

Mathematical methods for exploring the cognitive drivers of animal movement

by

Peter Thompson

A thesis submitted in partial fulfillment of the requirements for the degree of

Doctor of Philosophy

in

Ecology

Department of Biological Sciences

University of Alberta

© Peter Thompson, 2023

Abstract

The spatial distributions of animals have fascinated scientists for centuries. Understanding where animals go and why helps ecologists conserve their populations. Technological advances during the 21st century have allowed scientists to record the spatial location of animals over time, motivating the development of models that explain these patterns. Animals use external factors, such as qualities of their environments, and internal processes, such as memory, when deciding where to move. Interest in models that relate these internal processes to movement has increased in the last decade. In this thesis, I expand on existing work to model how perception, memory, and learning affects the way animals move. The methods described here incorporate different mathematical perspectives with a collective goal of identifying how moving animals account for temporal variation in their environments, predictable or unpredictable.

Temporal environmental variation results from many biological processes. When this variation is directly caused by animals themselves (e.g., through resource depletion), these animals navigate away from patches they visited (and depleted) recently. Resources may also vary independently from the animal, and when this variation is predictable, animals may benefit from learning schedules of resource availability. Chapter 2 describes a model that uses animal tracking data to identify patch revisitation patterns. The model's ability to quantify these patterns was verified on simulated data before being fit to brown bear (*Ursus arctos*) data from the Canadian Arctic. These bears live in an environment where food resources vary seasonally, and the model suggested that they use spatiotemporal memory to leverage these predictable patterns. Using advanced model-fitting techniques to obtain maximum likelihood estimates and confidence intervals, the model suggested that brown bears wait approximately

one year before navigating to resource-rich patches they visited previously.

When temporal variation in an animal's environment is not so predictable, animals must learn and adjust their foraging behaviour to survive. Psychologists and ecologists have theorized that animal learning resembles Bayesian inference, suggesting that animals refine their prior knowledge by incorporating the outcome of subsequent experiences (data). Chapter 4 incorporates this theory into a mechanistic model that simulates how animals learn, using Bayesian Markov chain Monte Carlo sampling to model how animals optimize a task with a quantifiable outcome. Using a mechanistic model that simulates the movement of spatially informed foragers within a home range, we apply this framework to predict how animals may learn to adjust to rapid and unpredictable changes in their environments. At larger spatial scales, predictable temporal variation in the environment may give rise to migratory behaviour. Chapter 5 presents a model that can statistically identify the beginning and end of migration from animal tracking data. This model can be used to partition animal location data into biologically reasonable behavioural segments for further analysis.

Movement ecologists have used statistical models to identify important biological patterns from data, and mechanistic models can incorporate causal links to make important predictions about how animals may move in the future. The work presented in this thesis advances movement ecology by introducing statistical and mechanistic tools that describe how cognitive processes inform animal foraging patterns.

Preface

This thesis is an original work by Peter Thompson. Some of the research included in this thesis was conducted as a part of collaborations. Mark A. Lewis is a supervisory author on Chapters 2, 3, 4, and 5, and Andrew E. Derocher is a supervisory author on Chapters 2, 3, and 5. Both of them contributed invaluable to the study design and provided substantial feedback to the writing. Mélodie Kunegel-Lion, helped design the modelling framework from Chapter 4. She also assisted in developing figures and revising the writing of the chapter. Chapter 5 uses data from ferruginous hawks (distributed by Erin M. Bayne), barren-ground caribou (distributed by Conor Mallory and Mitch Campbell), and brown bears (distributed by Mark A. Edwards). All of these collaborators provided feedback to the writing and analysis from Chapter 5. Subhash R. Lele and Peter D. Harrington helped design the model and provided feedback on the writing in Chapter 5.

A version of Chapter 2 has been published as: Thompson, P. R., Derocher, A. E., Edwards, M. A., & Lewis, M. A. (2021). Detecting seasonal episodic-like spatiotemporal memory patterns using animal movement modelling. *Methods in Ecology and Evolution*, 13(1), 105–120. Mark A. Edwards distributed the brown bear movement and environmental data for this chapter, and also contributed to the design of the model and analysis.

A version of Chapter 3 has been published as: Thompson, P. R., Lewis, M. A., Edwards, M. A., & Derocher, A. E. (2022). Time-dependent memory and individual variation in Arctic brown bears (*Ursus arctos*). *Movement Ecology*, 10(1), 18. Mark A. Edwards contributed significantly to the writing and analysis for this manuscript.

The brown bear data used in Chapters 2, 3, and 5 were collected by Mark A.

Edwards and Andrew E. Derocher. The University of Alberta Animal Care and Use Committee for Biosciences approved all animal capture and handling procedures, which were in accordance with the Canadian Council on Animal Care (ACUC412305, ACUC412405, ACUC412505, ACUC412605 and ACUC412705). Capture was conducted under permit from the Government of the Northwest Territories (WL3104, WL3122, WL3282, WL5352 and WL5375).

Acknowledgements

Thank you to my supervisors, Dr. Mark Lewis and Dr. Andrew Derocher, who have been the perfect team for the past three-and-a-half years. Mark and Andy were always available to provide kind, encouraging words alongside thorough, constructive feedback. Mark's vast experience with mathematical modelling and Andy's expertise in mammalogy synergize perfectly for the questions addressed in my thesis. Mark comes from a multidisciplinary background and his wide breadth of modelling experience has broadened my horizons as a scientist. Under Mark's supervision I have learned about the philosophy of science, which has encouraged me to think critically about how I answer scientific questions. I have been consistently inspired by Mark's unwavering passion for science over the past few years. Andy has enriched and supported my graduate education, and it has always been very clear to me that he cares deeply about my success and happiness, both as a student and in the future. He has always been available at a moment's notice, whether I needed to briefly discuss some minute aspect of my thesis or I needed urgent, time-sensitive feedback. I was incredibly fortunate to join him for fieldwork, where I was exposed to the hands-on component of ecology for the first time. I learned so much from Andy during this life-changing experience. I feel incredibly fortunate to have had Mark and Andy as supervisors during my time at the University of Alberta and I view them both in high esteem as role models.

I would like to thank my colleagues in the Lewis Research Group and Derocher Lab. These talented and passionate scientists have enriched my experience as a Ph.D. student through thought-provoking scientific discussions and memorable time spent together. There are too many names to name here, but I will never forget all the office conversations that have forged important scientific

ideas and kept my spirits high. The work in this thesis, particularly Chapters 4 and 5, would not have been possible without my lab-mates, but more importantly, neither would so many of the friendships I now cherish. I would also like to thank Kimberley Wilke-Budinski, the Lewis Research Group's administrator, for keeping the lab up and running. Kim is amazing at what she does and is a joy to be around.

I would like to thank Dr. Erin Bayne, who, along with Mark and Andy, made up my Ph.D. supervisory committee. Erin's commitment to thorough, rigorous, and effective science has positively influenced my thought process. I greatly appreciate his enthusiastic involvement in Chapter 5, which included distributing the ferruginous hawk data necessary for the analysis. I would also like to thank all the wonderful scientists outside my committee who I have had the pleasure of collaborating with during my Ph.D.: Dr. Mark Edwards, Dr. Mélodie Kunegel-Lion, Dr. Kimberly Mathot, Jonathan Farr, Elène Haave-Audet, Dr. Conor Mallory, Dr. Subash Lele, Dr. Peter Harrington, and Dr. Mitch Campbell. I would also like to thank Dr. Evelyn Merrill, who I worked with first as a student in her Landscape Ecology course and then as her teaching assistant. I am incredibly grateful to have worked with and learned from Evie, whose contributions to landscape ecology and habitat selection over the past four decades are foundational to my thesis work.

As a Ph.D. student I was fortunate to receive external funding from a number of organizations. I would like to thank Alberta Innovates, UAlberta North, the Andrew Stewart Memorial Fund, the Alberta Society for Professional Biologists, and the Alberta Graduate Excellence Scholarship for their financial support.

Contents

1	General introduction	1
1.1	Movement ecology as a discipline	1
1.2	Spatiotemporal cognition in wild animals	4
1.3	Dissertation outline	6
2	Detecting seasonal episodic-like spatiotemporal memory patterns using animal movement modelling	10
2.1	Introduction	10
2.2	Materials and Methods	14
2.2.1	Modelling framework	14
2.2.2	Statistical inference	27
2.2.3	Simulation studies	31
2.3	Results	35
2.3.1	Model verification: simulated data	36
2.3.2	Model application: grizzly bear case study	38
2.4	Discussion	41
2.5	Conclusions	46
3	Time-dependent memory and individual variation in Arctic brown bears (<i>Ursus arctos</i>)	48
3.1	Introduction	48
3.2	Materials and Methods	51
3.2.1	Study area	51
3.2.2	Brown bear data	53
3.2.3	Model design	54
3.2.4	Fitting the model to data	58

3.3	Results	59
3.3.1	Model selection	60
3.3.2	Parameter estimation	65
3.4	Discussion	67
3.5	Conclusions	74
4	Simulating how animals learn: a new modelling framework ap- plied to the process of optimal foraging	76
4.1	Introduction	76
4.2	Methods	81
4.2.1	The learning model	81
4.2.2	Application of the model to foraging	83
4.3	Results	90
4.3.1	Posterior distribution of parameters	90
4.3.2	Posterior distribution of objective function values	90
4.4	Discussion	93
5	A parametric model for estimating the timing and intensity of animal migration	99
5.1	Introduction	99
5.2	Methods	102
5.2.1	The model	102
5.2.2	Parameter estimation	104
5.2.3	Simulation analysis	106
5.2.4	Case studies	107
5.3	Results	113
5.3.1	Simulation analysis	114
5.3.2	Ferruginous hawks: stopovers and fix rates	114

5.3.3	Caribou: incorporating calving phenology	116
5.3.4	Brown bears: application to non-migrants	117
5.4	Discussion	118
6	General conclusion	132
6.1	Statistical models as a window into animal cognition	132
6.2	Spatiotemporal predictability and memory	134
6.3	Management applications	136
6.4	The future of movement ecology	137
	References	141
	Appendices	169
	Appendix A: Supplementary Figures and Tables for Chapter 2	170
	Appendix B: Supplementary Material for Chapter 3	172
	Appendix C: Overview, Design Concepts, and Details (ODD) protocol for Chapter 4	174
	Appendix D: Determining the appropriate number of MCMC iterations	184
	Appendix E: Simulation study for Chapter 5	185

List of Tables

2.1	Description of model parameters	26
2.2	Breakdown of model selection counts using BIC for the simulated tracks	37
2.3	Estimates of bias and MSE for each parameter in the resource-memory model	39
2.4	Model selection results for eight bears in the Mackenzie Delta population	40
3.1	dBIC (difference in BIC from the "best model") values for each model and bear, with resource covariates set to be temporally constant	61
3.2	dBIC (difference in BIC from the "best model") values for each model and bear, with resource covariates set to be temporally variable	63
3.3	Parameter estimates for the "best model" (as identified by BIC) for each bear	68
4.1	Learning model parameters and variables	82
5.1	Bias and MSE value for migration timing parameters	114
A.1	Description of all functions and quantities included in the model that were not fit as parameters	170
A.2	Breakdown of model selection counts using AIC for different types of simulated tracks	171
A.3	Breakdown of likelihood ratio test results for different types of simulated tracks	171
B.1	Classification method used to generate the berry density raster for the resource-only and resource-memory models	173

B.2a 95% lower confidence bounds for the "best model" (as identified
by BIC) for each bear 175

B.2b 95% upper confidence bounds for the "best model" (as identified
by BIC) for each bear 176

B.3 Parameter estimates for the "best model" (as identified by BIC)
for each bear with explicit expression of resource seasonality . . . 177

List of Figures

2.1	Schematic describing our modelling framework	15
2.2	Diagram describing how an animal's cognitive map Z changes over four discrete time steps	18
2.3	Violin plot of parameter estimates for β_1	38
3.1	Simulated animal movement tracks (300 steps per track) on a randomly generated landscape displaying behaviours consistent with each hypothesis	55
3.2	Movement track for bear ID GM1046 for the years 2004 and 2005	64
4.1	Schematic describing cognitive map calculation	85
4.2	Scenarios of environmental change	89
4.3	Posterior density of learning parameters	91
4.4	Posterior distribution of f_i with different values of k	92
4.5	Posterior distribution of f_i in different environmental scenarios .	92
4.6	Posterior distribution of f_i with different values of k and in dif- ferent environmental scenarios	94
5.1	Ferruginous hawk spring migration	123
5.2	Ferruginous hawk fall migration with stopover behaviour	125
5.3	Ferruginous hawk fall migration with premigratory behaviour . .	127
5.4	Caribou migration identified by our model without <i>a priori</i> in- formation	128
5.5	Caribou migration identified by our model with <i>a priori</i> information	130
5.6	Model fits for brown bear movement data	131
A.1	Violin plot of parameter estimates for α parameter in the resource- memory model	172

C.1	Flowchart describing the individual-based simulation model for animal movement	180
D.1	Relationship between the number of iterations in a MCMC chain used to simulate the foraging task and distributional similarity .	185

1 General introduction

1.1 Movement ecology as a discipline

Almost all animal species must move to survive. Moving allows these animals to acquire nutrients, evade predation, or find conspecifics to reproduce with. As one of the most fundamental components of an animal's survival, ecologists have been fervently interested with studying movement for decades. The field of "movement ecology" (Nathan et al., 2008) has expanded into a discipline of its own and has garnered widespread attention. The effects of anthropogenic global change on these movement patterns, and their corresponding consequences for animal population persistence, have elevated movement ecology's importance (Tucker et al., 2018). Understanding not just where animals go, but why they decide to go there, allows ecologists to pinpoint how to manage and conserve at-risk animal populations.

For centuries, ecologists have learned about animal behaviour and cognition by observing how animals move. Ecological pioneers like Charles Darwin observed and documented large-scale migrations long before methods existed to rigorously track and/or study these patterns (Darwin, 1839). In the early 20th century, live-traps were used to estimate the size of spatial areas used by non-migratory animals, which came to be known as an animal's "home range" (Burt, 1940, 1943). Methods for characterizing the size and shape of animal home ranges continue to evolve (Worton, 1989; Moorcroft et al., 2006; Fleming and Calabrese, 2017), and in turn so has the desire to identify what qualities constitute a valuable home range. Ideal free distribution theory (Fretwell and Lucas, 1969; Calsbeek and Sinervo, 2002), which postulates that animals distribute themselves according to the spatial distribution of resources, and optimal foraging theory (Charnov, 1976; Krebs et al., 1978), which introduces energetic

and economic principles to suggest foraging procedures that would maximize the fitness of wild animals, are among the many theoretical frameworks developed to answer these questions. These ideas influence how we think about animal movement to this day (Fagan et al., 2022; Martin et al., 2022; Netz et al., 2022; Railsback, 2022; Scott and Resetarits, 2022). The seminal work of Charnov and others focused the budding movement ecology community on how spatial heterogeneity in resources leads to spatial heterogeneity in animal distributions. The application of the use-available model design to animal movement data inspired the development of widely used resource selection functions (Manly, 1974; Johnson, 1980; Manly et al., 1993; Arthur et al., 1996; Boyce and McDonald, 1999). These methods rely on the proposition that animals can only occupy regions that are spatially available to them, and thus their habitat preferences must be analyzed within that domain of availability. Despite decades of innovation and research, identifying why animals go where they do is still one of the most important questions facing ecologists today (Nathan et al., 2008, 2022).

The 21st century brought about technological advances that advanced movement ecology through animal tracking, remote sensing, and more. Live-traps and direct observations have been replaced by tracking apparatuses that, when attached to wild animals, record a discrete sample of the animal's movement path. These data have been crucial for advancing movement ecology in terrestrial and marine systems (Hussey et al., 2015; Kays et al., 2015; Wilmers et al., 2015). This trend will likely continue as animal tracking technology evolves in the future (Jetz et al., 2022). Increased data availability has been accompanied by innovative mathematical models. Advances in computational technology have produced complex numerical techniques ranging from numerical analysis of differential equations to simulation of animal movement paths (Moorcroft et al., 2006; Schick et al., 2008; Tang and Bennett, 2010). Perhaps

the most notable consequence of this uptick in movement ecology research has been its application to conservation (Fraser et al., 2018). Understanding animal movement and space-use has clear conservation implications and the movement ecology has grown to address these increasing concerns (Barton et al., 2015; Hays et al., 2019; Davidson et al., 2020). To this day, there is still much we do not know about animal movement, motivating the development of models that can fill important knowledge gaps.

Fitting models to animal tracking data can uncover new details about the cognitive and behavioural drivers of movement. Nathan et al. (2008) characterized animal movement as a complex process resulting from external and internal factors. From this framework, an animal's decision to move somewhere would come about as a result of its internal interpretation of the external environment, limited by its locomotive and navigational capabilities. Notably, the majority of movement ecology studies have focused solely on how these external factors affect movement, often ignoring internal processes (Joo et al., 2022). Animal movement depends heavily on learning and spatial memory, as has been demonstrated in laboratory experiments for decades (Castro and Wasserman, 2010; Jacobs and Menzel, 2014). Uncovering these phenomena in the wild typically requires coupling high-resolution tracking data with mathematical and statistical models (Fagan et al., 2013; Lewis et al., 2021). Such approaches have suggested that home range emergence and migration, along with many other important behavioural patterns, would be impossible without spatial memory (van Moorter et al., 2009; Merkle et al., 2019; Ranc et al., 2022). There is still much to be learned about exactly how animals perceive and memorize the environment around them, though, and modelling the movements of wild animals is likely to provide insight on the problem (Lewis et al., 2021).

1.2 Spatiotemporal cognition in wild animals

The cognitive capabilities of animals have been of great interests to biologists and psychologists alike for decades. For many years, animals were a proxy used by psychologists to learn about human cognition, inspiring pioneering work on conditioning, discrimination learning, and sociality (Pavlov, 1927; Rescorla and Wagner, 1972; de Waal, 1991). Neuroscientific approaches have pinpointed brain regions that control spatial cognition in animals, enhancing our understanding of animal and human cognition (O'Keefe and Nadel, 1978). The popularity of Bayesian statistics has led cognitive ecologists to suggest that animals may learn in a way that resembles Bayesian inference (Green, 1980; Berger, 1985; Valone, 2006). Recently, interest in animal cognition has expanded past its application to humans due to conservation and management applications. In many cases, laboratory experiments often fail to encompass the overwhelming complexity of real-world environments, focusing recent work on spatial cognition in wild animals (Jacobs and Menzel, 2014; Pritchard et al., 2016). Identifying how animals memorize the spatial location of landmarks, patches, or other important areas, a process known as spatial memory, has emerged as an important study area for movement ecologists (Collett et al., 2013; Fagan et al., 2013; Vámos and Shaw, 2022). Spatial memory appears to be pivotal in forming many fundamental movement patterns (Clayton and Dickinson, 1998; van Moorter et al., 2009; Riotte-Lambert et al., 2015; Jesmer et al., 2018; Merkle et al., 2019), but different life history strategies may necessitate the use of different memory processes (Mueller and Fagan, 2008; Fagan et al., 2013). Specifically, incorporating temporal variability in an animal's landscape, and thus, its spatial memory, has been studied for animals with a variety of movement strategies (Schlägel and Lewis, 2014; Oliveira-Santos et al., 2016; Abrahms et al., 2019). "Spatiotemporal memory" in wild animals has not been extensively studied as there

is no all-encompassing framework for how these mechanisms facilitate optimal foraging in different animal populations.

Identifying patterns of spatial (or spatiotemporal) cognition in wild animals typically involves developing mathematical models and, if possible, fitting them to animal tracking data (Fagan et al., 2013). The wealth of modelling approaches take on many mathematical forms that can typically be classified as mechanistic or statistical. Statistical models characterize and identify consistent patterns, such as memory, from animal tracking data. Spatial memory is often quantified using the rate at which animals revisit areas they have been before (Berger-Tal and Bar-David, 2015). An exceptional number of these "recursive" movements in a dataset suggests that animals can navigate back to areas they visited previously (Merkle et al., 2014; Falcón-Cortés et al., 2021; Ranc et al., 2022). Similar approaches have been applied to migratory animals (Merkle et al., 2019; Kürten et al., 2022). More complex techniques have explored the temporal context of these revisitations, unearthing important knowledge about animal foraging (Schlägel and Lewis, 2014; Lafontaine et al., 2017). These models must statistically eliminate the possibility that patterns observed in the data could have arose from memory-less movement, which often requires designing competing alternative hypotheses (Fagan et al., 2013). In some cases, eliminating memory-less mechanisms for movement is difficult, but mechanistic models address this issue by directly including a mathematical causality between variables. These models need not incorporate data and can instead attempt to simulate realistic movement patterns for individuals or populations. These simulation-based analyses can fill important knowledge gaps about animal cognition and movement (van Moorter et al., 2009; Mueller et al., 2011; Potts and Lewis, 2016). An exciting new body of work has focused on how mechanistic and statistical models can be linked, mathematically and biologically (Potts et al., 2022). Ultimately, both

approaches are useful and can be especially powerful when taken together.

Developing models for how animals incorporate spatiotemporal memory into their movements will connect empirical observations with ecological theory. The utility of memory-informed movement, and consequently the way that animals incorporate memory into their movement decisions, depends on the spatiotemporal heterogeneity and predictability of their environments (Mueller and Fagan, 2008; Fagan et al., 2013). For example, when resources vary temporally but this variation is predictable, animals may move cyclically between resource-rich areas, and the temporal context to spatial memory would heavily influence these movements (Mueller and Fagan, 2008). These types of movements can be characterized as migration or seasonal home-range use depending on their scale, but may be brought about by similar cognitive mechanisms (Dingle and Drake, 2007). Many of these theoretical predictions have not been confronted with animal tracking data and some of them have not even been addressed with data-free mechanistic models. The links between learning and animal movement, which are vital in an age where animals are frequently met with novel stimuli, are under-explored (Lewis et al., 2021). True learning is more difficult to observe in the wild, and typically requires environments rife with novel and unpredictable change. Translocation experiments (Jesmer et al., 2018; Falcón-Cortés et al., 2021) can address the problem, but the way animals learn to adjust to environmental change is a still major knowledge gap in movement ecology. Modelling advances can close these gaps and enhance our understanding of why animals go where they do.

1.3 Dissertation outline

The work described below represents an array of statistical and mechanistic approaches for characterizing spatiotemporal memory and learning processes in

animals. These models determine how animals decide where to go and when, with a particular emphasis on the temporal context of these decisions. The models encompass a spectrum of movement strategies, ranging from home ranging to migration, and mathematical formulations, ranging from simulations to statistical functions. The work was made possible by innovative numerical and computational techniques that are relatively new to movement ecology, promoting the possibility of future work expanding on these approaches. Chapter 6 synthesizes the inference drawn from modelling efforts discussed in Chapters 2-5.

Chapter 2 contains methodological details behind the development of a statistical movement model used to identify the spatial and temporal characteristics of revisitations within an animal's home range. The model builds on existing statistical techniques to identify whether animals use spatial memory to navigate to previously visited locations, and if they do, how long they wait before revisiting these locations. The timing and strength of this spatial signal are estimated, along with other behavioural qualities, as parameters, by fitting the model to tracking data. The temporal complexity of some parameters in the model made it difficult to fit with simple, traditional methods. We applied a recently developed likelihood profile algorithm for identifying accurate confidence intervals to ensure we properly handled the uncertainty of our results. Special cases of the model (with certain parameter values fixed) correspond to different hypotheses about memory and movement, so we used information theory to elucidate which hypothesis was most likely to be true. We verified that the model properly identifies memory-informed and memoryless movements using a simulation study, which also estimated the amount of data required for reasonable model inference.

In Chapter 3 we fit the model to 21 adult brown bears (*Ursus arctos*) collared

in the Mackenzie Delta region of the Northwest Territories, Canada. Brown bears are omnivorous and typically eat many different foods. In the Canadian Arctic, these foods are not available year-round and thus remembering the temporal availability of food resources is important for brown bears. We fit the model described in Chapter 2 to the bears and identified temporally consistent spatial revisitations in a majority of the individuals. We found that brown bears typically navigated towards regions of their home range that they visited approximately one year prior, suggesting that they are aware of seasonal patterns in food availability. Our model outperforms memory-less approaches even when the temporal availability of the resources is explicitly defined.

Chapter 4 discusses a mechanistic model that simulates how animals learn. The model builds on theoretical work suggesting that animals learn and make decisions using principles similar to Bayesian inference. Taken literally, this would suggest that Bayesian Markov chain Monte Carlo (MCMC) samplers can be used to simulate animal learning, given some sort of task with "parameters" and a "reward" function. We applied this framework to a foraging task, which simulates the movement of a spatially informed, non-migratory animal. The model yields notable conclusions about behavioural plasticity, adaptation to rapidly changing environments, and learning. Our framework is flexible and can be applied to many other tasks, and there is potential to corroborate the model with laboratory experiments or even empirical data from wild animals.

Chapter 5 summarizes a model that quantifies the temporal extent of migration in animals. Migration is a widespread, complex, and diverse behavioural process, but there are still not many approaches that can characterize migration phenology for a variety of ecological systems. The approach described here uses simple movement metrics (step lengths and turning angles) to identify abrupt behavioural shifts in animal movement patterns. We developed a grid-

based temporal likelihood optimization approach to accurately identify these timings. In addition to a brief simulation analysis, we tested the model on three case studies: ferruginous hawks (*Buteo regalis*), barren-ground caribou (*Rangifer tarandus groenlandicus*), and the brown bears from Chapter 3. The model identified migrations for the hawks and caribou, and failed to identify any consistent "migratory" patterns in the non-migratory bears. The confidence intervals for our model parameters, including those for migration timings, were obtained using parametric bootstrapping and indicate that these quantities can be estimated with high certainty.

Chapter 6 summarizes and synthesizes the analysis conducted in Chapters 2-5. This includes a discussion of how these mathematically unique modelling approaches connect with one another to answer the same questions in ecology: how animals know where to go, and why they go where they do. There is so much more to learn about animal cognition and movement, and Chapter 6 describes how the results from Chapters 2-5 can be elaborated on to fill important knowledge gaps in movement ecology. Specific attention is given to applications with significant implications for wildlife conservation and management.

2 Detecting seasonal episodic-like spatiotemporal memory patterns using animal movement modelling

2.1 Introduction

Animal movement modelling has rapidly emerged as a subfield of ecology (Nathan et al., 2008) due to advances in animal tracking (Kays et al., 2015) and computational technology (Kristensen et al., 2016). The products of these advances have been widely applied to conservation and management (Fortin et al., 2005; Graham et al., 2012; Gerber et al., 2019). These models allow ecologists to understand the size and shape of an animal’s home range (Worton, 1989) as well as what habitat attributes animals prefer on a finer scale (Gaillard et al., 2010). To address the latter, ecologists have developed tools such as resource selection functions (RSFs; Boyce and McDonald, 1999) and step selection functions (SSFs; Fortin et al., 2005). These allow for inference on an individual’s habitat preference in what is known as third-order selection (Johnson, 1980; Thurfjell et al., 2014). The fine temporal and spatial resolution of these models allows ecologists to draw inference about a variety of behavioural processes, such as how an animal’s movement rates are affected by its environment (Avgar et al., 2016; Prokopenko et al., 2017) and how movement patterns change at different temporal scales (Oliveira-Santos et al., 2016; Richter et al., 2020). And yet, even with the advances that have been made in animal movement modelling, some notable behavioural mechanisms are often not considered.

Spatial memory, defined by Fagan et al. (2013) as memory of the spatial configuration of one’s environment, is one of the most important influences on animal movement patterns. The idea of episodic-like memory, which hypothesizes

that animals can remember the "what", "where", and "when" associated with specific events, is often intertwined within the intersection of spatial memory and foraging (Munoz-Lopez and Morris, 2009; Eacott and Easton, 2010; Allen and Fortin, 2013; Crystal, 2018). Many well-known behavioural processes, such as home range emergence (van Moorter et al., 2009; Riotte-Lambert et al., 2015), food caching (Clayton and Dickinson, 1998), and even migration (Bracis and Mueller, 2017; Merkle et al., 2019), require the ability to remember the spatial location of landmarks or regions, which often requires some form of episodic-like memory of previous events. Animal species use spatial memory in different ways (Fagan et al., 2013), and the benefits an animal may receive from memory often depend on its environment (Mueller and Fagan, 2008; Mueller et al., 2011). Theory on animal cognition has proposed that animals encode this spatial information in their brain as a cognitive map (Tolman, 1948; O'Keefe and Nadel, 1978). Ecologists have proposed multiple theories for the structure of these maps, with debate arising over whether a spatially explicit Euclidean map or a network-based topological map is more accurate (Bennett, 1996; Sturz et al., 2006; Normand and Boesch, 2009; Asensio et al., 2011). The true structure of these cognitive maps in animals is still unclear and may vary in different animal species. In the least, a cognitive map is an effective mathematical vehicle to quantify how animals remember to revisit valuable places within their home ranges. The link between memory and movement has long interested ecologists (in the case of Siniff and Jessen, 1969, for the purposes of home range modelling), but there are still ample opportunities for modelling.

Attempts to model these revisitations have proposed cognitive maps with spatial and temporal components, but have neglected to make inference about the specific nature of these influences. While many such approaches exist (Dalziel et al., 2008; Avgar et al., 2013, 2015; Vergara et al., 2016; Harel and

Nathan, 2018), a common and simple technique involves integrating cognitive maps into SSFs (Merkle et al., 2014; Oliveira-Santos et al., 2016; Marchand et al., 2017). A notable example is the model developed by Schlägel and Lewis (2014), where cognitive maps are based on time since last visit (a form of episodic-like memory) for each point in space. It is proposed that animals will only be encouraged to revisit locations when they have not visited them recently, as seen in some ecological systems (Davies and Houston, 1981). This model was used to draw inference from gray wolf (*Canis lupus*) movement patterns (Schlägel et al., 2017), but it does not provide detail on when animals choose to revisit portions of their home range. The model only considers the last visit to any point in space, disregarding any previous visits to that point. Time since last visit alone is insufficient to model the complex time-dependent spatial memory that inspires movement patterns described above, because waiting longer to revisit such locations may not always be beneficial for the animals (e.g., trees that lose their ripe fruit after too long).

Here we describe a model that mathematically estimates the timing and precision of these seasonally recursive movements (Fig. 2.1). We employ innovative model fitting techniques (Kristensen et al., 2016; Fischer and Lewis, 2021) brought about by advances in computational methods to detect patterns in animal location data. Our modelling framework characterizes the movement of simulated or real animals according to four hypotheses: (N) the null hypothesis, assuming random walk behaviour; (R) the resource-only hypothesis, assuming animals move entirely according to nearby resources without memory; (M) the memory-only hypothesis, assuming animals exhibit seasonal revisitation patterns within their home range with a prescribed mean lag time; and (RM) the resource-memory hypothesis, assuming animals are simultaneously influenced by local resources and spatial memory. This model expands on pre-

vious work, which has provided detail on how animals react to previously visited locations (Schlägel and Lewis, 2014), how animals react to familiar locations at different times of day (Oliveira-Santos et al., 2016), and how memory may decay over time (Avgar et al., 2015). Riotte-Lambert et al. (2017) have even developed a movement metric capable of gauging how often recursions are present in animal movement data. We add to this rich array of literature by developing a model that quantifies how long animals may take to revisit certain regions of their home range, and how much a resource landscape plays a part in these movements, by analyzing the animal’s entire movement path as opposed to the recursion events themselves. The model is not intended to answer the question of *if* animals use memory, but instead *how*, testing the prevalence of temporally consistent recursive movements in foraging animals.

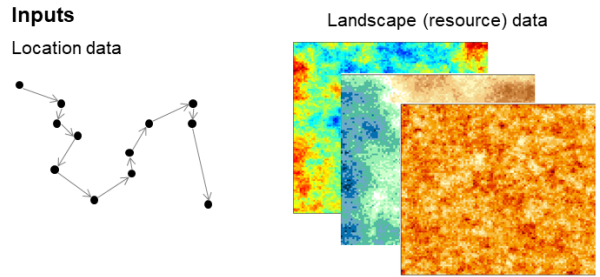
To test our model, we first simulated movement tracks according to the model’s prescribed rules on simulated environments, subsequently analyzing how sample size affects both model selection and parameter estimation. We found that even with data sizes equivalent to roughly one year of animal tracking data, the model accurately identified movement patterns consistent with the four different hypotheses and produced accurate parameter estimates. These results improved when tracks with more locations were simulated. We then fit the model to telemetry data from a population of Arctic grizzly bears (*Ursus arctos*) and performed the same simulation analysis with real landscape data and movement parameters estimated for the bears. These bears live in a harsh environment where food resources are seasonal (Edwards and Derocher, 2015) and sparsely distributed (Edwards et al., 2009). We found a heavy influence of spatiotemporal memory in the bears’ movement patterns, although we determined that more data may be required to analyze these populations than for simulated movements.

2.2 Materials and Methods

Here we introduce a new modelling framework based on step selection functions that accounts for temporally consistent revisitations by animals that forage on ephemeral resources (Fig. 2.1). We developed a nested structure of four models in discrete time and continuous space (see Table 2.1 and Table A.1 for a summary of the parameters and models) to address our four alternative hypotheses (N, R, M, RM). Our model fitting process, made possible through advanced automatic differentiation techniques, allows for further inference about the specific nature of these cognitive mechanisms. The novelty and complexity of the computational processes used to analyze animal location data with our model motivated multiple simulation-based studies to identify the statistical power and parameter estimability of our models.

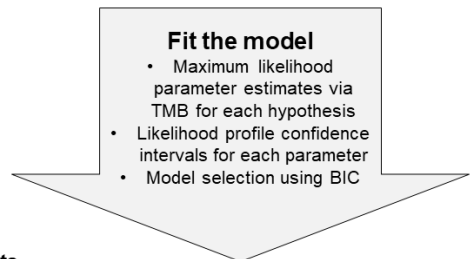
2.2.1 Modelling framework

We fit a hidden Markov model (HMM) to animal movement data to incorporate switching between stationary (or quasi-stationary) and non-stationary states. HMMs are a first-order Markov process, implying that the animal's current state is entirely dependent on its most recent state. This approach is common in movement ecology due to the multitude of behavioural strategies observed in foraging animals (Morales et al., 2004; Jonsen et al., 2013). We employ this approach to differentiate resting or other stationary behaviour from what the model would otherwise identify as spatial memory. Our model identifies time lags at which the animal moves particularly close to its previously visited locations, and staying put for one time step is interpreted mathematically by the model as strong recursive behaviour with a time lag of one time step. Without including the stationary behavioural state, the model erroneously identifies this one-step time lag in most animal data.



4 Alternative Hypotheses → 4 Movement Models

Null	Resource-only
Animals move without regard to their external environments or memory	Animals move only according to local gradients in their environments
Memory-only	Resource-memory
Animals return to previously visited locations with repeated time lags	Animals select for local resources while also returning to resource-rich locations they previously visited



Outputs

- Explicit description of animal movement behavior via **parameter estimates** and **confidence intervals**
- Relative likelihood of each hypothesis via **BIC**

Figure 2.1: Schematic describing our modelling framework. Given an animal's movement track, quantified as a set of spatial coordinates, as well as landscape data describing an animal's environment, we fit four nested, competing models using maximum likelihood estimation. The insight we gain from this process allowed us to make conclusions about the mechanistic drivers of animal behaviour.

An HMM consists of a Markov matrix \mathbf{A} of state-switching probabilities as well as conditional probability distributions of the animal's spatial location for each state (Jonsen et al., 2013). For a model with n different movement states, \mathbf{A} maps from $\mathbb{R}^n \rightarrow \mathbb{R}^n$, with each column summing to 1. Our model has two states, so we can infer the structure of \mathbf{A} from its diagonal. We denote these entries λ and γ , representing the probability that the animal will stay in the stationary or non-stationary state, respectively, given it was just there. Explicitly, it takes the form below:

$$A = \begin{pmatrix} \lambda & 1 - \lambda \\ 1 - \gamma & \gamma \end{pmatrix} \quad (2.1)$$

While our model is meant to be applied to continuous-space animal data, we make an approximation by discretizing our landscape over a two-dimensional square grid. Empirical landscape data is rarely continuous in space, and the resolution of this data can suggest a clear choice for the resolution of the domain grid. We define points in continuous space as \mathbf{x} (or \mathbf{x}_t to represent the animal's location at time t) and their corresponding grid cells as z or z_t . Thus, $\mathbf{x}_0 \in z_0$ is the animal's initial location.

We define our conditional probability density functions for the stationary and non-stationary state f_s (which remains the same in all four models) and f_{ns} , respectively. Each conditional probability distribution represents a first-order Markov process modelling the animal's location \mathbf{x}_t and its heading ϕ_t over time, which depend only on \mathbf{x}_{t-1} and ϕ_{t-1} from the previous time step. Due to observation error in animal tracking data, we assumed that the animal's observed location may change slightly even if it is not moving (Jonsen et al., 2013), so we allowed for small "movements" in our stationary state. The probability distribution for headings in the stationary state, $g_s(\phi_t|\phi_{t-1})$, is a uniform

distribution since we assume no directional autocorrelation here, so

$$g_s(\phi_t|\phi_{t-1}) = \frac{1}{2\pi}, \quad (2.2)$$

$$f_s(\mathbf{x}_t, \phi_t|\mathbf{x}_{t-1}, \phi_{t-1}, \rho_s) = \frac{2}{\pi\rho_s} g_s(\phi_t|\phi_{t-1}) \exp\left(-\frac{\|\mathbf{x}_t - \mathbf{x}_{t-1}\|^2}{\pi\rho_s^2}\right). \quad (2.3)$$

We modelled the probability of the animal moving from \mathbf{x}_{t-1} to \mathbf{x}_t when in the stationary state using a half-Gaussian distribution with a fixed mean ρ_s . The half-Gaussian distribution has thinner tails than the more traditionally used exponential distribution, decreasing the probability of longer movements from this state. We fix ρ_s to reduce model complexity, noting that it is fairly straightforward to do so based on the known degree of observation error or the resolution of environmental data.

In the non-stationary state, we use a cognitive map structure to keep track of the animal's spatiotemporal movement experiences (Fig. 2.2). Our implementation of a cognitive map expands on the concept of time since last visit (Davies and Houston, 1981; Schlägel and Lewis, 2014; Schlägel et al., 2017) by allowing for the memory of more than just the last location to any point in space. Instead, we formulate the animal's cognitive map as the set of times since previous visits (TSPVs) for any area in space. This formulation allows for a form of seasonal episodic-like memory that expands on the "time since last visit" framework (Clayton and Dickinson, 1998; Martin-Ordas et al., 2010). We define this map Z_t at each time t as a function over the domain grid. At each grid cell z , $Z_t(z)$ is a linked list of integers, with each element of the list representing an animal's visit to a point inside that cell. Z_0 is a grid full of empty linked lists, except for z_0 ; $Z_0(z_0)$ is a list with one element, 0. We can

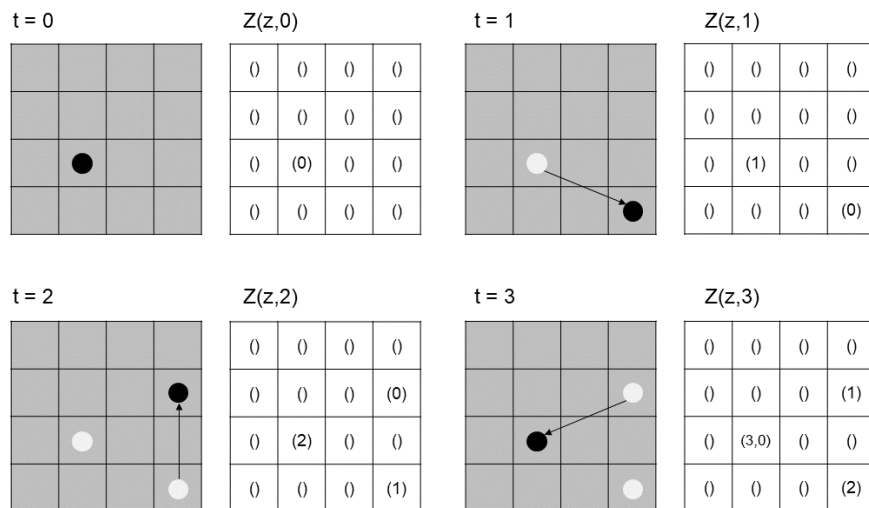


Figure 2.2: Diagram describing how an animal's cognitive map Z changes over four discrete time steps, given an animal's movement track, which is illustrated in the shaded panels. Each cell of Z contains a linked list that starts out empty but is iteratively appended as the animal traverses its environment.

obtain Z_t if we know Z_{t-1} as well as the animal's location at time t . When t is incremented by 1, so is every entry on every linked list across the grid, and a new entry (0) is added to the linked list corresponding to the animal's new location:

$$Z_t(z) = \begin{cases} Z_{t-1}(z) + 1 & \mathbf{x}_t \notin z \\ [Z_{t-1}(z) + 1, 0] & \mathbf{x}_t \in z \end{cases}. \quad (2.4)$$

where $[Z_{t-1}(z) + 1, 0]$ implies adding 1 to every entry of the linked list $Z_{t-1}(z)$ and appending it with a new value 0.

The function f_{ns} , which models the animal's location and heading in the non-stationary state, resembles a step selection function (Fortin et al., 2005; Forester et al., 2009), with two main components: k , the resource-independent movement kernel; and W , the environmental (or cognitive) weighting function.

The function k describes the animal’s locomotive capability while W , which may depend on the animal’s cognitive map Z_{t-1} , describes how attractive the point is to the animal. This yields the following expression for f_{ns} :

$$\begin{aligned}
 f_{ns}(\mathbf{x}_t, \phi_t | \mathbf{x}_{t-1}, \phi_{t-1}, Z_{t-1}, \Theta_1, \Theta_2) \\
 = \frac{k(\mathbf{x}_t | \mathbf{x}_{t-1}, \phi_{t-1}, \Theta_1) W(\mathbf{x}_t | Z_{t-1}, \Theta_2)}{\int_{\Omega} k(\mathbf{x}' | \mathbf{x}_{t-1}, \phi_{t-1}, \Theta_1) W(\mathbf{x}' | Z_{t-1}, \Theta_2) d\mathbf{x}'}. \quad (2.5)
 \end{aligned}$$

The integral in the denominator serves as a normalization constant to ensure that f_{ns} integrates to 1. The parameter vector Θ_2 represents parameters related to the W and Θ_1 represents the locomotive parameters associated with k , namely ρ_{ns} which describes the animal’s mean step length and κ which describes the degree of directional autocorrelation in the animal’s movements. For each of our four models (null, resource-only, memory-only, resource-memory), the animal’s resource-independent movement kernel k (as well as Θ_1) has the same formulation. We modelled the distance between \mathbf{x}_t and \mathbf{x}_{t-1} , known as a step length, using an exponential distribution with mean parameter ρ_{ns} , and modeled the heading ϕ_t using a von Mises distribution centred at ϕ_{t-1} with concentration parameter $\kappa \geq 0$ (Equation 2.6). Higher values of κ indicate straighter movement. We assume here that the animal’s step lengths and turning angles are independent. This modelling structure, known more generally as a correlated random walk, has been applied to a variety of ecological systems (Fortin et al., 2005; Auger-Méthé et al., 2015; Duchesne et al., 2015), and the exponential and von Mises distributions are both particularly easy to deal with analytically while still providing accurate fits for a majority of field data (Codling et al., 2008; Thurfjell et al., 2014). We formulate k such that

$$g_{ns}(\phi_t|\phi_{t-1}) = \frac{\exp(\kappa \cos(\phi_t - \phi_{t-1}))}{2\pi I_0(\kappa)}, \text{ and} \quad (2.6)$$

$$k(\mathbf{x}_t|\mathbf{x}_{t-1}, \phi_{t-1}, \Theta_1) = \frac{\exp\left(-\frac{\|\mathbf{x}_t - \mathbf{x}_{t-1}\|}{\rho_{ns}}\right)}{\rho_{ns}} g_{ns}(\phi_t|\phi_{t-1}), \quad (2.7)$$

where $I_0(\kappa)$ is the modified Bessel function of order 0. Notice that ϕ_t , the animal's heading at time t , is not explicitly included in the left side of Equation 2.7; it can instead be calculated easily if \mathbf{x}_t and \mathbf{x}_{t-1} are known (Fortin et al., 2005). Note that g_{ns} , just like g_s , is separate from the rest of k , following our assumption that the animal's step lengths and bearings are independent.

The only mathematical difference between the four models is the formulation of W . To differentiate between these different formulations, we refer to them as W_N , W_R , W_M , and W_{RM} for the null, resource-only, memory-only, and resource-memory models, respectively. The set of parameters we estimate in each model also varies, so we define $\Theta_{2,N}$, $\Theta_{2,R}$, $\Theta_{2,M}$, and $\Theta_{2,RM}$ in a similar respect.

2.2.1.1 Null model

The null model describes an animal's locomotive capability and directional autocorrelation based on its observed movement track. As a result, there is no extra weighting, so $W_N(\mathbf{x}_t|\Theta_{2,N}) = 1$ for all \mathbf{x}_t in space, and $\Theta_{2,N}$ is the empty set. As a result, when considering the null model, f_{ns} is equal to k .

2.2.1.2 Resource-only model

The resource-only model has the following key component:

- (R1) the animal's movement is driven by third-order selection for resources reachable within one time step.

As a result, W_R resembles the weighting function from an RSF or SSF (Boyce and McDonald, 1999; Fortin et al., 2005). If we are interested in P different resource covariates (expressed mathematically at each spatial location \mathbf{x} as $r_1(\mathbf{x}), \dots, r_P(\mathbf{x})$), we must estimate selection parameters β_1, \dots, β_P for each covariate. These parameters make up $\Theta_{2,R}$. The expression for our weighting function in the resource-only model is a linear combination of the covariates:

$$W_R(\mathbf{x}_t | \Theta_{2,R}) = \exp \left[\sum_{p=1}^P \beta_p r_p(\mathbf{x}_t) \right]. \quad (2.8)$$

2.2.1.3 Memory-only model

The memory-only model contains the following key components:

- (M1) the animal uses a cognitive map to remember the timing of previous visits to regions of its environment, and
- (M2) it will return to locations it previously visited after temporally similar time lags.

This type of cognitive map has been supported in the literature (Normand and Boesch, 2009; Martin-Ordas et al., 2010; Schlägel and Lewis, 2014) as has the validity of path recursions and revisitations as a foraging strategy for animals (Berger-Tal and Bar-David, 2015; Schlägel et al., 2017). Note that this behaviour could arise from multiple mechanisms: if an animal is foraging for periodically available resources, we can use its previous locations to determine where it might be in the future, and if an animal forages on some depleting resource, we could use this model to identify how long the animal waits before returning to a resource it had previously depleted. Note, though, that the memory-only model assumes a homogeneous landscape, as resource data are not included. While this assumption is usually unrealistic, we include it as

an alternate hypothesis to models including resource selection. In cases where appropriate resource data are not available, or the existing resource data are insufficient to explain patterns in the movement data, the memory-only model serves to identify if a pattern of timed re-visitation exists.

We calculate W_M based on distance to previously visited points on the animal's track. Given some time lag τ , we can use the cognitive map Z_t to find the point in space (or at least, the grid cell) where the animal was τ time indices ago. There is always exactly one grid cell $z_{t-\tau}$ where τ is an element of the linked list $Z_t(z_{t-\tau})$.

For each time lag τ , we compute the distance between the animal's current location and $z_{t-\tau}$, $\|\mathbf{x}_t - z_{t-\tau}\|$, and transform it using an exponential decay function with decay parameter 10^α . The primary role of α is to convert distances to unitless quantities representing attractiveness. Under the assumption that points closer to previously visited locations are more attractive, we use $\exp(-10^\alpha \|\mathbf{x}_t - z_{t-\tau}\|)$ as the transformation for the distance between \mathbf{x} and the centre of $z_{t-\tau}$. We include the power here so α can be any real number, and use 10 so its estimate can be interpreted more easily. The transformation with α produces a discounting of importance with distance, where α quantifies how quickly this importance is discounted spatially. If α is larger, then points must be very close to the previously visited location for the animal to deem them attractive. As α decreases, the mathematical difference between a step 1000 m away and a step 2000 m away is amplified, suggesting that the animal understands these differences in space on a wider scale. The value of α may be informative about the heterogeneity of the landscape, which can be informative about how animals value the importance of distance in predicting resource quality (Farnsworth and Beecham, 1999).

The animal's revisitation schedule, which is mediated by two parameters

μ and σ , dictates the weights for each of these exponentially transformed distances. The timing with which an animal navigates back to an existing location can be thought of as a random process, following a Gaussian distribution with mean parameter μ and standard deviation parameter σ . We can imagine that this timing reflects the state of the environment, with μ indicating the time scale at which resources may come and go and σ indicating the variability of these revisitations. For any given time lag τ , the exponentially transformed distance between \mathbf{x}_t and $z_{t-\tau}$ is weighted by the Gaussian probability distribution function $\varphi(\tau|\mu, \sigma)$. This produces a weighted mean of exponentially transformed distances, following the hypothesis that animals will navigate towards points they visited roughly μ time increments ago; the most "attractive" points for the animal are closest to z_μ . We introduce one final parameter, β_d , a "selection coefficient" for memorized locations. This parameter can be thought of as the relative probability of revisiting a memorized location instead of moving randomly or selecting for present-time resources. We restricted $\beta_d \geq 0.5$ (implying $\log \frac{\beta_d}{1-\beta_d} > 0$), in line with the hypothesis that animals select for (not against) previously visited locations.

The resulting formulation of W_M is as follows:

$$\begin{aligned}
 W_M(\mathbf{x}_t|Z_{t-1}, \Theta_{2,M}) \\
 = \exp\left(\tilde{\beta}_d \left[\frac{\sum_{\tau=1}^t \varphi(\tau|\mu, \sigma) \exp(-10^\alpha \|\mathbf{x}_t - z_{t-\tau}\|)}{\sum_{\tau=1}^t \varphi(\tau|\mu, \sigma)} \right]\right), \quad (2.9)
 \end{aligned}$$

where $\tilde{\beta}_d = \log(\frac{\beta_d}{1-\beta_d})$, and $\Theta_{2,M}$ contains μ, σ, β_d , and α .

W_M does not directly contain any periodic components (the Gaussian weight simply just has one mode around μ), and we do this to increase the flexibility of the model. In the event that an animal is pursuing resources that vary

periodically with a period of μ , its location at any point is likely to be nearby its location μ timesteps ago. Movements simulated from this model do also produce movements that are somewhat periodic, although the spatial correlation between an animal's location and its location μ time steps prior is stronger than locations separated temporally by 2μ , for example.

2.2.1.4 Resource-memory model

The resource-memory model incorporates both resource selection and memory into the animal's movements, so (R1) and (M1) still remain as components in this model. However, there is one additional component that is not present in the resource-only or memory-only models:

- (RM1) the animal will return to locations it previously visited at a prescribed and scheduled time if habitat conditions there were favourable; otherwise it will avoid these areas.

Models combining resources and memory in some way have proven to be effective in explaining movement patterns for many different animals (Dalziel et al., 2008; Merkle et al., 2014; Schlägel et al., 2017). The resource-memory model builds on the memory-only model, which is often unrealistic due to the omission of environmental data, by truly quantifying an animal's episodic-like memory, capturing the "when" and "where" of an animal's spatial experience via Z and augmenting this with the "what": the resource quality at these previously visited points. The addition of hypothesis RM1 produces memory that is resource-dependent, whereas the memory-only model works under the typically false simplifying assumption of a spatially homogeneous landscape.

The linear combination of resource covariates $\sum_{p=1}^P \beta_p r_p(\mathbf{x})$ is relative, so we introduced an additional parameter β_0 representing the relative probability of visiting a faraway location depending on its resource quality. As β_0 approaches

1, the animal perceives all previously visited locations as "attractive" for re-visitation. We transform this parameter with an inverse logistic function so it represents a pseudo-intercept (recall that traditional SSFs and are conditional models and do not require an intercept; Fortin et al., 2005).

The weighting function now includes present-time resource selection in the first sum and memorized information in the second term:

$$W_{RM}(\mathbf{x}_t|Z_{t-1}, \Theta_{2, RM}) = \exp \left(\sum_{p=1}^p \beta_p r_p(\mathbf{x}_t) + \tilde{\beta}_d \left[\frac{\sum_{\tau=1}^t \varphi(\tau|\mu, \sigma) \exp(-10^\alpha \|\mathbf{x}_t - z_{t-\tau}\|) (\tilde{\beta}_0 + \sum_{p=1}^P \beta_p r_p(z_{t-\tau}))}{\sum_{\tau=1}^t \varphi(\tau|\mu, \sigma)} \right] \right), \quad (2.10)$$

where $\tilde{\beta}_d = \log(\frac{\beta_d}{1-\beta_d})$ and $\tilde{\beta}_0 = \log(\frac{\beta_0}{1-\beta_0})$.

	Units	Description	N	R	M	RM
ρ_{ns}	$\frac{\text{distance}}{\text{time}}$	Mean movement speed in non-stationary state	X	X	X	X
κ	N/A	Degree of directional autocorrelation	X	X	X	X
β_0	N/A	Probability of revisitation				X
β_i	$\frac{1}{r_i \text{ units}}$	Resource selection coefficient(s)		X		X
β_d	N/A	Strength of selection for memorized areas			X	X
μ	time	Mean time lag between revisitations			X	X
σ	time	Standard deviation in time between revisitations			X	X
α	$\log(\text{distance})$	Degree of perceptual resolution			X	X
λ	N/A	Probability of staying in stationary state	X	X	X	X
γ	N/A	Probability of staying in non-stationary state	X	X	X	X

Table 2.1: Description of model parameters, including units (N/A implies that the parameter is unitless) and models (N = null; R = resource-only; M = memory-only; RM = resource-memory) in which the parameters are estimated. For functions and other quantities that were not fit as model parameters, see Table A.1.

The null model is a special case of both the resource-only and memory-only models, which are both a special case of the resource-memory model. Setting $\beta_i = 0$ for $i = 1, 2, \dots, P$ and $\log\left(\frac{\beta_0}{1-\beta_0}\right) = 1$ in the resource-memory model yields the memory-only model, while setting $\beta_d = 0$ yields the resource-only model. Nesting models is advantageous for many mathematical reasons, including the ability to conduct likelihood ratio tests between models (Burnham and Anderson, 2004).

2.2.2 Statistical inference

We fit the four models to discrete-time, continuous-space animal movement data and used information theory to identify which corresponding hypothesis was most likely to be true. We identified the optimal set of parameters for a given track using maximum likelihood estimation, and used likelihood profiling to obtain accurate confidence intervals for our parameters.

2.2.2.1 Likelihood function

The likelihood of a set of model parameters for one step is a weighted sum of the conditional likelihood functions (f_s and f_{ns}), weighted by the probability of being in each state. These state probabilities depend on probabilities for the previous step, so for the first point we fit (there is no previous step), we fixed δ_s , the probability of being in the stationary state right before the data begins, as the proportion of steps shorter than ρ_s .

The likelihood function for the entire track is a product of the likelihoods for each step included in model fitting. We omitted all animal locations before some time t^* , since our model (or at least, the memory-only and resource-memory models) relies on past information to explain where the animal may go. We left the portion of the track that happened before $t = t^*$ to "train" the model on what the animal remembers. Thus, our iterative formula for the likelihood function begins at $t = t^*$. We define $\Phi_t \in \mathbb{R}^2$ as the vector of state probabilities for time $t \geq t^*$, and we calculate our likelihood using the iterative equations below:

$$\Phi_{t^*} = (\delta_s, 1 - \delta_s)^T, \quad (2.11)$$

$$\mathbf{P}_t = \begin{pmatrix} f_s(\mathbf{x}_t | \mathbf{x}_{t-1}, \rho_s) & 0 \\ 0 & f_{ns}(\mathbf{x}_t, \phi_t | \mathbf{x}_{t-1}, \phi_{t-1}, Z_{t-1}, \Theta_1, \Theta_2) \end{pmatrix}, \quad (2.12)$$

$$\Phi_t = \frac{\Phi_{t-1}^T \mathbf{P}_{t-1}}{\|\mathbf{P}_{t-1} \Phi_{t-1}\|} \mathbf{A}. \quad (2.13)$$

Then, following Whoriskey et al. (2017), the overall likelihood for the model is $\prod_{t=t^*}^{t_m^{ax}} \Phi_t^T \mathbf{P}_t \mathbf{1}$, where $\mathbf{1} = (1, 1)^T$.

We approximate the denominator of Equation 2.5 with a sum so we do not have to integrate every time we evaluate the likelihood function. As is commonly done with SSFs (Thurfjell et al., 2014), we calculated W at a set of "control points" for each observed point \mathbf{x}_t . If \mathbf{x}_t , the endpoint of a step from \mathbf{x}_{t-1} , is a random variable conditional on Z_{t-1} , Θ_1 , and Θ_2 , the integral in the denominator of Equation 2.5 is $E(W(\mathbf{x}_t))$. Thus, we can approximate it by estimating the mean value of W at a set of simulated draws from \mathbf{x}_t , which has probability density function k . This gives us the following approximation for f_{ns} :

$$\begin{aligned} \tilde{f}_{ns}(\mathbf{x}_t, \phi_t | \mathbf{x}_{t-1}, \phi_{t-1}, Z_{t-1}, \Theta_1, \Theta_2) \\ = \frac{k(\mathbf{x}_t | \mathbf{x}_{t-1}, \phi_{t-1}, \Theta_1) W(\mathbf{x}_t | Z_{t-1}, \Theta_2)}{\frac{1}{K} \sum_{j=1}^K W(\mathbf{x}_{t,j} | Z_{t-1}, \Theta_2)}, \end{aligned} \quad (2.14)$$

where $\mathbf{x}_{t,j}$ represents the j^{th} control point (a simulated step starting at \mathbf{x}_{t-1}) and K is the number of control points per observed step. From this approximation, it becomes evident that each model compares W from steps the animal actually took to steps that are simulated from a random walk. This implies that

if an animal occasionally returns to previously visited locations as a result of random movement, the model will account for this and identify the null model as a more parsimonious explanation of the data than the other models. For the memory-only model to truly be an effective explanation of movement patterns observed in the data, these revisitations must be frequent and temporally consistent.

2.2.2.2 Fitting the model

We fit the model to data using maximum likelihood estimation, with the Template Model Builder (TMB) R package (Kristensen et al., 2016) improving numerical accuracy for this complex problem. TMB has been used to fit complex animal movement models, including HMMs (Albertsen et al., 2015; Auger-Méthé et al., 2017; Whoriskey et al., 2017). TMB uses automatic differentiation to calculate the gradient of a multidimensional likelihood function using pseudo-analytical methods, as opposed to traditional finite-difference methods that are slow and frequently result in numerical errors (Skaug and Fournier, 2006). We wrote a likelihood function for each model in C++, which TMB compiles and returns as a callable function in R (Kristensen et al., 2016). This allowed us to use an R optimizer of our choice while also benefiting from C++'s superior programming speed.

We used the R *nminb* function to obtain maximum likelihood estimates for the negative log of our likelihood function. To prevent our model from producing errors or unrealistic results, we imposed various bounds on some of the parameters. We bounded the estimation for μ at t^* because if $\mu > t^*$, we would not be able to identify a signal due to a lack of training data. We also put a lower bound on σ ; when this parameter was small, the partial derivative of our likelihood function with respect to μ became noisy, leading to computational errors in optimization. We found that a lower bound of approximately 20 time

indices eliminated this problem. We additionally required estimates for $\alpha < -\log_{10}(\bar{\rho})$, where $\bar{\rho}$ is the animal's empirical mean step length (for context, we expect $\bar{\rho}$ to be close to but slightly smaller than ρ_{ns}). Values of α above this bound imply that the animal cannot perceive a difference between a few step lengths, which is unreasonable biologically. For parameters with fairly restrictive bounds (λ , γ , β_d , and β_0 , which are bounded between 0 and 1), we performed logit transformations ($\tilde{\lambda} = \log \frac{1}{1-\lambda}$, for example) so the optimizer would more effectively traverse the parameter space.

We tested two "initial values" for μ for each dataset we fit the model to, picking the fit that gave us the best likelihood function value. When profiling the likelihood surface with respect to this parameter, we often found many local optima, so we fit the model with initial values of t^* and $\frac{t^*}{2}$. Fitting with different initial values incurs additional computational time (we are effectively running the optimization algorithm twice) but is necessary due to the importance of picking a good initial value for each parameter (Pan and Wu, 1998). Using a different number of initial values for μ may be advantageous for some datasets.

For a model as complicated as this one, obtaining confidence intervals (CIs) using traditional Wald-type methods does not always produce accurate results. We frequently found this to be true for our model in practice so we used the likelihood profiling from Fischer and Lewis (2021). Given a multidimensional objective function with a known optimum, this algorithm finds confidence intervals for one parameter at a time by performing a binary search algorithm for a target function value (typically, the optimum minus some small confidence threshold). The algorithm starts searching at the optimal parameter value, and tries an initial step, fixing the parameter in question at this value and optimizing the rest of the function parameters. This process is repeated subsequently until the lengths of each step in parameter space are small enough for the algorithm

to converge (Fischer and Lewis, 2021).

We used the Bayesian Information Criterion (BIC) to rank the four models by their likelihood and identify the hypothesis that was most likely to be true. BIC has a stronger penalization for model complexity than the more commonly used Akaike Information Criterion (AIC), and is a more useful criterion for model selection when one is interested in the truth of a hypothesis rather than the predictability of a model (Burnham and Anderson, 2004).

2.2.3 Simulation studies

Before applying our model to an ecological system, we simulated data and used it to test the model. These simulations are individual-based representations of our model that produce movement patterns associated with our four hypotheses. We performed this analysis as a means to ensure that our fitting methods could accurately identify the parameter values prescribed by the model. At each time index, we used our Markov matrix \mathbf{A} to decide whether the animal would change its behavioural state. If the animal was in the stationary state we simulated a random step from f_s (half-Gaussian step length, uniform turning angle). For the non-stationary state, we simulated from f_{ns} using a Monte Carlo method (Parzen, 1961). We first calculated W for the entire grid, then we simulated a large number of random steps from k (Equations 2.6 and 2.7). This simulation process resembles the generation of control points in Equation 2.14, but we simulated $N_r = 10000$ steps at each point in time. Making N_r very large did not greatly affect computational time, so we did so in the interest of accurately approximating Equation 2.5. These simulations took place on a bounded grid representing the hypothetical landscape, and any of the N_r proposed steps that took the animal off this grid were re-sampled until they were on the grid. While this resembles reflective boundary conditions, the animal is not assumed to "bounce off" the boundary or interact with it in any way other than avoiding

it. Note that it is possible to tune the animal's mean step length as well as the size of the landscape in simulations to drastically reduce the probability of this happening, which we did. We then randomly choose one of the steps based on the values of W at each step, with the probability of any step $\mathbf{x}_{t,i}$ being chosen described below:

$$\frac{W(\mathbf{x}_{t,i}|Z_{t-1}, \Theta_2)}{\sum_{j=1}^{N_r} W(\mathbf{x}_{t,j}|Z_{t-1}, \Theta_2)}. \quad (2.15)$$

For models that incorporate memory, we simulated memoryless training data ($W_M = W_N$ for the memory-only model, and $W_{RM} = W_R$ for the resource-memory model) for $t < t^*$. As expected, these initial points are omitted from model fitting.

2.2.3.1 Model verification: simulated data

We simulated tracks on artificial landscapes with preset model parameters, then fit the model to these tracks to explore parameter estimability and model selection accuracy. We varied the length of these tracks, $T = t_{max} - t^*$, as well as K , the number of controls points per step, to evaluate the amount of data required for accurate inference. Specifically, we tested four "treatment groups": $T = 600, K = 10$; $T = 600, K = 50$; $T = 1200, K = 10$; and $T = 1200, K = 50$.

We used the R NLMR package (Sciaini et al., 2018) to simulate spatially autocorrelated Gaussian random fields representing our resource covariates. For each treatment group, we simulated 50 random movement tracks for each hypothesis. Each group of 50 tracks had the same set of parameters. In our simulations, we simulated environments for $P = 3$ resource covariates per track using the `nlm_gaussianfield` function in R. We then fit all four models to each track individually, then used BIC to identify how often the "correct" model was selected for each movement track. We compared these results with AIC to

confirm that BIC is the most suitable information criterion for our modelling framework. We also estimated the bias and mean squared error (MSE; the mean squared difference between the parameter estimate and the true value) for each parameter with each model.

2.2.3.2 Model application: grizzly bear case study

We applied the model to grizzly bears in the Canadian Arctic, and then repeated the simulation study with data and model parameters from this system. Bears were captured from 2003 to 2006 and released with global positioning system (GPS) collars. Collars returned a location every four hours while the bear was not hibernating, and remained on the bears for up to four years (Edwards et al., 2009). The University of Alberta Animal Care and Use Committee for Biosciences approved all animal capture and handling procedures, which were in accordance with the Canadian Council on Animal Care. Capture and tracking was conducted under permit from the Government of the Northwest Territories, Department of Environment and Natural Resources, Inuvik Office (Permit numbers: WL3104, WL3122, WL3282, WL5352, and WL5375) following methods approved by the University of Alberta Animal Care and Use Committee for Biosciences (Permit numbers: ACUC412305, ACUC412405, ACUC412505, ACUC412605, and ACUC412705) in accordance with the Canadian Council on Animal Care guidelines.

The bears were collared in the Mackenzie River Delta region in the Northwest Territories (Edwards et al., 2009). Resources in the region are sparse and heterogeneous both in space and time (Shevtsova et al., 1995; Edwards and Derocher, 2015). To survive and forage optimally, bears take advantage of ephemeral, unpredictable, or seasonally available resources through a variety of foraging strategies (Edwards et al., 2009, 2011; Edwards and Derocher, 2015).

We analyzed grizzly bear habitat selection using multiple sources of environ-

mental data describing the Mackenzie Delta region. Vegetation class data for the region assigned a one of 46 classes (indicating the dominant plant type or terrain) to each 30x30 m cell. A digital elevation model for the region (with 30x30 m cell resolution) provided information on elevation and slope. We also used an RSF layer estimating resource use for Arctic ground squirrels (*Urocitellus parryi*), a common grizzly bear prey item (Barker and Derocher, 2010; Edwards and Derocher, 2015). We considered $P = 6$ resource covariates: berry density, represented as a likelihood of having berries for each vegetation class; distance to turbid water, an indicator of broad whitefish (*Coregonus nasus*; a grizzly bear prey item; Barker and Derocher, 2009) density as well as riparian habitat; Arctic ground squirrel density, taken directly from the RSF; sweetvetch (*Hedysarum alpinum*; a key grizzly bear food item; Edwards and Derocher, 2015) density, estimated by the vegetation class data; distance to the nearest of two towns in the region; and distance to six remote industrial camps (likely with little human activity). We modelled these resources in two different ways, fitting the resource-only and resource-memory models twice to each bear with different interpretations: resources constant in time and resources that explicitly vary throughout the year. We expected that if the movement patterns we had observed were simply a result of the resource variation, as opposed to the bears memorizing the location and timing of these resources, then the resource-only model with seasonal resources would outperform any of our models including memory. We defined an interval of availability based on the literature (Macdonald et al., 1995; Buck and Barnes, 1999; Gau et al., 2002; MacHutchon and Wellwood, 2003), and assigned the value 0 to every point on the grid outside the time interval for that resource. The null and memory-only model, which do not incorporate resources, are unaffected by this change, but since we needed to generate new available points for the seasonally varying resources, the model

fits were slightly different for these models as well.

Of the 21 bears with enough data for model fitting (at least two years of GPS collar data), we selected the eight with the most GPS fixes (these bears had at least three years of collar data). We set $\rho_s = 30$ metres, corresponding to the length of one grid cell for the environmental raster data, and we set $t^* = 365$ days. We used $K = 50$ control points when fitting the models. For each of these bears, we fit the models to the entire track as well as each year individually, comparing model selection between years. We then replicated that analysis using simulated bear tracks; for each bear, we simulated 100 movement tracks using the optimal parameters for each bear and the Mackenzie Delta environmental data. We simulated tracks of length $T = 600$ (approximately one year of grizzly bear GPS data, accounting for missed fixes and hibernation) and $T = 1200$ to evaluate how model selection accuracy changed with sample size. We used BIC to identify the hypothesis that most accurately explained each movement track, and also conducted likelihood ratio tests for each pair of nested models to determine the significance of specific behavioural signals.

2.3 Results

Our modelling structure allows ecologists to explain movement patterns identified from location data according to a set of four hypotheses, of which two incorporate complex time-dependent spatial memory. For animals that appear to use memory, our parametric approach evaluates the temporal consistency of navigations to previously visited locations in an animal’s home range. By fitting the model to simulated data we showed that the accuracy of the model is improved by sample size, and ecologists can also increase parameter estimability by simulating additional control points. Still, the amount of data required to draw accurate inference from the model is not large, as we show both with

simulated environments and real-life landscape data (where the model is slightly less accurate).

2.3.1 Model verification: simulated data

The model's ability to accurately characterize each type of movement behaviour increased with the amount of location data (T) but not with the number of control points (K ; Table 2.2). The model identified null and resource-only movements accurately at all treatment levels, but the model's ability to identify memory-only and resource-memory movement increased for longer simulated tracks. As a whole, increasing K does not improve model selection accuracy for either choice of T . The most common misidentification at all sample sizes was mistaking resource-memory movement for resource-only or memory-only movement.

		$K = 10$				$K = 50$			
		N	R	M	RM	N	R	M	RM
$T = 600$	N	48	0	0	2	47	0	0	3
	R	0	45	0	5	0	46	0	4
	M	7	0	40	3	4	0	44	2
	RM	0	5	7	38	0	8	7	35
$T = 1200$	N	49	0	0	1	45	0	0	5
	R	0	46	0	4	0	47	0	3
	M	2	0	47	1	0	0	50	0
	RM	0	3	2	45	0	7	2	41

Table 2.2: Breakdown of model selection counts using BIC for the simulated tracks. The row represents the "true" model that the tracks were simulated from (N = null; R = resource-only; M = memory-only; RM = resource-memory), while the column represents the model that was identified as the most parsimonious explanation of the data using BIC. Treatment groups (based on T , the length of the fitted movement track, and K , the number of available points per timestep)

are identified by the outer left and upper portions of the table and are separated by shading.

Using AIC instead of BIC resulted in a higher rate of "false positives" for memory (i.e., the resource-memory or the memory-only model was identified as the most parsimonious explanation for memoryless simulated tracks), and made model selection less accurate overall (Table A.2). Likelihood ratio tests on the same dataset for each pair of nested models revealed a similar trend; the likelihood ratio test often identified memory when it was not incorporated into the simulated tracks (Table A.3).

The model produced more accurate parameter estimates with larger values of T and K (Table 2.3). When focusing on β_1 in the resource-memory model, we can see that bias does not change as much with different treatment groups as

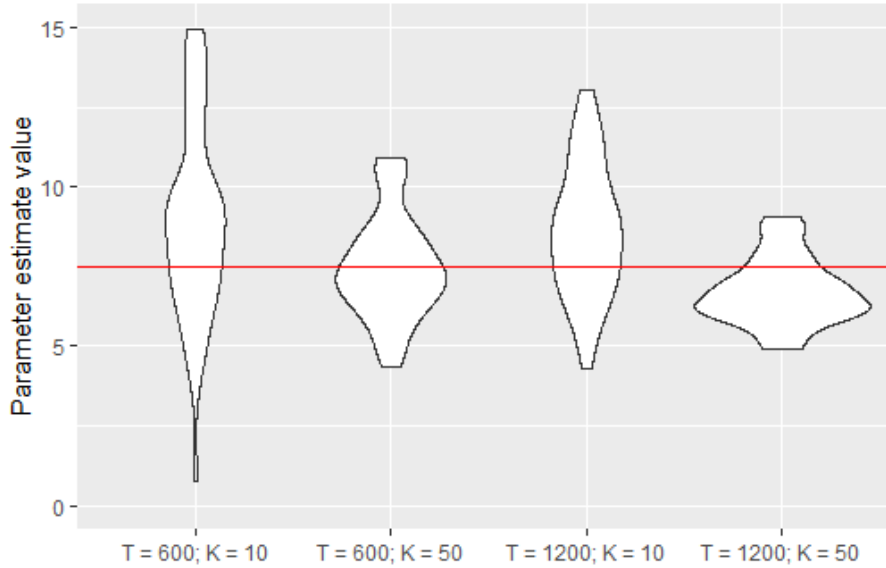


Figure 2.3: Violin plot of parameter estimates for β_1 in the resource-memory model for our four treatment groups (listed on the x-axis), with 50 simulations per plot. The true value of 7.5 is denoted by a horizontal red line.

MSE (Fig. 2.3). For the simpler movement parameters $(\rho_{ns}, \kappa, \lambda, \gamma)$, parameter estimates were consistent even with smaller values of T and K (Table 2.3).

2.3.2 Model application: grizzly bear case study

According to our modelling framework, five of the eight grizzly bears exhibited consistently timed revisitations to previously visited locations in their home ranges (Table 2.4). When the data were broken up into one-year increments, model selection results varied annually, and sometimes differed even from the full dataset. For three of the bears (GF1008, GF1016, GM1046), the model identified as most explanatory of the bears' movement behaviours by BIC was different for the full dataset, the first subset, and the second subset. The resource-memory model was the most parsimonious explanation of the movement patterns of four bears, while the resource-only (2), memory-only (1), and

	True value	$T = 600$ $K = 10$		$T = 1200$ $K = 10$		$T = 600$ $K = 50$		$T = 1200$ $K = 50$	
		Bias	MSE	Bias	MSE	Bias	MSE	Bias	MSE
ρ_{ns}	0.75	-0.17	0.03	-0.18	0.04	-0.14	0.03	-0.17	0.04
κ	0.75	-0.21	0.05	-0.21	0.05	-0.19	0.04	-0.19	0.04
β_0	0.50	0.06	0.12	0.04	0.12	0.13	0.11	0.18	0.12
β_1	7.5	1.3	10.1	1.6	13.4	0.0	2.6	-0.7	1.7
β_2	-7.5	-1.2	7.8	-1.1	5.5	0.2	3.8	0.5	1.5
β_3	0.0	-0.1	5.0	0.4	4.3	-0.1	2.5	0.0	1.7
β_d	0.999	-0.04	0.02	-0.04	0.02	-0.01	0.00	-0.03	0.02
μ	500	-8	795	-13	543	-22	7819	-25	7277
σ	25	2	341	-3	32	1	197	-1	217
α	-1.78	-0.45	2.64	-0.28	1.30	-0.14	1.81	-0.67	2.17
λ	0.85	-0.02	0.001	-0.02	0.001	-0.02	0.002	-0.03	0.001
γ	0.90	-0.03	0.001	-0.03	0.001	-0.03	0.001	-0.03	0.001

Table 2.3: Estimates of bias and MSE for each parameter in the resource-memory model, averaged from 50 simulated movement tracks per treatment group. True values for each parameter are displayed on the left.

null (1) models were also identified as most parsimonious in some cases. Four of the five memory-informed bears exhibited seasonal memory timescales close to one year ($\mu > 320$ days), while GF1016 had a μ value of 3 days. The six bears with resource selection included in their "best model" displayed similar resource selection patterns: significant selection for areas indicative of berries and Arctic ground squirrels, avoidance of areas indicative of sweetvetch, and indifference to towns and cabins. When we considered the resources to be explicitly seasonal, the memory-only model was most commonly the "best model" for the bears, with models including resources being much less common (Table 2.4).

Bear ID	Full data	First subset	Second subset	Seasonal resources
GF1004	RM (38.54)	N (1.11)	RM (1.15)	RM (3.50)
GF1008	RM (17.53)	R (39.78)	N (4.90)	M (21.34)
GF1016	M (5.99)	N (18.24)	R (1.84)	M (22.32)
GF1041	RM (45.74)	R (18.24)	RM (24.62)	N (4.29)
GF1086	R (49.35)	R (5.45)	RM (19.68)	R (16.78)
GF1107	R (33.63)	R (30.17)	RM (83.54)	M (15.25)
GF1130	N (12.87)	RM (73.82)	N (17.13)	RM (16.71)
GM1046	RM (40.32)	R (6.03)	M (10.06)	M (19.71)

Table 2.4: Model selection results for each bear in the Mackenzie Delta population. We list the hypothesis (N = null; R = resource-only; M = memory-only; RM = resource-memory) identified by BIC as most likely to be true given the data for the full dataset, the first subset, and the second subset. We also include results for the full dataset when resources were modelled as being explicitly seasonal. The numbers in parentheses are the difference in BIC between the best model and the second-best model.

Our simulation study revealed that at smaller sample sizes, the model occasionally failed to identify memory from memory-informed simulated tracks, but this issue is remedied with double the data. An example was GF1008, where only 10 of the 100 simulated tracks were correctly identified as "resource-memory" movements at $T = 600$. With $T = 1200$, this improved to 89. When we used likelihood ratio tests to compare the resource-memory model with the resource-only model (a special case of the resource-memory model) for GF1008, we found that at $T = 600$, 76 of our 100 simulated tracks registered a p-value below 0.05, indicating that the resource-memory model was significantly more explanatory than the resource-only model 76% of the time. With $T = 1200$, this increased to 95. We observed similar trends for the other three resource-memory bears (GF1004, GF1041, GM1046) but not as strongly. It should be noted that GF1008 had the smallest estimate for β_d (2.3) of these bears. When

we performed BIC model selection on simulated tracks based on GF1086, a "resource-only" bear, a false memory signal was identified more frequently with larger T (from 4 to 12 out of 100). This trend was not replicated for GF1107, the other "resource-only" bear (decrease from 10 to 7).

2.4 Discussion

Our model builds on existing literature to identify unique behavioural and cognitive mechanisms from animal movement data. Using advanced computational techniques, this novel and complex modelling framework can provide statistical inference for a variety of ecological systems. Our simulation studies provided insight on the viability of the model for different amounts of data.

We formulated a model that expresses parameters with clear biological implications to aid in the interpretation of our results, but we had to do so carefully to ensure that these parameters could be estimated accurately. Finding a set of biologically meaningful parameters with low mean squared error (Table 2.3) required a degree of trial and error, especially for β_0 and β_d . We chose to express them in a way that makes sense both biologically (where they represent relative probabilities) and mathematically (where they can easily be estimated with less error). While we can redefine these parameters without actually changing our likelihood function, we made sure to define parameters that are easy to estimate and biologically meaningful.

Our results provided support for a positive effect of the amount of location data and control points on parameter estimation, with the number of control points having a negligible effect on model selection accuracy. However, at all treatment groups, parameter estimates were occasionally inaccurate (Fig. 2.3, Table 2.3), and the model occasionally mistook the movement mechanisms driving the simulated tracks (Table 2.2). These outliers may be due to the stochastic-

ity of simulated movement tracks; for example, a resource-only simulated animal may happen to visit similar portions of its landscape at a coincidentally regular interval, which the model might mistake for memory-informed movement. Conversely, an animal following the "memory-only" rules may coincidentally visit locations that happen to be particularly high (or low) in specific resource values, resulting in the movement track being best explained by the resource-memory or even the resource-only model.

Increasing the number of observed animal locations (T) improved our results, but we are more encouraged by the positive effects of simulating additional control points (K). While increasing T may require such costly tasks as using longer-lasting tracking devices, re-capturing animals and equipping them with new tracking devices periodically, or increasing the temporal resolution of tracking devices, increasing K is easy to do post-hoc. While increasing K may not yield benefits as large as increasing T , the cost of increasing K is much smaller.

Our simulated tracks consistently underestimated ρ_{ns} and κ in the resource-only and resource-memory models (Table 2.3), which is an artifact of the way we simulated the data. In these models, the animal "chooses" a step from N_r proposed steps, which are simulated from k , which depends on ρ_{ns} and κ . Our simulated landscapes are spatially autocorrelated, so if the simulated animal found itself in a resource-rich patch, it would be very likely to stay put. These movements are also less directionally autocorrelated than would be suggested by κ for similar reasons. Using an integrated step selection function (Avgar et al., 2016) could remedy these issues but for our purposes, it adds additional complexity to the model and is not our primary concern.

Our estimates of bias and MSE for α did not consistently decrease with increases in the amount of location data or the number of control points, potentially because of an odd bimodal distribution of parameter estimates (Figure

A.1). The larger portion of this bimodal distribution is clearly centred around the true value of approximately -1.78 for all four treatment groups, but curiously the "second" mode, which appears to be centred around -4.5, seems to account for more of the estimates T and K increase. These smaller estimates for α would imply that the hypothetical organisms moving according to our simulation rules occasionally behave with a much wider understanding of their environment, which they perceive to be spatially heterogeneous. The exact cause of these patterns requires further investigation.

When we applied the analysis to field data, we notice that the model's effectiveness, especially when it comes to identifying a memory signal, increased greatly with sample size. Our simulations revealed that the model may miss a memory signal with inadequate data, which could explain the disparity between subsets of the data in Table 2.4. It must also be noted that, as stated in the Introduction, the goal of this model is not to determine whether or not grizzly bears have spatial memory; we are more interested in if they use that memory the way we have hypothesized. If the resource-only model is the "best model" for a bear, it may just mean that they are using memory in some other way. While it is possible that grizzly bears, especially females that take on different reproductive roles in different years, would change their movement strategies between years, it is also likely that the model may have not had enough data to identify a memory signal in an individual year. With twice data, the simulations accurately identified memory more often, suggesting that the memory signals identified for the entirety of each bear's track are legitimate. Nevertheless, even with these considerations, we see that half the bears in the dataset exhibited patterns following the resource-memory hypothesis, suggesting a strong influence of both habitat selection as well as spatial memory on the movement of grizzly bears in the Mackenzie Delta.

We occasionally observed "false positives" (the model identified memory as a driver of movement from memoryless simulated data) that increased in longer animal tracks ($K = 1200$ vs. $K = 600$) when simulating tracks with the grizzly bear data. This trend may be an artifact of how the Mackenzie Delta landscape data influenced simulated tracks, since false positives were much less frequent in the simulation study with artificial landscapes. When comparing this result with the real-life subsetting for the bears, we saw examples of subsetting data registering memory when the full data set did not, but we also saw examples of the opposite.

Our modelling framework operates under the assumption that resources vary in time, forcing animals to exhibit seasonal movement patterns within their home ranges. We handled this assumption in two different ways: by explicitly defining this temporal variation, and by indirectly incorporating it into the resource-memory and memory-only models. In this case, explicitly defining the seasonality of the grizzly bear resources made the memory-only model (which is primarily meant for situations when sufficient environmental data may not be available) much more effective. We suggest that making arbitrary assumptions about these timings may not always improve model parsimony, and instead may overshadow patterns and behaviours we are interested in. An alternative method to capture this variation would be to assume that μ is informative about how long resources take to re-appear, and as a result how long animals take to return to them.

Due to the novelty of this contribution, we accept that there will be opportunities to build on and improve the approach. Particularly interesting is the addition of more behavioural states to the model. We applied a hidden Markov component to the model mainly to avoid mistaking stationary periods for recursive movement on a short timescale, but adding many states (e.g., a

memoryless searching state and a memory-informed navigating state) could provide insight on the frequency of these movements. One such adjustment could involve changing the form of W_M and W_{RM} such that they are truly periodic; this could be done by changing φ from a traditional Gaussian to a wrapped Gaussian. Making this change would imply that animals are influenced to re-visit locations they visited $k\mu$ time steps ago for all positive integers k . Including such a mechanism would also potentially warrant the incorporation of explicit memory decay, which we omitted but could be useful when longer timescales or wrapped distributions are involved. Revising φ to a mixture of multiple Gaussians instead could also be used to test the hypothesis that animals perform recursive movements on different, asymmetrical scales. Modifying the formulation of the cognitive map Z (e.g., to something resembling a discrete-time analog of the territory interaction model from Potts and Lewis, 2016) could also be an opportunity to improve and tweak the model. Connections to the work of Potts and Lewis (2016) could also be made by incorporating territoriality or the presence of other individuals into the model somehow, potentially as a "resource" covariate. A final point for future work would be to redevelop this model from the perspective of integrated step selection analysis (iSSA; Avgar et al., 2016). Here, we could analyze how animal movement behaviour is directly influenced by covariates such as its distance from previously visited locations or the strength of its reliance on spatial memory.

While we used grizzly bears as a case study, the model was designed to be general and can be applied to a variety of different systems. Many animals, including turkey vultures (*Cathartes aura*; Holland et al., 2017), black vultures (*Coragyps atratus*; Holland et al., 2017), caribou (*Rangifer tarandus*; Lafontaine et al., 2017), and eastern indigo snakes (*Drymarchon couperi*; Bauder et al., 2016), perform seasonal movements within their home ranges. For data

with higher temporal resolution, it would be possible to model complex time-dependent recursive movements on a diel scale, since many animals exhibit repetitive day-to-day movements within their home range (Christiansen et al., 2016; Herbig and Szedlmayer, 2016). Collecting data at finer temporal resolutions would be beneficial for inference on memory-informed movement, assuming observation errors are accounted for. Even patrolling predators, which were modelled by Schlägel and Lewis (2014), could be modelled using our framework, although we may expect estimates for μ to be smaller than in the grizzly bears. Schlägel et al. (2017) displayed the importance of time since last visit for gray wolves, but insight on when exactly wolves deem parts of their home range "re-visitable" could be interesting. Of course, migration is also seasonal and predictable, and although it is typically difficult to obtain environmental data for an animal's entire migratory route, spatial memory has been identified as a key driver of migration in many instances (Mueller and Fagan, 2008; Mueller et al., 2011; Fagan et al., 2013; Bracis and Mueller, 2017; Merkle et al., 2019). Fitting this model to migratory populations could provide insights on how to quantify or potentially even predict these mechanisms.

2.5 Conclusions

Our model uses patterns in animal movement data to obtain information on complex time-dependent spatial memory patterns. Made possible by advanced computational techniques, we expand on existing literature from animal movement modelling as well as animal cognition to generate a model that can be applied to a variety of ecological systems. The model can estimate the timing of recursive movement patterns observed in an animal, which is novel, and also allows for the interaction of present-time resource selection and memory-informed navigation. We verify our model fitting process using simulated data

before testing its utility on GPS collar data from grizzly bears, finding that this very complex model can be effective without need for immense data collection. We hope to apply this model more broadly to animals with different foraging strategies as a means to compare the nature of time-dependent memory mechanisms in different ecological systems.

3 Time-dependent memory and individual variation in Arctic brown bears (*Ursus arctos*)

3.1 Introduction

Ecologists have used animal movement data to answer many important ecological questions in recent years (Nathan et al., 2008; Joo et al., 2020). Models have been developed to explore the qualities of an animal’s home range (Worton, 1989; Dahle and Swenson, 2003; Borger et al., 2008; Edwards et al., 2009), large-scale movements such as migration (Dingle and Drake, 2007; Merkle et al., 2019), and species-habitat relationships (i.e., habitat selection; Boyce and McDonald, 1999; Fortin et al., 2005; Thurfjell et al., 2014). Habitat selection analyses, in particular, have advanced due to the increasing availability of remote sensing data, which can describe large-scale environmental patterns, as well as animal movement data itself (Kays et al., 2015). These analyses provide solutions to difficult problems concerning how animals interact with their environment (Muhly et al., 2019; Suraci et al., 2019). Understanding these interactions, however, is limited without incorporating how animals perceive their environments cognitively (Fagan et al., 2017). This realization in movement ecology has inspired the growth of memory-informed movement modelling.

By including spatial memory, we can quantitatively model animal cognition using movement data. Animals use spatial memory to encode, store, and retrieve information about the location of landmarks in an animal’s environment (Fagan et al., 2013). Ecologists have included memory into habitat selection models by hypothesizing that animals will select for areas they have visited more frequently (Dalziel et al., 2008; Oliveira-Santos et al., 2016), assuming animals will select against areas they have just visited (Schlägel and Lewis, 2014), or modifying

habitat selection models such that animals will not be attracted to high-quality patches unless they can perceive this quality (van Moorter et al., 2009; Avgar et al., 2013). Most of these models lack attention to temporal memory, where animals remember not just where they have visited but how long ago they were there. While the "time since last visit" construct incorporated by Schlägel and Lewis (2014) is a noteworthy exception, they assumed patches become increasingly attractive to the animal as time passes, which is not realistic in seasonally variable environments. For animals with seasonally varying home ranges, the energetic value of visiting a food patch may vary periodically or seasonally. Animals that live in such environments may change the size and shape of their home range seasonally, implying that they only visit specific parts of their home range at specific times of year (Wiktander et al., 2001). On a smaller timescale, spatiotemporal memory allows animals to capitalize on ripe fruit, which loses its energetic return if visited too late (Janmaat et al., 2016). Despite the occurrence of such patterns, which may be either ephemeral or seasonal, animal movement models rarely incorporate a time-dependent spatial memory mechanism that accounts for them.

The brown bear (*Ursus arctos*) is a widespread, omnivorous mammal found in the Northern Hemisphere (Pasitschniak-Arts, 1993), and populations in seasonal regions of the species' range are likely to benefit from remembering the timing of food resources. The Canadian Arctic is an example of such an environment, and brown bears that live here are especially opportunistic, taking advantage of a wide variety of food resources (Edwards and Derocher, 2015). Most brown bear food resources here are only available for a fraction of the bears' active season (Nagy and Haroldson, 1990; Burn and Kokelj, 2009; Edwards and Derocher, 2015), resulting in seasonal variation in their habitat selection (McLoughlin et al., 2002). Brown bears in the Arctic also display individual

dietary variation due to sexual size dimorphism as well as the reproductive constraints of adult females (Edwards et al., 2011). Theoretical studies have displayed the utility of memory-informed movement in environments with predictable temporal variation (Mueller et al., 2011). Evidence of memory-informed movement in other brown bear populations includes oriented movement towards previously visited kill sites (Selva et al., 2017), scent marking to identify territorial boundaries (Clapham et al., 2012), fidelity to the same salmon-rich stream each year (Wirsing et al., 2018), and repeated use of the same denning area each year (Manchi and Swenson, 2005; Sorum et al., 2019). These studies demonstrate the cognitive and perceptual capabilities of the species, suggesting that brown bears in the Canadian Arctic may incorporate time-dependent spatial memory into their movement patterns.

We applied a new animal movement model that incorporates a unique form of complex, time-dependent spatial memory to global positioning system (GPS) data for brown bears from the Mackenzie Delta region of the Canadian Arctic. Chapter 2 describes a model with four special cases, each concerning its own hypothesis about cognition and movement: a null hypothesis; a resource-only hypothesis assuming simple resource selection; a memory-only hypothesis assuming resource-less seasonal revisitation patterns within an animal's home range; and a resource-memory hypothesis assuming animals are simultaneously influenced by local resources and spatial memory. Fitting each of these four models to animal location data provides inference on the likelihood of each hypothesis being true, and the parameters in each model describe explicit components of the animal's foraging behaviour. We obtained parameter estimates and performed model selection analysis for 21 individual bears, allowing us to explicitly examine variation at the individual level. We found that amid high individual variation within the population, movement patterns from a majority

of the bears supported the resource-memory hypothesis. These results represent the first application of a novel model to a population of opportunistic and potentially sensitive omnivores.

3.2 Materials and Methods

We applied the model described in Chapter 2 to global positioning system (GPS) location data from a population of brown bears in the Canadian Arctic. We used the model to test four alternate hypotheses stated above about animal movement and cognition (Figure 3.1). We drew inference from maximum likelihood estimates for the model parameters to quantify characteristics of the bears' behaviour (Table 2.1). We describe the biological function of the model here, noting that it is described in full detail in Chapter 2.

3.2.1 Study area

The Mackenzie River empties into the Arctic Ocean in the northern Northwest Territories, in NW Canada. Our study area, the Mackenzie Delta region, spans 23,000 km² of wet Arctic tundra, interspersed with many lakes and smaller streams (Edwards et al., 2013). The Mackenzie Delta region is a harsh environment for brown bears, with minimal food availability that results in short active seasons (Ferguson and McLoughlin, 2000). There are two human settlements in the region, Inuvik and Tuktoyaktuk, in addition to some remote and rarely inhabited industrial camps.

Our landscape data provide information on the spatial heterogeneity in vegetation and topography. We used three 30 x 30 m raster layers to describe the study area: a digital elevation model (DEM) measuring elevation (ranging from 0 m to 1676 m), a vegetation class raster describing dominant vegetation in each portion of the landscape, and a raster approximating the density of Arctic

ground squirrels (*Urocitellus parryii*), which are a common brown bear prey species (MacHutchon and Wellwood, 2003; Barker et al., 2015). The vegetation class raster classified each 30 x 30 m grid cell into one of 46 vegetation classes, describing the age, size, and/or dominant plant species present in each area (Ducks Unlimited, 2002; but also see Appendix B). The ground squirrel raster is a product of a resource selection function from an existing study, so it quantifies the likelihood (based on environmental conditions) for any spatial region to support ground squirrels (Barker and Derocher, 2010).

We manipulated our landscape data to produce six resource covariates. Berries (including but not limited to *Empetrum nigrum*, *Shepherdia canadensis*, *Vaccinium uliginosum*, and *V. vitis-idaea*) are an important dietary item for most individuals (Edwards et al., 2011; Edwards and Derocher, 2015). In the Canadian Arctic, berries are generally found in dwarf shrub areas (Porsild and Cody, 1980; Shevtsova et al., 1995; Norment and Fuller, 1997), but they can also occur beneath the canopy of northern woodlands (Murray et al., 2005). We do not have an explicit berry density survey, so we used the vegetation class data along with knowledge of common berry species to infer the probability of berries occurring at each spatial grid cell (Table B.1).

We included a covariate representing the Euclidean distance from turbid water to gauge the extent to which brown bears select for riparian areas. These regions support food resources such as horsetails (*Equisetum* spp.) and wetland sedges (*Carex* spp.) that are important in the early summer (Edwards and Derocher, 2015). Brown bears in the Mackenzie Delta region also fish broad whitefish (*Coregonus nasus*) beside streams and rivers when the fish migrate (Barker and Derocher, 2009).

We also included covariates representing the possible presence of Arctic ground squirrels and alpine sweetvetch (*Hedysarum alpinum*), two common di-

etary resources in the area (Edwards and Derocher, 2015). We used the ground squirrel RSF from Barker and Derocher (2010) as a covariate for squirrel selection. Sweetvetch occurs in dry, shrubby uplands (Porsild and Cody, 1980), so we used an interaction between slope (from our DEM) and dwarf shrub vegetation classes to quantify sweetvetch density.

Brown bears are affected by the presence of humans in many ways (Mace et al., 1996; Steyaert et al., 2016; Lamb et al., 2017), so we included covariates measuring the Euclidean distance from various human settlements or dwellings. The first covariate measured the distance from the nearest human settlement in the Mackenzie Delta region (either Inuvik or Tuktoyaktuk). Brown bears that come near human settlements are often deterred by the residents or wildlife officials in a forceful manner (Kellert et al., 1996), so we expected bears whose home ranges overlap one of the settlements to avoid them. Some more remote industrial buildings are occasionally inhabited but often lack the constant human presence brown bears face near Inuvik or Tuktoyaktuk. As opportunistic omnivores, brown bears commonly use anthropogenic food sources (Kavčič et al., 2015) and may visit these buildings. Our second anthropogenic covariate measured the Euclidean distance from the closest of the 6 cabins in the region.

3.2.2 Brown bear data

Between 2003, and 2006, 31 brown bears (24 female, 7 male) were captured and equipped with GPS collars (Telconics Inc., Mesa, AZ, USA) that provided the bear’s spatial location every four hours. The collars used long temporal sequences without movement to identify denning periods, and did not record any signals until the bear began to move again in the spring. The collars were removed and/or stopped recording bear locations after one to four years. The University of Alberta Animal Care and Use Committee for Biosciences approved all animal capture and handling procedures, which were in accordance with the

Canadian Council on Animal Care. Capture was conducted under permit from the Government of the Northwest Territories. A subset of these data were analyzed in Chapter 2 as a preliminary analysis of the model.

3.2.3 Model design

We fit a discrete-time hidden Markov model (HMM) that assesses the nature of complex time-dependent spatial memory mechanisms in Arctic brown bears. The model has two movement states: one representing resting or not moving (stationary), and one representing movement (non-stationary). In a HMM, the state is not explicitly known but can be inferred from observed data (e.g., if consecutive GPS locations are only 1 m apart, we can infer that the bear is likely in the stationary state), which is mathematically expressed with conditional likelihood functions (Jonsen et al., 2013). Like other HMMs, the bear’s movement state at any point in time depends only on the previous state as well as fixed state-switching probabilities: λ and γ (Table 2.1). The conditional likelihood functions for the non-stationary and stationary states can be found in Equations 2.5 and 2.3, respectively. See Section 2.2.1 for more modelling details.

3.2.3.1 Null model

In the null model, we assume that the bear moves randomly, so the only parameters of concern are those dictating movement speed (ρ_{ns}), directionality (κ), and state-switching (λ and γ ; Table 2.1). If the 95% confidence interval for κ excludes 0, we can conclude that there exists significant directional autocorrelation in the bear’s movements. The weighting function $W_N(x_t|Z_{t-1}, \Theta_{2,N}) = 1$ for all x_t in space.

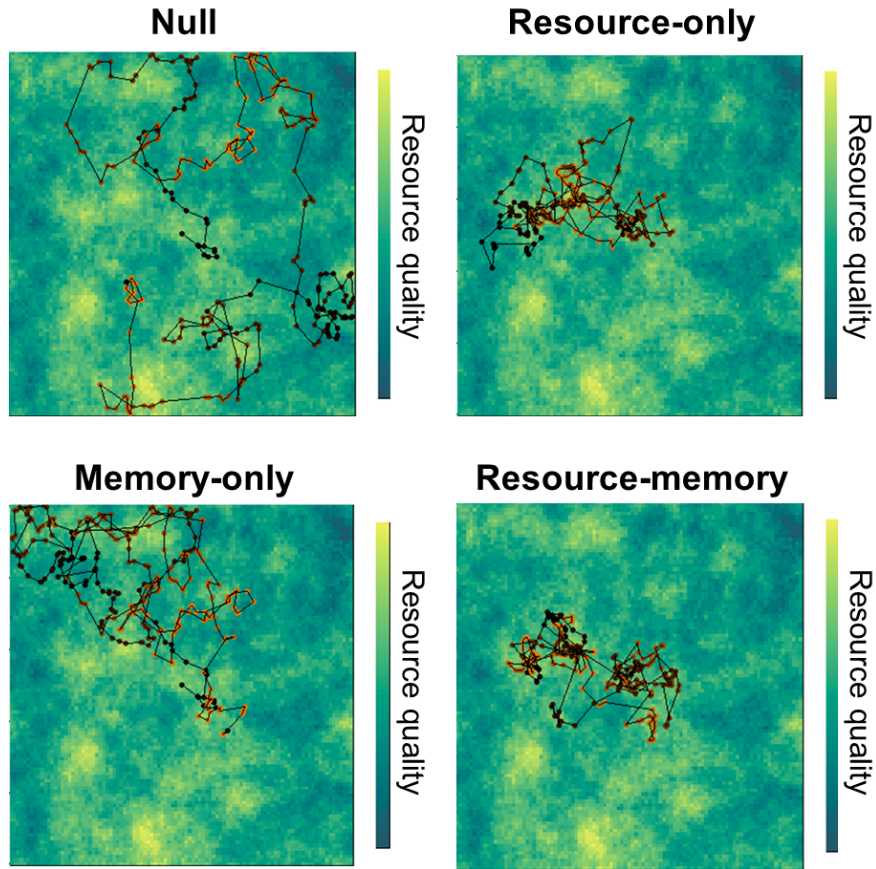


Figure 3.1: Simulated animal movement tracks (300 steps per track) on a randomly generated landscape displaying behaviours consistent with each hypothesis (and model). The colour of each point on this simulated movement track represents the hypothetical time in the animal's memory "cycle", which is here set to 100 time units (points at $t = 75$ have the same colour as $t = 175$). The null model implies completely random movement, while the resource-only model implies that the animal will locate nearby resources and select for those areas. The memory-only model implies that the animal relocates itself to areas it visited 100 time units before. The resource-memory model combines mechanisms in the resource-only and memory-only models.

3.2.3.2 Resource-only model

The resource-only model tests the hypothesis that bears select for nearby locations with high habitat quality. We define W_R in Chapter 2 (Equation 2.8). If the 95% confidence interval for any of these parameters excludes 0, we can conclude that the animal significantly selected for (or against) that variable.

To ensure that the seasonal revisitation patterns we observed were a result of spatial memory, we tested an alternate version of the model where resource covariates were restricted to seasons of availability. In the original versions of the resource-only and resource-memory model, each resource covariate $r_i(x)$ retains the same value throughout the year. This follows the assumption that our covariates measure the habitat conditions necessary to support seasonally available resources, not the resources themselves. For example, $r_2(x)$, the distance from x to the nearest riparian area, does not change seasonally, but the likelihood of obtaining valuable food resources from that region does vary seasonally. That being said, identifying memory based solely on movement patterns requires rigorously eliminating any other mechanisms that could cause those patterns (Fagan et al., 2013), so we designed an alternate model where resources were explicitly seasonal.

We identified temporal intervals in which each resource would be treated as present on the landscape, and assumed that $r_i(x)$ would be equal to 0 outside of these intervals. Berries are available in smaller portions year-round (Edwards and Derocher, 2015), but the primary period of occurrence lasts from approximately August 1 until the end of the active season, which we considered to be November 30, when bears had entered dens and GPS collars turned off (Gau et al., 2002; MacHutchon and Wellwood, 2003). The food available in riparian habitats (including whitefish, which generally migrate in early October; Barker and Derocher, 2009) is most prominent from May 10 to October 16 (Macdonald

et al., 1995) when the ice has melted from the Mackenzie River. Arctic ground squirrels are always present, but they are easier for brown bears to hunt when they are hibernating (Barker et al., 2015), so we used an interval from September 11 to November 30 to approximate when most squirrels would be dormant (Buck and Barnes, 1999). Sweetvetch is also available year-round, but provides the highest nutritional return in the early spring, so we used an interval from April 1 (the beginning of the active season) to June 15 (MacHutchon and Wellwood, 2003). We left r_5 and r_6 , the covariates relating to presence of humans, temporally constant.

3.2.3.3 Memory-only model

The memory-only model quantifies the hypothesis that brown bears remember the spatial location of areas they have visited previously, with the intent to return there after a consistently scheduled time lag. The cognitive map associated with this model builds on the idea of time since last visit proposed by Schlägel and Lewis (2014), where previously visited locations become increasingly more attractive to the animal as time increases. We model this structure with a discrete-space cognitive map Z_t where the animal keeps track of all its previous locations (Figure 2.2). The weighting function for the memory-only model W_M incorporates this cognitive map structure through Equation 2.9.

The memory-only model follows the hypothesis that there is some "peak" in attractiveness that represents the periodicity of habitat quality in the environment (see μ and σ in Table 2.1). Higher values of σ indicate that bears are less precise in their revisitation patterns, and may also be indicative of lower temporal predictability in the environment. Each distance is transformed using an exponential decay function with parameter α (Table 2.1). As α decreases, the mathematical difference between a step 1 km away and a step 2 km away is amplified, suggesting that the animal understands these differences in space

on a wider scale. We propose $\log_{10}(\rho_{ns})$ as an important cutoff point for this parameter, as the decay term for these distances is equal to ρ_{ns} , the animal's mean step length (Equation 2.9). The memory-only model includes one last parameter β_d ($\tilde{\beta}_d = \log(\frac{\beta_d}{1-\beta_d})$), representing the probability of moving in a way that incorporates Z , relative to moving randomly or selecting for present-time resources. As β_d approaches 1, the animal will approach oriented movement towards previously visited locations, and if the 95% confidence interval for this parameter excludes 0.5, we can conclude that the animal is displaying significant selection for memorized areas.

3.2.3.4 Resource-memory model

The resource-memory model combines the principles of the resource-only and memory-only models. Bears moving according to this model consider present-time resources in nearby locations as well as previously visited locations. We additionally hypothesize that bears will only be attracted to previously visited locations that had food, and will not revisit previously visited locations with low resource quality. This mechanism is mediated by "threshold" parameter β_0 , which approximates the probability of returning to a previously visited location (Table 2.1). We can infer about the habitat quality necessary to influence revisitations from a bear if the 95% confidence interval for β_0 overlaps 0.5, which would imply no selection for these areas. The weighting function for the resource-memory model includes two terms, one representing present-time resource selection and one representing memorized information (Equation 2.10).

3.2.4 Fitting the model to data

We used maximum likelihood estimation to fit the four models to each individual, comparing each model using the Bayesian Information Criterion (BIC). In Chapter 2, we found that BIC was more accurate than AIC in terms of se-

lecting the most parsimonious model for simulated data, suggesting that BIC makes more sense for this modelling framework. A difference in information criteria greater than 2 between the best and second-best models indicates greater support for the best model (Burnham and Anderson, 2004). We used maximum likelihood estimates (MLEs) along with 95% confidence intervals for each parameter in the best model to obtain further information on the bears' movement behaviours. We removed the first year of GPS data from model fitting for every bear because we could not determine enough about the bear's previous movement experience to identify memory. We refer to this first year as "training data", and removed bears with only one year of GPS data from the analysis. The models are computationally complex, so we used advanced automatic differentiation techniques to obtain MLEs (Albertsen et al., 2015; Kristensen et al., 2016; Whoriskey et al., 2017) and likelihood profiling to obtain confidence intervals (Fischer and Lewis, 2021). See Section 2.2.2 for additional details on model fitting.

We fit all four models to each bear under the assumption of temporally constant resources, then fit the resource-only and resource-memory models with the explicit inclusion of seasonal resource variation. Resources are not included in the null or memory-only models so they are mathematically equal in both cases.

3.3 Results

Of the 31 bears for which we had GPS data, 21 (18 females, 3 males) bears had enough data (at least one year excluding the first year of training) for model fitting. We fit all four models to each bear and used BIC to identify which associated hypothesis was most heavily supported by the data. Once we identified the best model for each bear, we calculated MLEs and 95% confidence

intervals for all parameters in that model. We found that despite a large degree of individual variation, bears generally exhibited movement informed by resources as well as memory, with a revisitation scale close to 365 days. We also confirmed that memory, not the seasonality of resources, was the primary mechanism causing brown bears to return to previously visited food patches in a periodic fashion.

3.3.1 Model selection

The Mackenzie Delta brown bear population displayed a variety of movement behaviours, although the resource-memory model was most frequently selected as the most parsimonious explanation of the bears' movement patterns (Table 3.1). It was identified as the "best model" (using BIC) for 9 of the 21 bears. The resource-only and memory-only models also received some support within the population; these models were the best model for 5 and 4 bears, respectively. For 3 of 21 bears, the null model was the most parsimonious explanation of bear movement patterns. There were only two cases where the difference in BIC between the two best models was < 2 (Table 3.1).

Bear ID	Null	Resource-only	Memory-only	Resource-memory
GF1004	70.8	51.7	76.3	0.0
GM1046	148.3	42.3	98.9	0.0
GF1008	49.2	0.0	19.1	33.2
GF1086	99.1	19.4	100.6	0.0
GF1016	22.3	11.8	0.0	30.5
GF1041	100.9	0.0	109.6	34.3
GF1107	228.7	0.0	237.9	2.4
GF1130	0.0	28.4	18.6	42.6
GF1005	65.3	0.0	52.0	16.5
GF1096	60.9	0.8	58.5	0.0
GF1167	16.6	21.0	0.0	4.8
GF1079	121.6	5.0	123.1	0.0
GF1089	8.0	16.1	0.0	20.2
GF1141	0.3	24.3	0.0	24.9
GM1133	85.2	85.5	0.0	4.4
GF1087	32.6	43.2	8.0	0.0
GF1108	0.0	9.4	0.1	15.6
GF1143	19.5	10.2	12.3	0.0
GM1147	1041.4	1021.3	0.0	960.1
GF1092	39.4	9.1	30.5	0.0
GF1146	2.0	19.6	0.0	7.8

Table 3.1: dBIC (difference in BIC from the "best model") values for each model and bear, with resource covariates set to be temporally constant. Cells shaded gray represent the model that best explains the movement patterns of each bear (dBIC = 0), and cells shaded light gray represent models < 2 BIC above the best model. Bears are sorted in descending order by number of data points (i.e., bears with more data at the top of the table).

3.3.1.1 Seasonal resource modelling

When we revised our resource covariates by adding time dependence, the memory-only model was a much more parsimonious explanation of the data (Table 3.2). It was the "best model" for 14 of the 21 bears when resource covariates were restricted to our prescribed seasons. The resource-only model was the best model for three bears, and the null and resource-memory model were the best for two bears each. There were three cases where the difference in BIC between the best model and the other models was < 2 (Table 3.2).

Bear ID	Null	Resource-only	Memory-only	Resource-memory
GF1004	3.5	11.4	9.0	0.0
GM1046	49.4	43.0	0.0	19.7
GF1008	30.1	51.8	0.0	21.3
GF1086	39.8	0.0	41.3	16.8
GF1016	22.3	41.3	0.0	33.4
GF1041	0.0	4.3	8.7	23.5
GF1107	17.1	25.2	0.0	15.2
GF1130	16.7	41.4	30.9	0.0
GF1005	14.9	41.9	0.0	33.8
GF1096	2.4	16.8	0.0	27.9
GF1167	16.6	28.4	0.0	47.6
GF1079	39.1	0.0	40.6	17.7
GF1089	9.4	0.0	1.3	1.9
GF1141	0.3	29.2	0.0	38.3
GM1133	85.2	90.2	0.0	106.3
GF1087	24.6	43.8	0.0	25.9
GF1108	0.0	31.5	0.1	36.6
GF1143	7.2	30.9	0.0	26.8
GM1147	1041.4	977.4	0.0	953.8
GF1092	8.9	34.5	0.0	32.9
GF1146	2.0	57.2	0.0	22.9

Table 3.2: dBIC (difference in BIC from the "best model") values for each model and bear, with resource covariates set to be temporally variable. Cells shaded gray represent the model that best explains the movement patterns of each bear (dBIC = 0), and cells shaded light gray represent models < 2 BIC above the best model. Bears are sorted in descending order by number of data points (i.e., bears with more data at the top of the table).

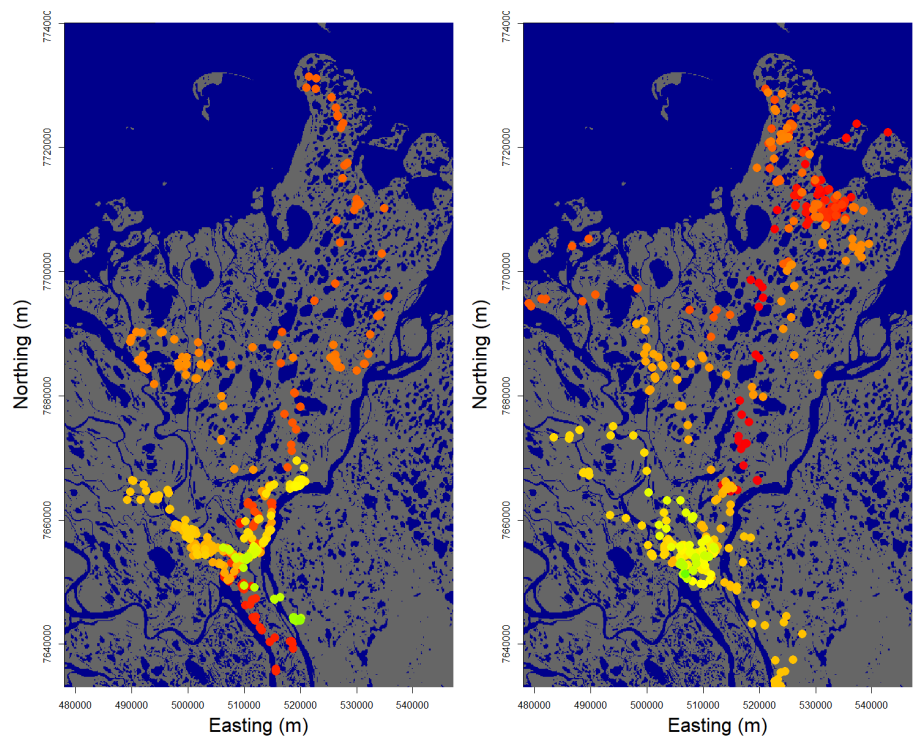


Figure 3.2: Movement track for bear ID GM1046 for the years 2004 (left) and 2005 (right). Each point on the animal's track is coloured according to the day of the year. Note the extended visitation of the southern part of the bear's home range in 2003, followed by a directed navigation towards that same area at the same time in 2004. The movement patterns of GM1046 were best explained by the resource-memory model (Table 3.1).

3.3.2 Parameter estimation

Most of the results below concern the "traditional" model, where we did not explicitly set the seasonality for the resource parameters. See Table B.3 for parameter estimates when resources were explicitly seasonal.

3.3.2.1 Movement parameters

Brown bears varied in their movement speed and directional autocorrelation (Table 3.3). Mean movement speed in the non-stationary state (ρ_{ns}) varied from 0.22 (GF1086) to 0.65 (GF1005) km/h. Parameter estimates for κ varied from 0 (GF1092) to 0.7306 (GF1143), and 19 of the 21 bears exhibited some significant directional autocorrelation (i.e., the 95% confidence interval for κ excluded 0).

Every bear spent more time in the non-stationary state than the stationary state, with estimates for λ (the probability of remaining in the stationary state given the bear was already in it; Table 2.1) being significantly lower than γ . The 95% confidence intervals for γ , the probability of remaining in the non-stationary state, were entirely above 0.5 for every member of the Mackenzie Delta population, implying that all bears were significantly more likely to stay in the non-stationary state than leave it at any given time. Conversely, 10 of the 21 bears had 95% confidence intervals for λ that were entirely below 0.5, and only two bears (GF1016 and GF1041) had a confidence interval for λ that was entirely above 0.5. Dividing λ and γ each by $\lambda + \gamma$ estimates the percentage of time each bear spent in the stationary and non-stationary states, respectively, and we found that most bears spent between 30 and 40% of their time in the stationary state.

3.3.2.2 Resource selection parameters

Of the 21 bears in the population, 12 (8 resource-memory + 4 resource-only) had resource selection in their "best model". Some resource covariates displayed more within-population variation than others (Table 3.3). Only one (GF1143) of the 12 bears did not display significant selection for areas likely to contain berries (i.e., the 95% confidence interval for β_1 was entirely above 0). The parameter estimate for GF1143 was positive but the lower confidence bound for β_1 overlapped 0 (Table B.2a). 6 of the 12 bears selected for areas closer to turbid water, suggesting attraction to riparian areas. None of the bears selected against this covariate. 11 of the 12 bears selected for areas indicative of high Arctic ground squirrel density, with GF1087 displaying neutral selection for this covariate. Curiously, parameter estimates for β_4 , the selection coefficient for sweetvetch habitat, were negative for all 12 "resource-informed" bears. 8 of the 12 bears displayed significant selection against these areas. Bears generally displayed minimal responses to anthropogenic dwellings in the region. Only one (GF1087) bear displayed any significant pattern in relation to human settlements (selecting closer to them), and only three displayed such behaviours with respect to industrial cabins (GF1087 avoided them while GF1008 and GF1086 selected for areas closer to them).

3.3.2.3 Memory parameters

15 of the 21 bears had memory incorporated in their "best model", and most of these "memory-informed bears" returned to previously visited locations between 300 and 365 days after their last visit (Table 3.3). These trends were similar when resources were explicitly assumed to be seasonal (Table B.3), where the memory-only model provided the best explanation of most of the bears' movements. Estimates of β_d were often close to 1, suggesting that memory played a

part in movement for all of the memory-informed bears. 9 of the 15 bears had estimates for μ that were close to one year (>10 months or 300 days), implying that the majority of the population used a revisitation schedule of approximately one year. The median estimate value for σ was 8.2 days. For 8 of the 15 bears, the confidence interval for σ excluded 3 days (the lower optimization bound for σ ; see Chapter 2 for more information), implying significant variation in the bears' revisitation schedules. Estimates for α also varied between bears, ranging from -2.91 (GF1086) to 0.11 (GF1016). Based on the confidence intervals for this parameter, we found that 4 (GF1079, GF1086, GF1087, GM1147) of the 15 bears exhibited significantly heterogeneous perception of their landscapes, while 3 (GF1016, GF1089, GF1096) exhibited the opposite.

Of the 8 bears whose movements were best explained by the resource-memory model, 5 displayed especially selective revisitations to locations along their track (based on whether the 95% confidence interval for β_0 was below 0.5). There was some individual variation in the estimates for β_0 themselves, ranging from approximately 0 (GF1079) to approximately 1 (GF1096) (Table 3.3). However, the confidence interval for β_0 was large for the latter. Figure 3.2 depicts an example of one of these 9 bears, GM1046, highlighted by clear navigations to previously visited locations approximately a year later.

3.4 Discussion

We used brown bear movement data from the Mackenzie Delta region to analyze the viability of a new model for an opportunistic omnivore living in a harsh and seasonal environment. This model incorporates a complex time-dependent spatial memory mechanism that allowed us to identify how long brown bears wait before returning to previously visited locations. We found a great deal of variation between individual bears, but this did not hinder our ability to observe

ID	Model	ρ_{ns}	κ	β_1	β_2	β_3	β_4	β_5	β_6	β_0	β_d	μ	σ	λ	γ	α
GF1004	RM	0.382	0.502	0.182	0.240	1.270	-0.008	0.017	-0.034	0.1764	~1	353.6	10.9	0.509	0.759	-0.015
GM1046	RM	0.427	0.517	0.477	-0.797	1.310	-0.015	0.049	-0.010	0.3412	~1	358.4	11.8	0.391	0.772	-0.100
GF1008	R	0.443	0.525	0.173	-0.440	2.049	-0.027	-0.056	-0.082	N/A	0	N/A	N/A	0.527	0.852	N/A
GF1086	RM	0.219	0.229	0.405	-0.897	3.855	-0.102	0.095	-0.203	0.0006	~1	0.8	3.0	0.404	0.770	-2.910
GF1016	M	0.301	0.220	0	0	0	0	0	0	0.7311	0.9783	3.0	3.0	0.601	0.758	0.112
GF1041	R	0.404	0.575	0.236	-0.885	3.177	-0.017	-0.109	-0.102	N/A	0	N/A	N/A	0.399	0.785	N/A
GF1107	R	0.256	0.259	0.338	0.049	2.848	-0.009	-0.092	-0.020	N/A	0	N/A	N/A	0.452	0.751	N/A
GF1130	N	0.429	0.528	0	0	0	0	0	0	N/A	0	N/A	N/A	0.487	0.767	N/A
GF1005	R	0.653	0.332	0.245	-0.240	4.646	-0.032	-0.085	-0.067	N/A	0	N/A	N/A	0.472	0.758	N/A
GF1096	RM	0.399	0.401	0.306	-1.400	2.793	-0.020	-0.040	-0.092	~1	0.5010	350.7	26.6	0.406	0.794	-0.079
GF1167	M	0.463	0.574	0	0	0	0	0	0	0.7311	~1	364.8	6.3	0.387	0.761	-0.126
GF1079	RM	0.377	0.731	0.259	-1.737	3.603	-0.002	0.029	-0.054	~0	0.7604	0.8	3.0	0.171	0.786	-1.729
GF1089	M	0.297	0.186	0	0	0	0	0	0	0.7311	0.9852	2.6	3.0	0.377	0.739	0.068
GF1141	M	0.419	0.270	0	0	0	0	0	0	0.7311	~1	365.0	11.9	0.606	0.754	-0.023
GM1133	M	0.374	0.080	0	0	0	0	0	0	0.7311	~1	54.5	26.7	0.595	0.768	-0.212
GF1087	RM	0.399	0.296	1.205	-0.536	-2.837	-5.431	-0.467	0.743	0.9996	~1	356.0	8.2	0.393	0.742	-0.728
GF1108	N	0.376	0.211	0	0	0	0	0	0	N/A	0	N/A	N/A	0.273	0.880	N/A
GF1143	RM	0.387	0.722	0.147	-0.742	4.983	-0.035	0.037	-0.027	0.1159	0.9997	352.2	14.5	0.179	0.848	-0.119
GM1147	M	0.556	0.115	0	0	0	0	0	0	0.7311	~1	260.9	3.0	0.204	0.742	-0.477
GF1092	RM	0.296	0.000	0.512	1.259	2.934	-0.054	0.125	0.161	0.8500	~1	361.9	42.0	0.463	0.708	0.106
GF1146	M	0.411	0.549	0	0	0	0	0	0	0.7311	0.9998	350.0	3.0	0.286	0.819	-0.162

Table 3.3: Parameter estimates for the "best model" (as identified by BIC) for each bear. Bears are listed in ascending order by number of GPS fixes. Note that the second letter of the bear ID indicates the sex of the individual. Gray text in the table indicates a parameter value that was fixed and not estimated for that model, and gray "N/A" values indicate parameters that are not influential in the "best model" for that bear. Parameter estimates for β_0 and β_d that are very close to but not exactly 0 or 1 are indicated as such with a "~". See Tables S2a and S2b for 95% confidence intervals for each bear and each parameter.

population-level trends in the bears' movement patterns. We also showed that representing resources as temporally constant was more effective in explaining the movement patterns of the brown bears than explicitly defining seasons for these resources.

The most common pattern observed in the population was a 365-day "circannual memory", implying that many bears returned to portions of their home range that they visited roughly a year before (Figure 3.2). While the model does account for bears potentially avoiding previously visited areas through β_0 , this behaviour was seldom observed in our population. Previous work on this population identified a pattern of annual home range shift for Mackenzie Delta brown bears (Edwards et al., 2009). Potentially, brown bears maintain fidelity to portions of their home range, visiting those portions of the environment at the same time each year, and displaying less annual fidelity to other portions of their home range. Our GPS data display the bears' movements as discrete-time "steps", but recent modelling advances have allowed for continuous-time modelling of animal location data (Wang et al., 2019). With more data, it may be more feasible to estimate these "steps" more explicitly and incorporate them into Z , the animal's cognitive map.

Some of the resource selection patterns observed in the "resource-informed" subset of the bear population could be explained by the nature of our landscape data. The lack of response to areas suggestive of sweetvetch presence was surprising, as almost every bear in the population displayed significant avoidance from such habitats. We based our estimate of sweetvetch presence on Porsild and Cody (1980), but other citations (e.g., Aiken et al. (2007)) indicate that they may appear closer to bodies of water, in sandy areas, or even in tundra (in fact, this could explain selection for areas closer to turbid water bodies such as rivers and coastlines).

Most bears did not display selection for or against anthropogenic structures, and when they did, the resulting behaviour was not always what we predicted. Bears are typically most affected by human presence when they have had a previous negative encounter with humans (Hertel et al., 2019), suggesting that this lack of significant selection could be explained by a lack of human-bear encounters. Many of the bears did not even go near Inuvik or Tuktoyaktuk while they were collared, suggesting a lack of encounters with humans.

When we adjusted our resource covariates such that they were explicitly assumed to only appear during a prescribed temporal interval, we found that the resource-only and resource-memory models were a significantly worse explanation of brown bear movement patterns. In fact, the number of bears that had resource selection included in their "best model" decreased from 12 with temporally constant resources to only 5 with explicitly seasonal resources. When resources were seasonally bounded, the memory-only model was much more effective than it was when resources were temporally constant. Recalling that the memory-only model is constructed independently of resources, this yields a clear ordering in the effectiveness of each model type for the entire population: resource-memory with constant resources > memory-only > resource-only with seasonal resources. We do not dispute that these resources are indeed seasonal, but instead suggest that the landscape data we included in the model represent more than just the seasonal resources we included them for. For example, it may be possible that brown bears select for (and remember the location of) shrubby, berry-rich habitats outside of berry season, when they may provide other foraging benefits. Brown bears are opportunistic omnivores, and even when one food resource is widely available, they still maintain a balanced diet with multiple food sources (Robbins et al., 2007). When we restricted our resource availability to seasonal intervals, we nearly limited brown bear habitat selection to one

resource covariate at a time, which may have been unrealistic. The correction we attempted in this model may not have worked for this population of bears, but in other systems (e.g., specialist herbivores in Kenyan savannas; Kartzinel and Pringle, 2020), it may be more appropriate.

The high inter-individual variation in the brown bear population is both interesting and unsurprising given what we know about the species and population. Brown bears undoubtedly possess the cognitive capability to remember the location of previously visited areas (Manchi and Swenson, 2005; Clapham et al., 2012; Selva et al., 2017; Wirsing et al., 2018), and the Arctic’s seasonal and spatial dynamics suggest that the spatio-temporal memory we tested here would be useful for optimal foraging (Fagan et al., 2013). It is then somewhat surprising that only 15 of the 21 bears in the population exhibited memory-informed movement according to our model selection process. One potential explanation is that if the temporal variation in the landscape is unpredictable, then periodic memory-informed movement may not improve foraging success (Mueller et al., 2011). Vegetation in the Mackenzie Delta region is somewhat unpredictable from year to year (Edwards et al., 2013), and while some resources may be available at the same place and time each year, memorizing the location of a patch that may not support resources in the future could be detrimental to foraging. It is also possible that bears remember the locations of previously visited areas, but take a different (possibly more efficient) route to these areas. This is just one example of a memory-informed movement that may not be identified by our memory-only or resource-memory models, as our models and hypotheses are concerned only with a specific kind of memory-informed movement. Our model also does not account for social dominance hierarchies that are often present in brown bear populations (Gende and Quinn, 2004). Including the paths of nearby conspecifics would be difficult given our data restrictions

(e.g., many bears in the population were not tracked) but would connect to innovative theoretical work (e.g., Potts and Lewis, 2014) to answer important questions about animal cognition and sociality.

The model used here may not reliably be able to identify the correct signal when fit to only one year of bear GPS data, forcing us to question our results for bears with this much data. In Chapter 2, although the simulation analyses performed with the model were effective for small data sizes, the model fits for individual years of data from the same bear, the "best model" often changed from year to year. A finer temporal resolution for our GPS data could also solve this problem, since processes such as movement autocorrelation are more difficult to identify with temporally sparse data. With the data we have, though, we can only postulate that either the bears are changing the way they move from one year to another, or that the model is unreliable in detecting a spatio-temporal memory signal without enough data. The former could arise as a result of reproductive activity in the population. When female bears have cubs, their movement strategies change as preventing infanticide and supporting their offspring become priorities (Edwards and Derocher, 2015). Male bears display much less behavioural plasticity with regard to reproduction, and all three of the male bears included in our analysis were best explained by the resource-memory model. Year-to-year variability in the landscape could also influence this behaviour; for example, if a bear finds food somewhere in one year, revisits that area 365 days later, and does not find food, it may use its cognitive map differently in subsequent years. Conversely, if a bear finds a new food source it may abandon its cognitive map and spend time at the newly found patch instead. We acknowledge that we cannot support or refute these hypotheses about within-individual variation without a longer temporal scale of data per individual.

One bear, GF1079, yielded noticeably different parameter estimates from the resource-memory model as its "best model". This bear had a β_0 value close to 0 and its estimate for μ was less than 1 day, which implies that it was consistently moving away from locations it had visited very recently. This would be expected from an animal performing correlated random walk behaviour (its estimate for κ was 0.731, the largest in the population), but in our model, we control for this behaviour by comparing observed steps to random steps simulated from a correlated random walk (as is done in traditional step selection analysis). This combination of parameter estimates only occurred with GF1079, which had only one year of location data (excluding the first year used for model training), suggesting that this occurrence is rare and may be alleviated with more data. Another bear, GM1147, exhibited movement patterns that were explained much better by the memory-only model than any other model we fit (Tables 3.1 and 3.2). A dBIC value of nearly 1000 from these data is difficult to explain, although once again, the infrequency of this situation implies that it may disappear if more data are included.

Our modelling framework focuses on behaviours that are observed in many other taxa, with potential for application in wildlife management. Boreal woodland caribou (*Rangifer tarandus caribou*) display site fidelity patterns that vary by season, displaying greater fidelity at different parts of the year (Lafontaine et al., 2017). Applying our framework to location data for woodland caribou, potentially breaking data up into seasonal partitions, would provide valuable inference about the extent of these patterns. The individual variation in brown bear movement behaviour was a key conclusion that we identified, which suggests that our modelling framework may be applicable to other ecological systems with high individual variation. As an example, black-legged kittiwakes (*Rissa tridactyla*) display individual differences in site fidelity when foraging

near nesting colonies (Harris et al., 2020). These birds may not only exhibit different degrees of support for the resource-memory model, but the rate at which previous foraging paths are revisited (μ) may differ between individuals. Our approach may also be useful when resources do not vary temporally, but other factors (such as prey vigilance or depletion-recovery dynamics) necessitate the use of spatio-temporal memory in animals (e.g., Schlägel and Lewis, 2014). Identifying the degree to which animals rely on memory is also important for translocation and reintroduction protocols. These protocols are often applied to animals that pose a high risk of coming into conflict with humans, transporting these animals to an environment they are unfamiliar with. Translocated animals that rely heavily on memory struggle to forage effectively in their new environments (Jesmer et al., 2018). Brown bears are frequently translocated, and these costly and time-consuming protocols significantly increase mortality risk if not executed properly (Milligan et al., 2018). These important and necessary decisions can be made more effectively with knowledge of how memory and familiarity impacts the movements of problem animals.

3.5 Conclusions

Animal movement is one of ecology’s most complex processes, with many potential drivers that undoubtedly vary between individuals and species alike. Brown bears in the Arctic display this complexity due to the heterogeneity of their environment and the high dietary variation between individuals. We applied a newly derived modelling framework to a subset of the Mackenzie Delta brown bear population and amid high variation between individuals, we found the most frequent movement strategy to be a circannual pattern of revisitation to resource-rich food patches, which our model suggests is driven by time-dependent spatial memory. These results highlight the ability of this modelling

framework to identify complex cognitive processes from discrete-time animal location data.

4 Simulating how animals learn: a new modelling framework applied to the process of optimal foraging

4.1 Introduction

Animals do not know everything about the environments they live in (Fagan et al., 2013), and even if they did, human-induced climate change is making the world very unpredictable (Masson-Delmotte et al., 2021). While evolutionary adaptations are typically too slow to match these changes (Bell and Collins, 2008; Chevin et al., 2010; Merilä and Hendry, 2014), many animals can exhibit multiple behavioral responses to a changing environment without modifying their genetic code in a phenomenon known as behavioral plasticity (DeWitt et al., 1998; Schmidt et al., 2010; Snell-Rood, 2013; Wong and Candolin, 2015). Examples of behavioral plasticity range from temporal adjustments in the phenology of frogs in the temperate forests of the eastern United States (Gibbs and Breisch, 2001) to the settlement of urban areas by birds in Europe (Møller, 2009). The ability to incorporate external information into a revised behavioral strategy may confer a fitness benefit to animals living in uncertain environments (Parrish, 2000; Donaldson-Matasci et al., 2008), but the conditions under which behavioral plasticity is adaptive are not well-understood (Wong and Candolin, 2015). Most forms of behavioral plasticity involve learning (Snell-Rood, 2013), which has a rich theoretical background (Pearce, 2008) that could provide important context to the problem.

Our understanding of how animals learn is largely derived from laboratory studies of simple tasks (Pearce, 2008), which elucidate important cognitive mechanisms for learning but do not particularly resemble the natural world.

This rich field of study can be traced back to Pavlov's work on conditioning and associative learning (Pavlov, 1927; Harris and Bouton, 2020), which spawned theoretical and experimental work assessing the formation and extinction of these associative relationships, along with an animal's ability to categorize stimuli into different groups (Spence, 1936; Rescorla and Wagner, 1972; Pearce, 1987; Katz and Wright, 2006). As food is often used as a positive reinforcer for animals (Pavlov, 1927), it follows logically that "foraging" tasks can effectively display how animals learn to prioritize different food resources based on their relative reward (Krebs et al., 1978; Lea et al., 2012). Many of these conclusions draw heavily from optimal foraging theory (Charnov, 1976), generating a connection between cognitive and spatial ecology. When the proper data are available, animal movement and foraging processes can characterize memory and learning in wild animals (Fagan et al., 2013; Lewis et al., 2021). The mechanistic clarity of laboratory experiments and the realism of animal movement models are difficult to combine into one analysis, but individual-based simulation modelling may be an effective tool for generating realistic patterns with clear mechanistic origins (Tang and Bennett, 2010; DeAngelis and Diaz, 2019; Murphy et al., 2020).

Cognitive psychologists and ecologists have identified a striking resemblance between learning and Bayesian inference. This is most clear when couched in terms of statistical decision theory (SDT; McNamara and Houston, 1980; Berger, 1985). Broadly speaking, SDT is a mathematical framework describing the optimal way animals or humans should make decisions according to learned information (Dall et al., 2005; Dayan and Daw, 2008; Schmidt et al., 2010). A key component of SDT is the use of Bayes's theorem to represent how prior knowledge is updated through learning to produce a refined, posterior distribution of belief (Berger, 1985). Bayes's theorem and its key principles have been used to explain many learning processes (Griffiths et al., 2001; McNamara

et al., 2006), including Pavlovian conditioning (Courville et al., 2006), mate choice (Luttbeg, 1996; Castellano et al., 2012), and optimal foraging (Green, 1980, 2006; Valone, 2006). The application of SDT to optimal foraging problems has inspired the term "Bayesian foraging", which describes how animals update their foraging preferences in a decision-theoretic manner (Green, 1980; Valone, 2006). Most of this work has focused on small-scale foraging tasks, but in reality, foraging is a complex process influenced by many cognitive cues (Fagan et al., 2013). Extending SDT to a model that wholly encompasses animal movement and foraging will produce results that are more realistic and applicable to vulnerable wildlife populations.

Bayesian Markov Chain Monte Carlo (MCMC) sampling is a simple algorithm that we can use to simulate how animals learn. MCMC sampling uses a stochastic approach to calculate the posterior distribution of a set of parameters based on prior distributions and data supplied by the user (Raftery and Lewis, 1992). When applied to learning, these parameters represent biological qualities of an animal, and the data represent information collected by animals through empirical experience. The structure of the prior and posterior distributions reflects the relative "belief" an animal possesses in a certain behavioral strategy (i.e., combination of parameters) before and after incorporating "data", respectively. The data enforce revised posterior belief in certain behavioral strategies through an objective function, which depends on the parameters and may also be stochastic. While the objective function in a MCMC sampling procedure is typically a probability distribution function (or likelihood function) of some sort, it does not need to be continuous nor does it need to integrate to 1 over the sampled domain. Instead of using MCMC to find the global optimum of a likelihood function, we can use it to identify behavioral strategies that result in globally optimal fitness. In this example, the objective function would represent

the net energetic yield afforded by a specific strategy. Under this framework, MCMC simulates how "animals" sample information by executing the task and evaluating the energy afforded by different behavioral strategies (i.e., parameter values). Behavioral strategies that consistently produce less favorable objective function values are less likely to accumulate probability mass in the posteriors.

One complete run of the MCMC algorithm, which we henceforth refer to as a "chain", consists of many iterations. In each iteration the sampler draws random parameter values and calls the objective function at those values, either accepting or rejecting the parameters based on the function value. The number of iterations in a chain has important mathematical and biological interpretations. Chains with more iterations allow for more extensive modification of the priors, which biologically represent a simulated animal's relative belief in different behavioral strategies. With that in mind, we suggest that the number of iterations in a chain represents the amount of information the animal gathers in its environment. We can more effectively ensure that the animal consistently develops the same posterior belief in identically parameterized, but independent, chains when these chains have more iterations (this is mathematically akin to ensuring the algorithm converges; Raftery and Lewis, 1992; Cowles and Carlin, 1996). Some MCMC algorithms leave iterations at the beginning of the chain out of the posterior distribution, classifying them as "burn-in" iterations. The burn-in period was designed to enhance chain convergence (Cowles and Carlin, 1996) but by omitting the behavioral strategies employed at the beginning of the simulation process, the posterior distributions no longer include information the animal gathered during the unrealistically "naive" (given the structure of the priors) stages of learning.

During the sampling process, MCMC allows for the acceptance of suboptimal objective function values (i.e., lower than previous values) to search the

parameter space more completely and avoid local optima. The rate at which these suboptimal values are accepted can be likened to the range of behavioral strategies an animal may try in a given environment. Animals that accept a wide variety of strategies, even when they may not be optimal, could be thought of as displaying behavioral plasticity. Consistently following the optimal behavioral strategy could be thought of as displaying environmental canalization, a term used to characterize a lack of phenotypic variation in reaction to environmental change (Gibson and Wagner, 2000; Gaillard and Yoccoz, 2003; Liefting et al., 2009). The simplest way to enforce this in the model is to introduce an exponent $k > 0$ which is applied to the objective function during sampling. We can think of k as an index of canalization, implying that lower values of k correspond to high behavioral plasticity. Animals that possess high plasticity frequently sample many behavioral strategies amid environmental uncertainty in what is commonly referred to as bet-hedging (Donaldson-Matasci et al., 2008; Nevoux et al., 2010).

We expanded on existing implementations of SDT by coupling an individual-based simulation model for animal movement with memory (Avgar et al., 2013) to a Bayesian model simulating how animals learn to forage optimally. Our algorithm incorporates an objective function measuring the net energetic intake of a foraging bout, given a set of parameters controlling animal behavior. To this end, the posterior distribution of these parameters obtained after sampling reflects what simulated animals learned about the efficiency of different foraging techniques. We tested how effectively animals adjusted to unexpected and abrupt changes in the distribution and abundance of resources on the landscape. We found that animals with higher behavioral plasticity performed more efficient foraging returns after these abrupt changes, but were less efficient when the environment did not change. Our framework displays how SDT can be

extended to the simulation of realistic ecological processes that, if formulated correctly, can make effective predictions when data are lacking.

4.2 Methods

4.2.1 The learning model

We used Bayesian Markov Chain Monte Carlo (MCMC) sampling to simulate how animals learn to adjust their behavior based on indicators of success. The effectiveness with which an animal executes a certain task was quantified by an objective function f . Animals "sample" different parameter values (i.e., behavioral strategies) and evaluate their optimality by calculating f ; depending on the value of f , the animal may be more or less likely to attempt similar strategies as represented by the posterior distribution of behavioral strategies.

We parameterized the MCMC sampler in a way that produced consistent and biologically realistic results. We used uniform priors for each of the behavioral parameters, which necessitated that we added a burn-in period to our chains, and we chose to omit the first $N_{burn} = 500$ iterations of each chain from the posterior distribution to this end. Choosing the number of iterations per chain (including burn-in), N_{iter} , was a careful optimization of the trade-off between computational expense and consistency. Chains with more iterations take longer to simulate but they also more accurately represent what simulated animals have learned. We analyzed chains of different sizes to evaluate the fewest iterations necessary to produce consistent posterior distributions, which supported our choice of $N_{iter} = 2000$ (see Appendix D for more detail). This produced posterior distributions with $N_{iter} - N_{burn} = 1500$ parameter values. We also tested many different values for k , the exponent applied to f during sampling: $k = 5, 10, 20, 50, 100, 200, 500, 1000$. Parameter values used in this study are summarized in Table 4.1. We ran our algorithm in Julia 1.6.2 using the Turing

Par	Description	Value
MCMC algorithm parameters		
N_{iter}	Number of MCMC iterations per chain	2000
N_{burn}	Number of iterations in burn-in period	500
k	Exponent of objective function f	Many values
Behavioral parameters		
β	Degree of reliance on memory	Not fixed
γ	Likelihood to make long navigations	Not fixed
q	Default expectation of habitat quality	Not fixed
h	Relative preference for resource Q_1	Not fixed
Movement parameters (see Appendix A)		
N_r	Number of potential points of interest simulated	1000
λ	Exponent of C values when choosing point of interest	10
ρ	Average step length on navigations	2
κ	von Mises angular correlation parameter for navigations	10
Objective function parameters		
T_{train}	Length of training portion of each track	1000
T_{test}	Length of test portion of each track	1000
v	Energetic loss per 1 cell length of movement	0.05
N_{avg}	Number of tracks incorporated into one f call	5
Landscape parameters (see Appendix A)		
Q	Threshold for landscape patches	0.6 or 0.9
d_L	Rate of resource depletion per time step	1.0
r_L	Recovery rate of depleted resources per time step	0.025

Table 4.1: Description of model parameters. The four parameters under the section "Behavioral parameters" are incorporated into the objective function f , and sampled in the Bayesian MCMC algorithm.

library, which offers a number of different MCMC samplers. We sampled different parameter combinations with the widely used Metropolis-Hastings algorithm (Hastings, 1970; Chib and Greenberg, 1995), using the "MH()" function from the Turing library. Parameters with infinite support were log-transformed and bounded on finite intervals determined by assessing their biological meaning.

4.2.2 Application of the model to foraging

We tested our modelling framework with an optimal foraging task involving the individual-based simulation of animal movement across a continuous-space landscape. Our individual-based model (IBM) for movement is heavily inspired by Avgar et al. (2013) and contains four parameters mediating the behavioral strategy of simulated animals. We provide a summary of the model and parameters below, but see Appendix A for a more detailed explanation of the process using the ODD (Overview, Design Concepts, and Details) protocol (Grimm et al., 2006).

Simulated animals move on a landscape characterized as a 100 x 100 arbitrary length unit (lu) square in two-dimensional continuous space. The landscape has two independently distributed "resources" that provide an energetic benefit to the animal. In the interest of producing movements similar to empirically observed location data, animals take discrete-time "steps" every 1 arbitrary time unit (tu). Animals perceive, remember, and recall the quality of previously visited foraging patches to make informed movement decisions. We make four key assumptions about how animals do this, listed below:

- (A1) Animals exhibit a preference for one of the two resources on the landscape and bias their movements accordingly.
- (A2) Animals remember the resource density of areas they have previously visited, but the animals' reliance on memory decreases over time.

- (A3) All points that the animal has not visited are perceived by the animal as having equal value, regardless of their spatial or temporal position.
- (A4) Animals are more likely to navigate to nearby points, all else held equal.

The foraging quality of any point \mathbf{x} at any time t , which we denote $Q(\mathbf{x}, t)$, ranges from 0 to 1 and is composed of two independent foraging resources, $Q_1(\mathbf{x}, t)$ and $Q_2(\mathbf{x}, t)$. While $Q(\mathbf{x}, t) = (Q_1(\mathbf{x}, t) + Q_2(\mathbf{x}, t))/2$ across the landscape, we allow animals to exhibit "habitat selection" for the different resources on the landscape (Assumption A1). The behavioral parameter h ranges from 0 to 1 and mediates the animal's relative preference for Q_1 and Q_2 . Simulated animals perceive Q_1 and Q_2 as independent entities, and when computing the animal's perceived foraging quality for any point \mathbf{x} and time t , we use $\tilde{Q}(\mathbf{x}, t) = hQ_1(\mathbf{x}, t) + (1 - h)Q_2(\mathbf{x}, t)$ as opposed to $Q(\mathbf{x}, t)$ (Figure 4.1).

Simulated animals perceive new information about resources on the landscape and encode this information into spatial memory. Many different animals use memory to guide their foraging movements (Panakhova et al., 1984; Clayton and Dickinson, 1998; Schlägel and Lewis, 2014; Potts and Lewis, 2016; Bracis et al., 2018; Ranc et al., 2021), but heavy reliance on spatial memory is accompanied by numerous energetic costs (Fagan et al., 2013). The behavioral parameter $\beta \geq 0$ quantifies the extent to which simulated animals rely on their memory of previous foraging experiences. As β increases the animal relies less on its memory, potentially a strategy to adapt to temporally variable environments (Fagan et al., 2013). We note that unlike memory decay, a neurological process (Thomas and Riccio, 1979), the mechanism displayed here represents the animal's conscious choice not to rely on the memory of previous experiences.

Animals make a naive, uninformed "guess" about the resource quality of locations they have not visited, and per Assumption A3, this guess is constant across space and time. Specifically, any location will be assigned the value

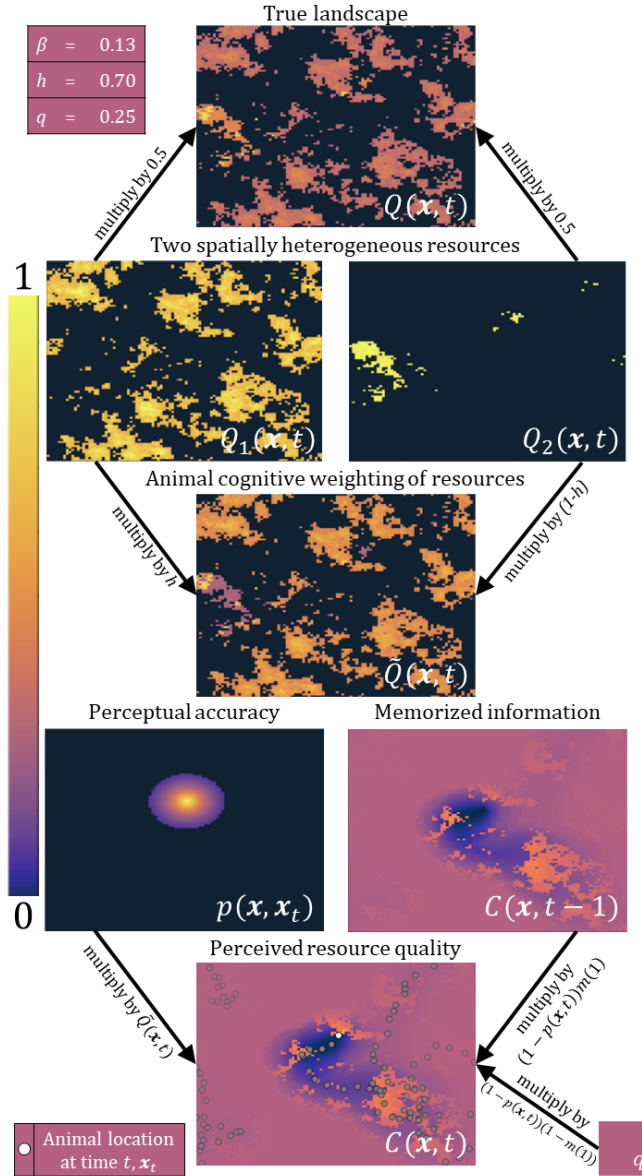


Figure 4.1: Schematic describing the generation of $C(\mathbf{x}, t)$, the animal's estimation of resource quality across the environment. The animal weights two independently distributed resources and incorporates newly perceived information into C based on the perception function $p(\mathbf{x}, \mathbf{x}_t)$. Note the incremental updating of C as the animal moves to a new location (\mathbf{x}_t , pictured in blue on the bottom right).

$q \in [0, 1]$ as long as that location remains unvisited by the animal. Larger values of q suggest that the animal is more "optimistic" about the quality of unexplored areas (Berger-Tal and Avgar, 2012; Avgar et al., 2013), and will more frequently visit these areas as a result.

Once the animal generates an expectation of resource quality across the landscape, it must choose a location to navigate to. Assumption A4 states that animals are more likely to navigate towards nearby points than faraway points. This idea follows logically from the marginal value theorem (Charnov, 1976), which considers the energetic cost of travel to other patches. We included behavioral parameter $\gamma \geq 0$ to quantify this relationship. As γ increases, the probability that the animal will navigate to a faraway point decreases; even if the animal believes there are resources far away, it may opt for nearby resource patches instead, a tactic many animals adopt as a risk avoidance mechanism (Gehr et al., 2020).

The animal's perceived resource quality for any point \mathbf{x} and time t , denoted $C(\mathbf{x}, t)$, depends on these four assumptions. This function consists of a weighted average of three quantities: newly perceived information (weighted by perception function $p(\mathbf{x}, \mathbf{y})$), memorized information (weighted by memory function $m(t)$), and the naive expectation q .

$$p(\mathbf{x}, \mathbf{y}) = \exp\left(-\frac{d(\mathbf{x}, \mathbf{y})}{\rho}\right), \quad (4.1)$$

$$m(t) = \exp(-\beta t), \quad (4.2)$$

$$C(\mathbf{x}, t) = \underbrace{p(\mathbf{x}, \mathbf{x}_t)\tilde{Q}(\mathbf{x}, t)}_{\text{perception}} + (1 - p(\mathbf{x}, \mathbf{x}_t)) \left(\underbrace{m(1)C(\mathbf{x}, t-1)}_{\text{memory}} + \underbrace{(1 - m(1))q}_{\text{expectation}} \right). \quad (4.3)$$

The perception function relies on the assumption that animals perceive nearby information more accurately than faraway information (Fletcher et al., 2013; Avgar et al., 2015; Fagan et al., 2017), where $d(\mathbf{x}, \mathbf{y})$ is the distance between \mathbf{x} and \mathbf{y} and ρ is the animal's average movement speed in lu/tu. A positive association between movement capability and perceptual range has been documented across many animal taxa (Kiltie, 2000; Møller and Erritzøe, 2010).

4.2.2.1 Calculating the objective function

We designed an objective function f measuring the energetic benefit afforded by a certain behavioral strategy. We divided these simulated foraging bouts into "training" and "test" sections of durations T_{train} and T_{test} , respectively, and only measured f over the test section. Avgar et al. (2013) made a similar correction to allow animals to develop an initial memory of their simulated landscape, producing movement paths that resemble empirically collected animal location data. We subtracted the animal's total resource intake across the simulation by the energetic loss as a result of movement, calculated as the animal's total distance traveled multiplied by a proportionality constant $v \geq 0$ (Table 4.1). Our function f consists of an average of N_{avg} independent movement tracks so it effectively characterizes the expected value of any parameter combination. We define f_i , the net energetic intake from the i^{th} of these tracks, by summing the energetic gains collected at each location \mathbf{x}_t along the animal's path:

$$f_i(\beta, \gamma, q, h|\mathbf{Q}) = \frac{\sum_{t=T_{train}+1}^{T_{train}+T_{test}} Q(\mathbf{x}_t, t) - v \sum_{t=T_{train}+1}^{T_{train}+T_{test}} d(\mathbf{x}_t, \mathbf{x}_{t-1})}{T_{test}}, \quad (4.4)$$

$$f(\beta, \gamma, q, h|\mathbf{Q}) = \frac{1}{N_{avg}} \sum_{i=1}^{N_{avg}} f_i(\beta, \gamma, q, h|\mathbf{Q}). \quad (4.5)$$

4.2.2.2 Scenarios of environmental change

We randomly generated spatially autocorrelated resource landscapes (see Appendix A for further detail) and used them to simulate abrupt landscape-level changes in the environment. Bayesian inference allows for the iterative updating of prior expectations based on previous analyses (Ellison, 2004). The posterior distributions of our behavioral parameters represent knowledge accumulated by a simulated animal, which we can use as more "informative" priors for a second MCMC chain. Each of our scenarios of environmental change contains two stages, where each stage has a unique Q_1 and Q_2 (Figure 4.2). The scenarios we generated incorporate two "types" of landscape, which can be visually compared in the first chain of Scenario A (Figure 4.2). Here, Q_1 is much more abundant and widely distributed than Q_2 , but Q_2 is richer than Q_1 in the small area where it can be found. Scenario A serves as a "control" where the environment does not change; we would expect the animal to identify an optimal strategy and retain this strategy for both chains. In Scenarios B and C, only one of the resources switches between being widely abundant and locally available (the difference being the directionality of this change), and in Scenario D, both resources swap.

We ran the MCMC algorithm with each of the four scenarios and a suite of k values (5, 10, 20, 50, 100, 200, 500, 1000) to evaluate how these quantities affected optimal foraging behavior. For each value of k and scenario, we ran algorithm 12 independent times. We obtained posteriors for the first and second chains of each run for the four parameters β , γ , h , and q , along with a posterior distribution of f_i values (1500 iterations after burn-in \times 5 f_i per f call \times 12 chains = 90000 total f_i calls) for each k and scenario.

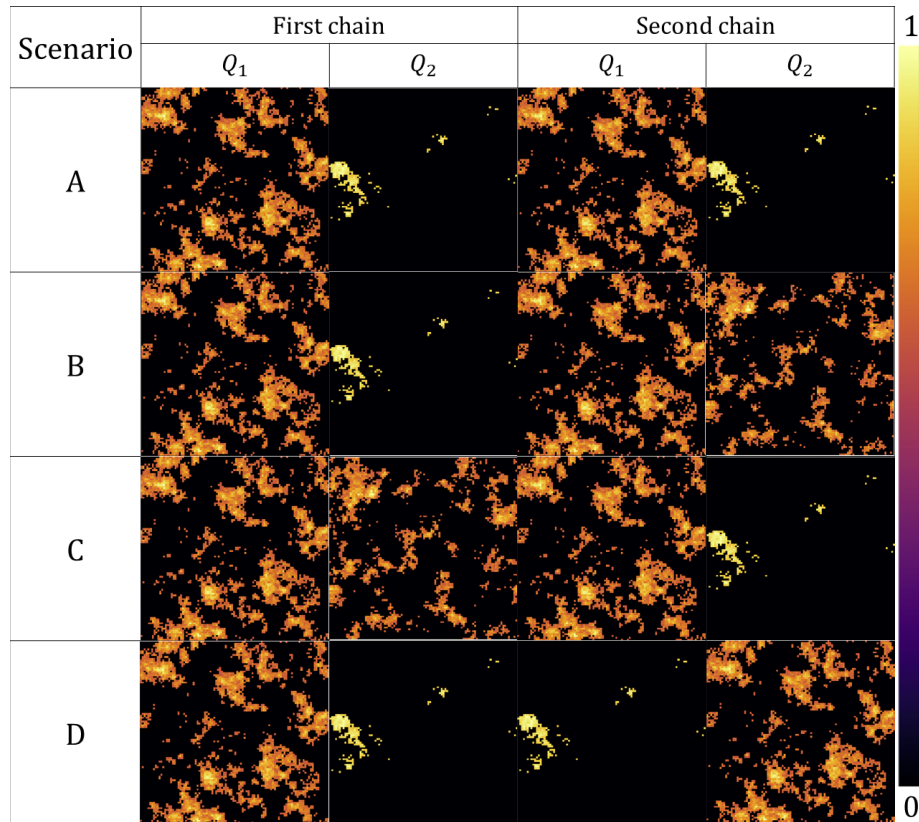


Figure 4.2: Different scenarios of environmental change used in our simulations. Scenario A is a “control” where the environment, composed of two resources Q_1 and Q_2 , does not change at all. In Scenarios B and C, Q_1 stays the same, but Q_2 becomes more or less abundant than Q_1 , respectively. In Scenario D, the distributions of Q_1 and Q_2 “swap”.

4.3 Results

4.3.1 Posterior distribution of parameters

Under the same environmental circumstances, 12 independently simulated MCMC runs produced similar posterior distributions, suggesting that $N_{iter} = 2000$ and $N_{burn} = 500$ is sufficient for convergence (a subset of these are displayed in Figure 4.3). In most circumstances, simulated animals displayed a relatively "pessimistic" expectation of unvisited food patches, as suggested by posterior distributions concentrated around low values of q . Posterior distributions of β were relatively spread out across all values, suggesting that long-term reliance on memory only has a minimal advantage over short-term reliance in these simulations. Simulated animals avoided long-distance navigations, opting instead for values of γ close to 1 frequently (Figure 4.3). Most notably, though, animals simulated in Scenario A (Figure 4.2) exhibited a strong preference for resource Q_2 , which was much less abundant across the landscape than Q_1 . This is indicated by posterior distributions for h concentrated around lower values.

4.3.2 Posterior distribution of objective function values

Both the scenario of environmental change and the MCMC parameter k affected the second chain's posterior distribution of f_i values. Typically, the spread of these distributions increased as k decreased, especially in Scenario A, where they appear similar to delta functions at $k = 500$ and $k = 1000$ (Figure 4.4). In scenarios where the environment changed dramatically (e.g., Scenario D; Figure 4.2), these distributions took on different shapes, sometimes becoming bimodal (Figure 4.5).

More specifically, the effect of MCMC parameter k on the distribution of objective function f_i values depended on the scenario of environmental change

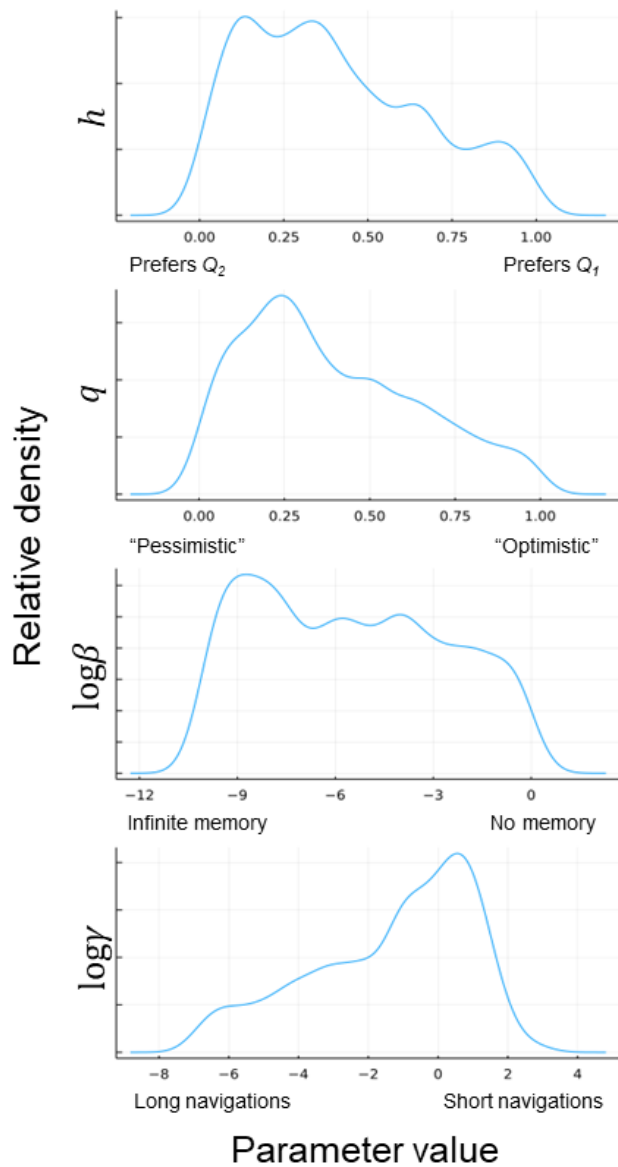


Figure 4.3: Posterior density plots for one independent runs of the MCMC algorithm, taken from the first chain of Scenario A (see Figure 4.2) with $k = 10$. Greater probability mass at certain parameter values indicates higher belief in that value optimizing the net energetic gain function f . Note, in particular, the animal’s preference for resource Q_2 , which in this case is much less widely available but provides a larger energetic benefit than Q_1 where it can be found (Figure 4.2).

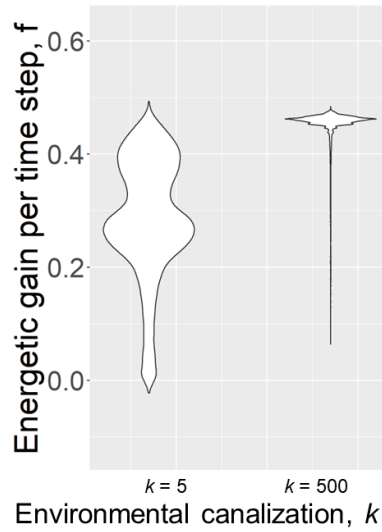


Figure 4.4: Example violinplots detailing the distribution of objective function f_i , which represents the net energetic gain from a simulated animal foraging bout. These two violinplots are taken from the second chain of Scenario A (see Figure 4.2), with k taking on two different values.

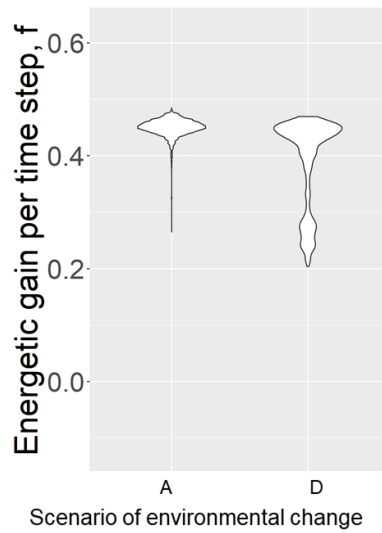


Figure 4.5: Example violinplots detailing the distribution of objective function f_i , which represents the net energetic gain from a simulated animal foraging bout. These two violinplots are drawn from the second chain of Scenarios A and D (Figure 2), respectively, with $k = 200$ for each.

(Figure 4.6). In Scenario A (Figure 4.2), simulated animals performed more consistently and efficiently with large values of k than with small k . In Scenario B, k had a much smaller effect on foraging success than Scenario A, although the spread of f_i values was larger with smaller k (Figure 4.6). The posterior distributions of f_i from Scenario C resemble those from Scenario A at low k , but appear to take on a skewed, slightly bimodal shape at higher k . In Scenario D, intermediate values of k ($k = 100$ and $k = 200$) produced foraging bouts that were, on average, more efficient than at large values of k (Figure 4.6). The distribution of f_i values was distinctly bimodal with large k , and as k increased, more probability mass was concentrated in the second, lower mode.

4.4 Discussion

Predicting how animals will adjust to environmental change is an important but complex ecological problem. We developed a Bayesian model that simulates how animals sample information about their environments to develop a posterior distribution of optimal foraging behavior. Our model builds on statistical decision theory, which has long been used to explain how animals learn from a Bayesian perspective (McNamara and Houston, 1980; Berger, 1985; Dall et al., 2005). We applied our learning model to a complex, continuous-space foraging task to be completed by simulated spatially informed foragers (Avgar et al., 2013). In the presence of two independently distributed resources with equal energetic return, animals simulated in our model prioritized resources that were concentrated within small, sparsely distributed patches. Animals that exhibited canalized behaviour displayed consistently efficient foraging returns in temporally predictable environments, but environmental canalization became maladaptive when we introduced sudden, unpredictable changes to the landscape. Our results suggest that Bayesian MCMC can be used to simulate how

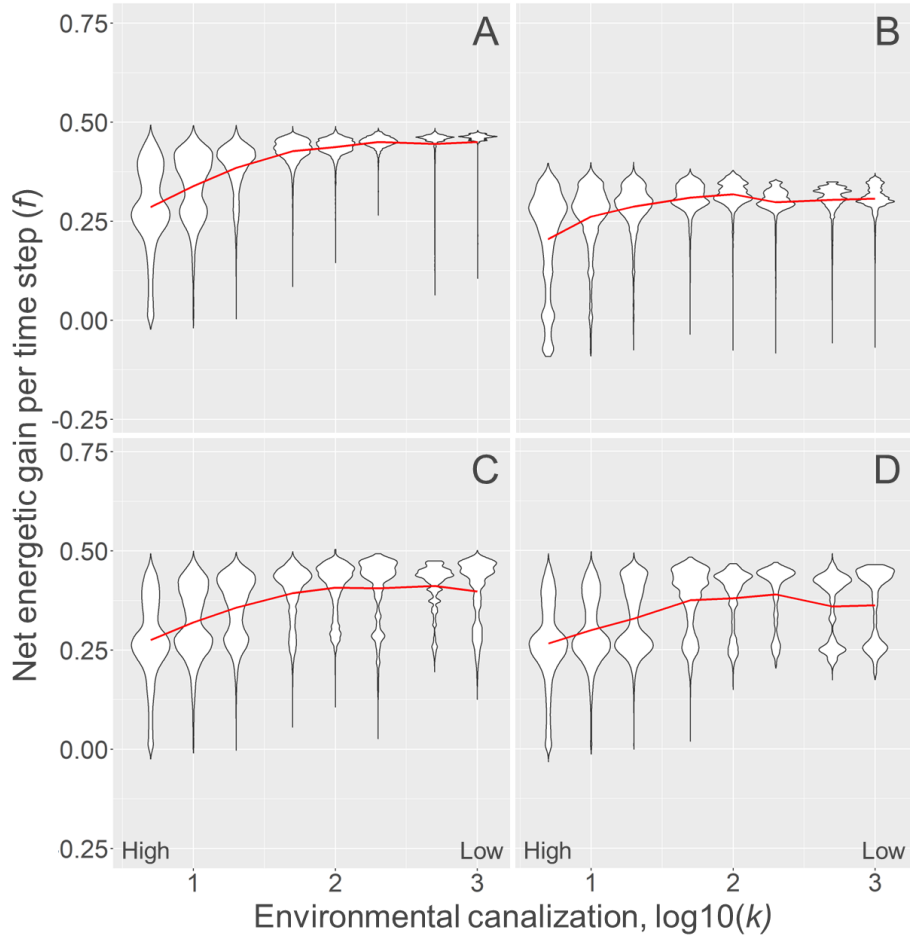


Figure 4.6: Effect of MCMC parameter k on foraging efficiency in simulated animals under four different scenarios of temporal environmental change (see Figure 4.2 for detail on each scenario). Each individual violinplot represents a sample of 90000 f_i values (12 independent runs of MCMC \times 1500 f values per run \times 5 f_i values per f call) representing the net energetic gain from a single simulated movement track. The red line represents the mean of all f_i values from each k value.

animals, and potentially even humans, learn a wide variety of tasks in an ever-changing world.

When faced with the choice of two resources, simulated animals chose the resource that was available in smaller, but more heavily concentrated patches (Figure 4.3). This finding suggests that simulated animals occupy areas with the highest possible habitat suitability, a key principle of ideal free distribution (IFD) theory (Fretwell and Lucas, 1969; Cantrell et al., 2007). Many patterns predicted by IFD theory can be seen in our results even though our IBM did not incorporate competition between individuals (this could be an interesting topic for future work). Specifically, IFD theory predicts that individuals residing in poor habitat will adjust for the lack of resource abundance by adopting larger home ranges (Haché et al., 2013). Simulated animals in our model centralized their movements around small plentiful resource patches, producing smaller home range sizes than individuals that foraged on less concentrated resources. Similarly, the resource dispersion hypothesis predicts that animals will occupy larger home ranges when resources are less spatially concentrated (Macdonald, 1983; Macdonald and Johnson, 2015). Increasing the speed or breadth of resource depletion or further decreasing the spatial availability of these concentrated resources could modify this relationship.

The wide variety of behavioral strategies adopted by simulated animals with high behavioral plasticity during sampling produced variable energetic outcomes. Behavioral plasticity allows animals to exhibit a variety of foraging strategies simply as a result of learning and adjusting to new environmental drivers (Parrish, 2000). Animals with highly canalized behavior (i.e., low plasticity) would be expected to perform one foraging strategy consistently (Gailard and Yoccoz, 2003; Snell-Rood, 2013; Wong and Candolin, 2015), and we frequently saw that in our simulations. This is also unsurprising from an analyt-

ical perspective, since k (specificity) also resembles the number of "clones" used in data cloning algorithms (Lele et al., 2007). This consistency also suggests that there is minimal stochastic variation in the value returned by our objective function f_i when our behavioral parameters were held constant.

Our simulations strongly suggest that behavioral plasticity is adaptive when the environment changes dramatically and unexpectedly. Animals simulated in temporally constant environments had unimodal distributions of energetic return, but those simulated in temporally unpredictable environments had a second mode centered around a lower energetic intake (Figure 4.5). The latter group of simulated animals foraged efficiently until the distribution of resources suddenly changed, rendering the original strategy suboptimal. Animals with high behavioral plasticity shifted their resource preferences depending on the environment, for better or for worse (Parrish, 2000; van Baaren and Candolin, 2018; Dunn et al., 2020). Animals with very low behavioral plasticity continued to forage according to their initial, now suboptimal, strategy, while animals with intermediate levels of behavioral plasticity adjusted their foraging strategies more effectively (Figure 4.6). Animals with very high behavioral plasticity performed a diverse array of foraging strategies, many of which were too inefficient to produce optimal foraging returns.

While behavioral plasticity is typically considered an adaptive trait, some animals suffer from it. Ecological traps are resources that appear beneficial to animals but, in reality, do not confer a fitness benefit (e.g., mayflies lay their eggs on asphalt because it reflects light similarly to water; Kriska et al., 1998). Ecological traps have become more frequent in the Anthropocene due to the proliferation of man-made novel objects in natural environments (Robertson and Chalfoun, 2016). A typical consequence of behavioral plasticity is an increased likelihood to explore unfamiliar stimuli (Mettke-Hofmann et al., 2009;

Snell-Rood, 2013), which is believed to associate behavioral plasticity and vulnerability to ecological traps (Robertson and Chalfoun, 2016). The results from our simulation study corroborate empirical evidence that environmental canalization can be more effective than behavioral plasticity in some environments.

Translocated animals represent an effective way to test our model, displaying behavior similar to our simulations. Animal translocation and reintroduction protocols have many purposes, ranging from the displacement of potentially dangerous animals (Milligan et al., 2018) to the restoration of populations and ecosystems (Seddon et al., 2007; Polak and Saltz, 2011). Translocated animals are abruptly brought to entirely new environments where they must learn to forage optimally or face heightened mortality risk. The nature of these protocols makes them an effective real-life test for our model, and many of the predictions offered by our model are verified from translocation studies. Translocated elk (*Cervus canadensis*) displayed different foraging behavior depending on the environmental conditions in their original home range and the environmental change they underwent (Falcón-Cortés et al., 2021). Specifically, elk translocated between two very different environments (resembling our Scenario D) were more exploratory and less reliant on memory than those translocated between similar environments, suggesting a shift in behavior from their original home ranges (Falcón-Cortés et al., 2021). As another case study, greater prairie-chickens (*Tympanuchus cupido*) typically sought out habitat similar to that of their natal ranges, suggesting a strong prior preference for resources found in their old environments (Kemink and Kesler, 2013). Here, canalization was detrimental to the birds' survival, adding support to the pattern observed in panel D of Figure 4.3. Translocations and reintroductions are frequently practiced across a wide array of animal taxa, but they are still risky and unpredictable (Berger-Tal and Saltz, 2014). The principles drawn from our analysis provide an improved

forecast for the efficacy of these protocols in different ecological systems.

In addition to the complex foraging task tested here, our framework for describing and simulating learning can be applied in many other situations. Much of what we currently know about animal learning comes from manipulative experiments conducted with captive animals (Pearce, 2008). Many of these studies have been critical for unearthing the mechanisms behind animal cognition, memory, and learning (Pavlov, 1927; Rescorla and Wagner, 1972), but they do not replicate the conditions wild animals experience. By incorporating the prevailing mathematical theory behind animal learning, our modelling framework fills this gap. Our results with respect to continuous-space foraging align with optimal foraging theory (Charnov, 1976), ideal free distribution theory (Fretwell and Lucas, 1969), and prevailing knowledge on behavioral plasticity (Wong and Candolin, 2015; Robertson et al., 2013). With that being said, our model for learning is general enough that it need not be confined to optimal foraging. Specifically, any problem that can be characterized in the form of an objective function and a set of parameters representing behavior is tractable for our framework. This could include movement on different spatial or temporal scales, social learning, or communication. Even more thought-provoking is the potential for our modelling framework to predict how humans learn and make decisions. Through these potential applications and more, our computational modelling framework has the capacity to address challenging problems in cognitive science.

5 A parametric model for estimating the timing and intensity of animal migration

5.1 Introduction

Migration is one of the most widespread and important ecological processes within the animal kingdom (Dingle and Drake, 2007; Bauer and Hoye, 2014). The process occurs in countless animal taxa and has evolved convergently many times (Pulido, 2007; Roff and Fairbairn, 2007; Fryxell and Holt, 2013). Owing in part to this convergent evolution, migration is a diverse process, occurring across a wide variety of temporal and spatial scales (Egevang et al., 2010; Hebblewhite and Merrill, 2011; Bohart et al., 2021; Abril-Colón et al., 2022). Understanding how and why animals migrate is important theoretically but understanding where these animals are going and when facilitates effective management (Middleton et al., 2020; Kauffman et al., 2021). As the world undergoes a period of rapid and unprecedented change, the migratory patterns of many animals have changed in response, particularly with respect to their spatial and temporal extent (Hardesty-Moore et al., 2018; Tucker et al., 2018). Recent advances in tracking technology have allowed ecologists to collect animal location data at unprecedented spatial and temporal resolutions, creating opportunities to answer more complex questions pertaining to migration (Kays et al., 2015). This influx of data describes the spatial extents of many animal migrations in detail. The temporal extent of migration is needed for phenological studies but is more difficult to quantify.

Ecologists have designed many approaches to identify the beginning and end of an animal's migration (Cagnacci et al., 2016; Soriano-Redondo et al., 2020). In some cases, the presence of ecological barriers along an animal's migratory

route make the onset of a migratory period easy to classify without explicit modelling (López-López et al., 2010; Rotics et al., 2018). When these barriers or thresholds are difficult to rigorously define, statistical methods can estimate migration timings. An often-used approach designed by Bunnefeld et al. (2011) relies on net squared displacement (NSD; the animal's distance from its initial location). The model fits non-linear curves representing different movement strategies (e.g., migratory, nomadic) to explain how an animal's NSD changes over time. The approach effectively differentiates migratory animals from non-migrants, but it only estimates the "centre" of migration as a parameter, not the beginning or end. Path segmentation analyses focus on dividing a movement path into segments with "change-points" that represent shifts in behaviour (Edelhoff et al., 2016). These models have often been used for identifying area-restricted searching bouts in foraging animals (Weng et al., 2008) but their principles can be extended to identifying migration (Limiñana et al., 2007; Madon and Hingrat, 2014; Mikle et al., 2019; Wolfson et al., 2022). Path segmentation approaches take many forms but broadly, they typically couple a movement metric (e.g., NSD) with a change-point algorithm that identifies changes in the distribution of this metric (Edelhoff et al., 2016). Methods that rely on NSD are sensitive to the animal's initial location and may break down depending on when data collection began (Singh et al., 2016). First passage time (FPT) is a similar metric that measures the amount of time required for an animal to travel a certain distance, and it has been used to identify changes in movement behaviour on many scales (Johnson et al., 1992; Fauchald and Tveraa, 2003; Le Corre et al., 2014). This distance must be user-defined beforehand, requiring unique assumptions for every dataset (Barraquand and Benhamou, 2008). Complex path segmentation approaches work even when the desired number of segments is not known (Lavielle, 2005; Gurarie et al., 2009; Madon and Hin-

grat, 2014). Among the plethora of migration models, movement ecologists are still searching for a model that accurately and precisely estimates biologically meaningful parameters that describe when and how animals migrate, with little to no prior knowledge of the system.

Dingle and Drake (2007) provide two separate definitions for migration in individual animals: a persistent period of directionally autocorrelated (or straight) movement, and a period of movement ranging over an exceptionally large spatial extent. Step lengths, the Euclidean distance between two consecutive tracked locations, and turning angles, the angle made by the animal's turn during three consecutive tracked locations, describe the speed and directionality of a movement track, respectively. Both of these metrics are widely used in movement ecology (Morales et al., 2004; Fortin et al., 2005; van Moorter et al., 2010; Avgar et al., 2016). The first definition of migration suggested by Dingle and Drake (2007) relates to directional persistence, and could be quantified by a change in an animal's turning angles, while the second definition relates to distance covered and could be quantified by a change in an animal's step lengths. While many path segmentation models combine these properties into one metric (e.g., NSD or FPT), we suggest that a path segmentation model that identifies simultaneous changes in two metrics (step lengths and turning angles) will allow ecologists to draw more biological context from migration data.

We designed a model that identifies the temporal extent of migration using step lengths and turning angles alone. We hypothesized that migration can be quantified by an abrupt change in an animal's observed movement speed and directionality for a sustained temporal interval. Unlike most path segmentation approaches, which focus on one all-encompassing movement metric, our model generates distributions for step lengths and turning angles concurrently. We designed a likelihood-based method for identifying the optimal sequence of

change-points (e.g., start and end of migration) and used a parametric bootstrapping algorithm to generate confidence intervals for the parameter estimates. Our model works for a diversity of migratory animals sampled at different temporal frequencies, which we display with three case studies: ferruginous hawks (*Buteo regalis*) in the Great Plains of central North America, and barren-ground caribou (*Rangifer tarandus groenlandicus*) and brown bears (*Ursus arctos*) in northern Canada. The inference that can be drawn from this model can have important management implications when applied to additional datasets.

5.2 Methods

5.2.1 The model

Our modelling approach builds on and simplifies existing approaches for estimating the start, end, and intensity of migration. This model only requires information on step lengths and turning angles calculated from a discrete-time sample of an animal’s movement path. If we define $\mathbf{z}_t = (x_t, y_t)$ to be the animal’s recorded location at time t , we calculate the step length r_t as follows:

$$r_t = \|\mathbf{z}_t - \mathbf{z}_{t-1}\|. \quad (5.1)$$

Step lengths are an indicator of the distance an animal travels per time step, and turning angles indicate the directional persistence (or straightness) of movement (Morales et al., 2004). We calculate the turning angle ϕ_t as follows:

$$\varphi_t = \begin{cases} \arctan \frac{y_t - y_{t-1}}{x_t - x_{t-1}} & x_t > x_{t-1} \\ \arctan \frac{y_t - y_{t-1}}{x_t - x_{t-1}} + \pi & \text{otherwise;} \end{cases} \quad (5.2)$$

$$\phi_t = [\varphi_t - \varphi_{t-1}] \% 2\pi, \quad (5.3)$$

where \arctan is the inverse tangent (arc-tangent) function. Applying the mod-

ulus operator % ensures that all values are between 0 and 2π . Smaller turning angles (closer to 0 or 2π) indicate straighter movement.

Step lengths and turning angles are well-studied and can typically be explained effectively using known distributions, which we leverage for our model (Auger-Méthé et al., 2016a; Avgar et al., 2016). We hypothesize that an animal’s step lengths follow an exponential distribution at all stages of movement, but during the animal’s migratory stage, the parameter dictating the mean step length increases. We also hypothesize that an animal’s turning angles follow a von Mises distribution, where the angular concentration parameter increases during migration. We assume there exist temporal parameters t_1 and t_2 that signal the start and end of migration, respectively. The likelihood function for any given point \mathbf{z}_t incorporates these conditions explicitly with model parameters t_1 , t_2 , ρ_0 , ρ_1 , κ_0 , and κ_1 . During the non-migratory period ($t < t_1$ or $t > t_2$) the animal’s step length distribution is parameterized by ρ_0 and the animal’s turning angle distribution by κ_0 . The parameters ρ_1 and κ_1 represent the additional movement distance and angular concentration incurred during migration, respectively. We define the likelihood function as follows:

$$I_{mig}(t) = \begin{cases} 1 & t_1 < t \leq t_2 \\ 0 & \text{otherwise,} \end{cases} \quad (5.4)$$

$$L(\rho_0, \rho_1, \kappa_0, \kappa_1, t_1, t_2 | \mathbf{z}_t) = \frac{\exp \left[(-\rho_0 - I_{mig}(t)\rho_1)^{-1} r_t + (\kappa_0 + I_{mig}(t)\kappa_1 \cos \phi_t) \right]}{(\rho_0 + I_{mig}(t)\rho_1) (2\pi I_0(\kappa_0 + I_{mig}(t)\kappa_1))}. \quad (5.5)$$

Here, $I_0(\kappa)$ is the modified Bessel function of order 0. The ratio between $\rho_0 + \rho_1$, the animal’s mean step length during migration, and ρ_0 , the mean step length outside of migration, approximates how much more quickly the animal moves when migrating. We denote this quantity R .

If necessary, we can also expand the model to account for multiple migratory periods within one dataset. This would necessitate the introduction of additional parameters $t_3, t_4, \dots, t_{2c-1}, t_{2c}$ for a model with c distinct periods of migratory movement. If $c > 1$, $I_{mig}(t)$ would be 1 when $t_{2n-1} < t \leq t_{2n}$ for any positive integer n . Unique step length and turning angle parameters (ρ_2, \dots, ρ_c and/or $\kappa_2, \dots, \kappa_c$) for each migratory period could be biologically realistic for some species. For any positive integers m and n , where $m < n$, the m -migration model is nested within the n -migration model; this can be verified by setting all ρ and κ equal to each other and fixing all t_i equal to each other for $i > 2m$.

5.2.2 Parameter estimation

Optimizing the likelihood function (Equation 5.5) is difficult because the function is not differentiable with respect to temporal parameters t_1 and t_2 . The easiest way to solve this problem is to fix all t_i and optimize the model for all ρ_i and κ_i . This process can be repeated for every meaningful set of t_i values (there is always a finite number of such combinations with discrete-time data) to find the overall maximum likelihood estimate.

With datasets spanning a wide temporal range (or with $c > 1$), the number of t_i combinations can become problematically large. In these cases, we use an iterative grid-search algorithm to find optimal regions of the likelihood profile quickly, before honing in on those regions with a finer grid. We optimized the t_i over a subsetted grid that only included properly ordered parameter combinations ($t_m < t_n$ if $m < n$). The number of grids used and their respective resolution depends on the temporal extent of the data as well as the desired precision with which one hopes to estimate the t_i parameters. The temporal extent of the movement paths varied between datasets but we used a minimum grid size of 1 day for all case studies. Optimizing over a coarse initial grid poses

risk of missing global optima but reduces computational times. We started by partitioning the temporal extent of each movement track into 14-day intervals and first found the optimal values of each t_i on this coarser grid. We then identified the t_i combinations that produced the five lowest values of the negative log-likelihood (NLL) function when optimized over ρ_i and κ_i ; this handles cases when the global optimum may not be near the lowest NLL value along a coarser grid. We then used a finer grid, this time with t_i values spaced 7 days apart, to more thoroughly search these optimal regions. Once again, the 5 lowest NLL values were taken from the 7-day grid for further exploration. We repeated this process with a 3-day grid before finally optimizing along a 1-day grid. By using many grids with a temporal resolution increasing roughly by a factor of two, our algorithm found the optimum much more quickly than using fewer grids, because within each grid there were few t_i combinations to be tested.

We generated a parametric bootstrapping algorithm that estimates 95% confidence intervals for our model's parameters. We cannot obtain confidence intervals using more standard methods (e.g., Wald-type estimations or likelihood profiles) because the likelihood function includes $I_{mig}(t)$, which resembles a step function. The likelihood function is not continuous with respect to the t_i parameters, which shift the position of $I_{mig}(t)$. To generate confidence intervals for an individual migration, we simulated random paths with the same size and temporal extent as the true migratory path. The number of random paths necessary to generate consistent confidence intervals varied depending on the dataset. These simulated paths were generated using the likelihood function and parameterized based on the maximum likelihood estimate for each of the model parameters from the true path. We then fit the model to each of these paths independently and used the distribution of the parameter estimates from each random path to obtain confidence intervals (taking the 2.5% and 97.5%

quantiles as lower and upper confidence bounds, respectively). The process of re-simulating data according to the estimated parameter values has been used in time-series data for many purposes, including calculating confidence intervals (Dennis and Taper, 1994; Kunst, 2008).

We conducted all data preparation and model fitting using R 4.2.1 (R Core Team, 2021). We obtained maximum likelihood estimates for the ρ_i and κ_i (with the t_i fixed) using the R Template Model Builder (TMB) package (Albertsen et al., 2015; Kristensen et al., 2016).

5.2.3 Simulation analysis

We simulated migratory movement as a series of random step lengths and turning angles, which form a complete path when taken together. Simulation analyses like these allow us to directly compare parameter estimates to "true" parameter values, which cannot actually be identified from animal tracking data. We simulated movement paths over 200 days with 1 observation per day (note that the use of "day" here is for clarity as the time units are arbitrary). Between days 70 and 100, we simulated step lengths from an exponential distribution with a mean step length of 45 km (once again, the spatial units are arbitrary) and turning angles from a von Mises distribution with concentration parameter $\kappa = 0.5$. Outside of this simulated "migratory period", these values changed to 5 km and $\kappa = 0$, respectively. Once we constructed complete movement paths, we randomly removed points such that approximately 150 of the 200 complete "steps" (groups of three consecutive points necessary for calculating turning angles) remained. We accomplished this by removing each point with a probability of 12.5%, which would remove approximately 25% of the complete steps in the data.

We compared our model to three commonly used approaches by fitting them to simulated migratory movement paths. In addition to our model, we fit the

NSD regression model from Bunnefeld et al. (2011), the FPT path segmentation model from Le Corre et al. (2014), and a path segmentation approach using daily movement distances (step lengths) from Madon and Hingrat (2014). The two path segmentation approaches use different algorithms for identifying the optimal change-points; Le Corre et al. (2014) use the penalized contrast method designed by Lavielle (2005) and Madon and Hingrat (2014) used the Pruned Exact Linear Time (PELT) algorithm designed by Killick et al. (2012). We fit the models to 50 independently simulated migratory paths, all with the same "true" parameters, and calculated the mean bias (estimated t_i - true t_i) and mean squared error (MSE; the mean of $(\text{bias})^2$ for all 50 samples). The variance of the estimator can be calculated by subtracting MSE from the square of the mean bias, gauging the precision of the model. We used the `adehabitatLT` R package (Calenge, 2006) to compute FPT time-series and identify change-points in those time series. We used the `changept` R package (Killick and Eckley, 2014) to run the PELT algorithm. We provide more detail on the implementation of each of these methods in the Appendix.

5.2.4 Case studies

5.2.4.1 Ferruginous hawks in the Great Plains

Ferruginous hawks are large, migratory raptors found in central Canada and United States (Schmutz and Fyfe, 1987; Schmutz et al., 2008). The shortgrass prairies of southern Alberta, Canada represent the northern edge of this species's breeding range, and birds breeding this far north make relatively long migrations to the southern Great Plains in the United States (Watson and Keren, 2019). Adult ferruginous hawks were captured at nest sites during the breeding season, using either a dho-gaza net or a bal-chatri trap (Watson, 2020). Captures were limited to nests in which the young had survived at least 10 days. Once

captured, the birds were fitted with solar ARGOS/global positioning system (GPS) platform transmitter terminals and solar Groupe Special Mobile (GSM) tags. ARGOS tags recorded a location every 1 hour and GSM tags recorded a location as frequently as every 1 minute (Watson, 2020), so we rarefied each movement track to one location per hour for consistency. Our dataset includes 50 individual hawks tagged on their breeding territories in southeastern Alberta and spans 10 years (2012-2021). The tags also provided estimates of dilution of precision (DOP) in the horizontal and vertical directions for every location. We removed any locations with a DOP over 5 in either the horizontal or vertical directions in preparation for our analysis (Edenius, 1997).

We isolated each individual migration (fall or spring) temporally so we could fit our model with $k = 1$ to them separately. Each hawk was originally tagged on its breeding territory so we used the date at which the first location was received for each individual as the cut-off point between spring and fall. To define a cut-off between the end of fall migration and the beginning of spring migration (i.e., the birds' arrival at the wintering grounds), we used the date at which the southernmost location was recorded in each year. Once these separations were made, we removed any migrations that were missing a significant section of data, either spatially (any migration containing a location that was further than 400 km away from the previous recorded location) or temporally (any migration containing a 14-day period without any recorded locations). The temporal resolution, or fix rate, of a movement dataset has a significant effect on the results of many movement analyses (Jerde and Visscher, 2005; Thurfjell et al., 2014), so we fit the model to the hawk movement tracks rarefied to 1-hour, 12-hour, and 24-hour fix rates. We bounded t_1 and t_2 such that $t_2 - t_1$ needed to be greater than 7 days, as anything shorter would represent a biologically unrealistic migration (Watson and Keren, 2019). We also estimated

95% confidence intervals for each individual migration using the parametric bootstrapping method described above. We simulated 100 random paths for each true migratory path. We ran the algorithm multiple times for the same migration and comparing the intervals to ensure that this number of paths produced consistent confidence intervals.

Like many animal species, ferruginous hawks display complex migratory patterns including stopovers and pre-migratory dispersal (Watson et al., 2018; Watson and Keren, 2019). Stopover behaviour is defined as the interruption of migration over some temporal period (Rappole and Warner, 1976) and is very diverse, just like migration itself (Salewski et al., 2007; Evans and Bearhop, 2022; Schmaljohann et al., 2022). Stopovers have many functions and differentiating long-term, foraging stopovers from shorter stopovers may be important in identifying critical habitat for migratory species (Green et al., 2002). During fall migration, many ferruginous hawks display long-term stopovers; Watson and Keren (2019) consider these fall movements to be two separate migrations partitioned by the stopover. Ferruginous hawks also frequently embark on pre-migratory movements, where they disperse from their breeding or winter territory before returning to the same general area (Watson et al., 2018). To evaluate whether our model could statistically identify stopovers and other complexities from the ferruginous hawk data, we compared our model fits with $c = 1$ (one migration) to those with $c = 2$ (two migrations) using Akaike Information Criterion (AIC) and Bayesian Information Criterion (BIC). AIC and BIC compare models by incorporating the maximum log-likelihood estimate along with the complexity of the model, quantified by the number of free parameters. Both metrics are used to select the most parsimonious model but when sample size is large, BIC is more likely than AIC to select models with fewer parameters (Burnham and Anderson, 2004). The model associated with the lowest AIC or

BIC value is assumed to be the most parsimonious, and the difference in AIC or BIC between the best model and other models (ΔAIC or ΔBIC , respectively) quantifies how much more parsimonious the best model is. The likelihood ratio test, another common model comparison metric, is not applicable to our model because our likelihood function is not continuous (Self and Liang, 1987).

We performed a short simulation analysis to evaluate whether AIC or BIC could reliably identify stopovers when they were knowingly present (i.e., incorporated into the simulation). We used the same process described in Section 5.2.3 to generate simulated movement paths but here, our simulation parameters were informed directly by the observed migration timings from ferruginous hawks. See the Appendix for more details on how we parameterized these simulations.

5.2.4.2 Barren-ground caribou in northern Canada

Caribou are one of the most well-studied species in the animal kingdom (Seip, 1992; Vors and Boyce, 2009; Festa-Bianchet et al., 2011). The many subspecies and ecotypes of caribou exhibit different life history and foraging strategies (Nagy et al., 2011), and the barren-ground caribou herds in the North American Arctic are notable for their migratory behaviour (Lent, 1966; Fleck and Gunn, 1982; Gunn and Miller, 1986; Torney et al., 2018). Our caribou data were collected for the Qamanirjuaq herd, which ranges across Nunavut’s Kivalliq region for much of the spring and summer. This herd moves annually between their more southern winter grounds and their calving and summer ranges further north. Caribou do not always display high inter-annual fidelity to their wintering grounds (Fullman et al., 2021) but, in part due to the gathering of large herds which facilitates social learning, the herd displayed high fidelity to their calving grounds for at least 40 years (Gunn et al., 2012). Pregnant females that arrive on the calving grounds give birth to their calves shortly after, and

dramatically reduce their movement for up to two weeks (DeMars et al., 2013; Mallory et al., 2020). Identifying the temporal extent of barren-ground caribou migration has management implications, especially as climate change and anthropogenic modifications to the landscape alter the phenology and availability of their food resources (Chen et al., 2018; Mallory et al., 2020). Many efforts have been made to identify these timings in other herds (DeMars et al., 2013; Le Corre et al., 2014; Torney et al., 2018).

We fit the migration model with $c = 1$ to data describing the spring migrations of barren-ground caribou. Caribou were pursued via helicopter and immobilized via net-gunning, before being fitted with a GPS collar (Mallory et al., 2020). Following approved protocols, caribou were collared between 2006 and 2016 and in total, we included 35 adult females in the dataset, of which 22 were tracked for more than 1 year. We isolated each individual year and sub-setted the data such that any locations after July 1 of that year were omitted. We chose this date because it is after the calving period (Mallory et al., 2020) but earlier than the onset of fall migration (Le Corre et al., 2017). The fix rates of each individual in the dataset varied from 1 hour to 1 day, so we rarefied all the data to a 1-day fix rate for consistency. Similarly to the ferruginous hawk dataset, we removed any migrations with significant spatial (150 km between two consecutive recorded locations) or temporal (any 14-day period without recorded locations) gaps from our dataset.

Caribou migrations are well-studied, so we compared migration timings from our model to those identified by an existing, commonly used approach (Bunnefeld et al., 2011). This approach involves fitting a non-linear (specifically, logistic) curve to an animal’s net squared displacement as a function of time. When only modelling one migration (and not the return back to the wintering grounds), the NSD model contains three parameters (see Equation 3 of

Bunnefeld et al., 2011): the asymptotic NSD value δ , the peak or "centre" of migratory movement θ , and the quarter-duration of migration ϕ . The beginning and end of migration are estimated based on the estimates of θ and ϕ :

$$\begin{aligned}\hat{t}_{1,NSD} &= \theta - 2\phi, \\ \hat{t}_{2,NSD} &= \theta + 2\phi.\end{aligned}\tag{5.6}$$

To leverage the wealth of information on barren-ground caribou migration and calving, we fit a second version of our model that incorporated *a priori* knowledge of calving phenology. Caribou calving can be identified from movement data because when females give birth to calves, they greatly reduce their movement rate (DeMars et al., 2013). We used the broken-stick regression method developed by DeMars et al. (2013) to identify the beginning of the calving period, which also conveniently signaled the end of spring migration. With this information to our advantage, we fit the migration model again, but this time we fixed t_2 to be equal to the date at which calving began, and only optimized along t_1 . This reduces the complexity of our grid and allowed us to optimize t_1 immediately along the 1-day timescale, without need for the iterative grid-search method described in Section 2.2. We visually compared the results from the NSD model, our model with no *a priori* information, and our model with *a priori* information to determine which model was most effective in identifying meaningful shifts in caribou movement behaviour.

5.2.4.3 Brown bears in northern Canada

Brown bears are opportunistic omnivores with a wide distribution across North America, Europe, and Asia (Pasitschniak-Arts, 1993). Brown bears in the Canadian Arctic are unique in comparison to their conspecifics worldwide, ex-

hibiting many adaptations to harsh environmental conditions (Edwards and Derocher, 2015). Brown bears are not considered migratory, but bears living in the Mackenzie River Delta region of northern Canada display annual home range shifts (Edwards et al., 2009) and, as demonstrated by Chapter 3, perform temporally oriented navigations to food resources visited a year prior. We used brown bear movement data from the Mackenzie Delta to evaluate if our model would identify any patterns in what biologists view as a non-migratory species. Brown bears were captured, immobilized, and equipped with GPS collars between 2003 and 2006 (Edwards et al., 2009). These collars were set to record GPS locations at a 4-hour fix rate. Brown bears in the Canadian Arctic spend up to 6-7 months of the year in a den where they hibernate (Halloran and Pearson, 1972; Nagy et al., 1983; McLoughlin et al., 2002). In total, we included 30 bears (24 females, 6 males) in our analysis.

Given the broad definitions of migration (Dingle and Drake, 2007) and the simplicity of our model, we saw value in searching for population-level trends in periods of high-intensity movement within the brown bear dataset. We fit the model with two migratory periods ($c = 2$) to every individual year in the dataset (many individuals had more than one complete year of data), under the assumption that bears would need to exhibit at least two periods of high-intensity movement to complete their theoretical migratory cycle. We then collectively analyzed the population-level distribution of t_i for each model to determine whether any trends persisted.

5.3 Results

The specific parameter estimates, confidence intervals, and more for each individual migration can be found in Supplementary File 1, which is stored online at github.com/pthompson234/migrationmodelling.

5.3.1 Simulation analysis

Our model was more precise and accurate than other migration modelling approaches when fit to simulated data (Table 5.1). When the number of change-points (here, two) is known, our model estimated the temporal duration of migration to within 1 day, on average. Applying the PELT algorithm (Killick et al., 2012; Madon and Hingrat, 2014) to daily distance time-series calculated from the simulated paths produced similarly accurate and precise estimates of migration timing. The NSD model does not explicitly estimate the beginning and end of migration as parameters but we calculated these quantities based on the parameters the model does estimate. These estimates displayed low bias and high variance, suggesting high accuracy and low precision. Estimating change-points with the penalized contrast method applied to first passage time data produced high bias and MSE.

Model	t_1 Bias	t_1 MSE	t_1 Variance	t_2 Bias	t_2 MSE	t_2 Variance
Our model	-0.1	2.7	2.7	0.5	1.4	1.2
NSD	4.1	182.4	165.6	-7.9	511.1	448.7
FPT	-10.4	435.7	327.5	22.0	1231.6	747.6
PELT	0.6	4.6	4.2	-3.2	45.6	35.4

Table 5.1: Bias (parameter estimate - true value) and mean squared error (MSE; bias squared) values for migration timing parameters t_1 and t_2 , estimated by fitting four different models to 50 randomly simulated migratory movement paths. Variance is calculated as the difference between MSE and (bias)². We compared our model to the net squared displacement (NSD) approach developed by Bunnefeld et al. (2011), the first passage time (FPT) approach from Le Corre et al. (2014), and the PELT algorithm used by Madon and Hingrat (2014).

5.3.2 Ferruginous hawks: stopovers and fix rates

We identified 99 unique ferruginous hawk migrations (35 fall, 64 spring). Our model precisely identified the beginning and end of these migratory movements

(a specific migration is shown in Figure 5.1). Ferruginous hawks rapidly increased their step lengths during migration but did not display as much change in their directionality. The average value of R was approximately 11.02 for ferruginous hawks sampled at a 1-hour fix rate. Before and after migration, ferruginous hawk step lengths averaged 1.34 km (the mean of all ρ_0 estimates for each migration), and this increased by 10.62 km (the mean ρ_1 estimate) during migration. Estimates of κ_0 , which quantified movement directionality outside of migration, were frequently 0, which would suggest a turning angle distribution that was either very close to uniform or not centred at 0 (Supplementary File 1). The median 95% confidence interval width for all six of our model parameters (0.39 days, 0.33 days, 0.10 km, 2.99 km, 0.06, and 0.18 for t_1 , t_2 , ρ_0 , ρ_1 , κ_0 , and κ_1 , respectively) suggests that all model parameters are estimable (Supplementary File 1). Independent runs of the parametric bootstrapping algorithm produced similar results for the same data. The largest confidence interval width for either timing parameter (t_1 or t_2) for any individual was 26.88 days, and no other confidence interval for these parameters was wider than 8 days.

The $c = 2$ model identified the timing and location of stopovers and pre-migratory movements in ferruginous hawks. Fall migrants frequently exhibited stopover behaviour, sometimes migrating for >500 km before drastically and temporarily reducing their movement rates. The $c = 1$ model occasionally identified only one portion of the fall migration in these cases, but sometimes ignored the stopover altogether (Figure 5.2). The $c = 1$ model typically ignored pre-migratory movements but sometimes included them as part of the migration (Figure 5.3). The $c = 1$ model was identified as less parsimonious than the $c = 2$ model when compared with AIC and BIC when these behaviours were present (Supplementary File 1). For example, the migration depicted in Figure 5.2 had much lower AIC and BIC values with the $c = 2$ model ($\Delta\text{AIC} = 1879.0$; $\Delta\text{BIC} =$

1866.6, with 1-hour fix rate). The results were similar for the migration depicted in Figure 3 ($\Delta\text{AIC} = 104.6$; $\Delta\text{BIC} = 93.6$, with 1-hour fix rate). Our simulation analysis provides further support for AIC and BIC as consistent identifiers of stopovers (Supplementary File 1).

Varying the fix rate of our data did not significantly affect the estimation of ferruginous hawk migration timings but did affect the estimates for step length and turning angle parameters. In some of the migrations with long-term stopovers or pre-migratory movements, the $c = 1$ model estimated different t_i values at different fix rates (e.g., Figure 5.2). For $c = 2$, temporal parameter estimates were more consistent (Supplementary File 1). Estimates for ρ_0 and ρ_1 were unsurprisingly highest at long fix rates. The mean values of ρ_0 and ρ_1 were 5.18 km and 131.40 km, respectively, when we fit the model to the 24-hour data. The hawks' proportional increase in movement speed, R , appear larger at higher fix rates (59.4 with the 24-hour data and 39.8 for the 12-hour data). Estimates for κ_0 were very close to, if not exactly, 0 at all fix rates. The mean estimate for κ_1 increased from 0.48 with 1-hour fix rates to 1.34 with 24-hour fix rates.

5.3.3 Caribou: incorporating calving phenology

After filtering the caribou data, we retained 57 individual spring migrations to which we fit the $c = 1$ migration model. In many cases, the model identified a biologically reasonable migratory period. The NSD model did the same but often failed to precisely estimate the beginning and/or end of migration. In the example from Figure 5.4, the NSD model estimated a migration that started 7 days later and ended 2 days earlier than our model. From visual inspection, it appears that our model correctly captures more of the linear migratory component than the NSD model. However, for some caribou-years, our model misidentified a period of sustained movement on the wintering grounds as migration,

rather than identifying the spring movement to the calving grounds (Figure 5.5, Supplementary File 1). In many of these cases, the NSD model picked a more appropriate midpoint but still failed to properly characterize the beginning and end of migration (Figure 5.5). By estimating t_2 from broken-stick regression models fit to caribou step length data (DeMars et al., 2013), the model consistently identified the biologically relevant spring migratory period. Supplying the model with this additional information remedied the problematic model fits like the example displayed in Figure 5.5, and allowed us to pinpoint the day at which each caribou began migrating.

Caribou did not increase their speed as much as ferruginous hawks during migration, as the mean value of R was 3.95 (Supplementary File 1). However, 49 of the migrations displayed significantly higher directional persistence on migration, with 95% confidence intervals for κ_1 excluding 0. The median confidence interval width for t_1 , ρ_0 , ρ_1 , κ_0 , and κ_1 were 16.5 days, 1.21 km, 9.43 km, 0.37, and 1.87, respectively. Individuals with low estimated values of ρ_1 and κ_1 were an exception, because paths simulated by our bootstrapping technique exhibited little change during the migratory period (Supplementary File 1). The six migrations with a 95% confidence interval for t_1 that was wider than 100 days all satisfied $\kappa_1 < 0.6$ (compared to the mean value of 2.05), and five of the six satisfied $\rho_1 < 4$ km (compared to the mean value of 9.14 km).

5.3.4 Brown bears: application to non-migrants

We fit the $c = 2$ model to 42 different bear-years and could not identify any trends throughout the population. According to the model results, 29 of the individuals spent over half of their active season "migrating", and 11 "migrated" for over 75% of the active season (Supplementary File 1). In other individuals, the duration of one or both of the theoretical migratory periods was 7 days or shorter. While the model appears to have identified periods in which brown

bears moved more quickly and/or less tortuously for a number of days or weeks, there was no consistency within the population as to when these periods took place or how long they lasted (Figure 5.6).

5.4 Discussion

Identifying when animals migrate is crucial to understanding and predicting changes in migration phenology as a response to climate change (Hardesty-Moore et al., 2018). We designed a model that synthesizes these existing approaches to estimate the timing of an animal's migration. Our model outperformed competing approaches when fit to simulated data (Table 5.1), and also identified biologically reasonable timings for migratory mammals and birds (Figures 5.1 and 5.4). We failed to identify any significant trends in migration-like behaviour for animals that are not considered migratory (Figure 5.6). The model relies on step lengths and turning angles, which are ubiquitous in animal movement modelling and can be calculated easily (Morales et al., 2004). As a result, the parameters we estimated with the model have direct biological interpretations that help describe multiple facets of migration. Our model explicitly estimated the beginning and end of migratory movement and was more accurate than commonly used methods, which we demonstrated using simulated migratory paths for which "true" parameter values were known. When fit to animal tracking data, our model estimated biologically reasonable (e.g., Figure 5.1) timings with high certainty, according to our 95% confidence intervals. The model does not require *a priori* biological knowledge of a system to identify timings, but is also flexible to include this information if it improves results (Figure 5.5). Applying our model to other migratory systems will further identify how it can most effectively be used.

In addition to the beginning (t_1) and end (t_2) of migration, our model es-

timated parameters that quantify exactly how an animal's movement changes during migration. By combining step lengths and turning angles to identify migration in ferruginous hawks and barren-ground caribou, our model facilitated a connection between parameter estimates and the biological definitions of migration for these species. We used $R = \frac{\rho_1 + \rho_0}{\rho_0}$ and $\kappa_1 - \kappa_0$ to quantify increases in speed and directionality during migration, respectively, as they can be easily compared between species. Ferruginous hawks moved in a more directed manner during migration, but also moved much more quickly (Supplementary File 1). Migratory ferruginous hawks typically moved 10 times as far during migration than they would otherwise, as the second definition of migration provided by Dingle and Drake (2007) postulates. Migratory barren-ground caribou dramatically increased the directional persistence of their movement during migration and did not "speed up" as much as the ferruginous hawks did (Supplementary File 1). These migrations resembled the "undistracted and persistent" definition of migration from Dingle and Drake (2007).

Fix rate did not dramatically affect t_i estimates for the ferruginous hawk dataset, but estimates of the ρ_i and κ_i varied. It is unsurprising that step lengths become longer as fix rates become longer, but notably, ρ_i estimates did not scale linearly with fix rate. In other words, the estimated value of ρ_0 with data sampled at 24-hour fix rates was less than 24 multiplied by the corresponding ρ_0 at 1-hour fix rates. We advocate for using R to compare how different animals migrate but this quantity also varies with fix rate, so this must be controlled before comparing different datasets (e.g., by subsampling, as we did here). Sampling data to coarser fix rates omits the tortuosity of movement at smaller scales, so longer step lengths underestimate movement speed (Postlethwaite and Dennis, 2013). Longer fix rates also produce straighter turning angles (Jerde and Visscher, 2005), which our model quantified with

larger κ_i values.

We applied parametric bootstrapping to our model to obtain confidence intervals, and in most cases these intervals suggest high certainty in our parameter estimates (Supplementary File 1). If ρ_1 and κ_1 are both small, the simulated path would not change much during the simulated "migratory" period, making the change-point difficult to estimate. Typically, this is not the case in migratory animals, although some of the caribou paths displayed this result. When this was the case, 95% confidence intervals for all parameters were concerningly wide (Supplementary File 1). These migrations were also difficult to estimate with the NSD model, which typically produced biologically suspicious results in these cases. Accounting for uncertainty in path segmentation models is difficult because of the focus on dividing movement into discernible sections (Edelhoff et al., 2016). We hope our application of parametric bootstrapping to this problem encourages ecologists to incorporate the uncertainty of change-point algorithms into their analyses.

Unlike simple threshold-based approaches, our model does not require any biological knowledge of the tracked animals. Nevertheless, incorporating *a priori* information about an animal's movement ecology is easy because of our grid-based temporal optimization approach. We directly controlled the set of t_i values included in our parameter space, allowing for the removal of biologically unreasonable timings. This process has the added benefit of reducing computational time. By estimating the beginning of the calving period in adult female caribou (DeMars et al., 2013), we removed an entire parameter (t_2) from optimization. The discrete-time nature of the data for which our model is intended along with our optimization algorithm allows for effective manipulation and improvement of the analysis, but only if necessary.

AIC and BIC were both effective at separating ferruginous hawk migrations

with stopovers or pre-migratory periods from those without. Here, AIC and BIC produced similar results but this may not hold at different sample sizes, and picking between AIC and BIC can be a complex problem (Burnham and Anderson, 2004). We note that our model was not effective at distinguishing between stopovers and pre-migratory periods, and this may require additional biological input. We did not test a version of the model with $c > 2$. The computational time allotted by the grid-search optimization algorithm increases exponentially with c . We are thus unsure if AIC and BIC are reliable when c is larger. Other path segmentation methods (including the PELT algorithm) use more complex techniques for identifying the optimal number of segments that make them extremely useful when the number of segments is unknown (Lavielle, 2005; Gurarie et al., 2009; Killick et al., 2012). In migratory animals, when the number of segments typically is known, our model outperformed other path segmentation approaches, but these competing models are likely more suitable otherwise.

Our model is intended to be fit to movement data for one individual, but fitting the model to several individuals in the same population characterizes the variation within that population. While analyzing the distribution of parameter values across a set of individuals (or individual migrations) is fairly straightforward (Figure 5.6), there is also an opportunity to regress our parameter estimates (particularly, the t_i parameters) against covariates. Animal populations display high individual variation with respect to their migratory behaviour (Hanski et al., 2004; Jesmer et al., 2018; Merkle et al., 2019; Byholm et al., 2022), and inter-annual variation in an animal's environment can cause an individual's migratory paths to vary from year to year (Tucker et al., 2018; Mallory et al., 2020; Franklin et al., 2022). Similarly, the effects of habitat modification and/or associated disturbance factors could also be assessed. With

the appropriate environmental data, our model could be used to explore these patterns for many animal populations.

Our model achieved the sought-after goal of determining when animals begin and end their migrations. By parameterizing time-dependent step length and turning angle distributions, we generated results that are easy to interpret biologically. Migration incurs an elevated risk to the negative effects of anthropogenic global change. Specifically, many animals are arriving at their breeding grounds earlier to capitalize on global warming-induced advances in green-up and prey availability (Haest et al., 2018; Mallory et al., 2020). Many ecologists expect (or are already observing) changes in when, where, and how animals migrate (Wilcove and Wikelski, 2008; Tucker et al., 2018). Our model provides unbiased, quantitative information on all three of these characteristics.

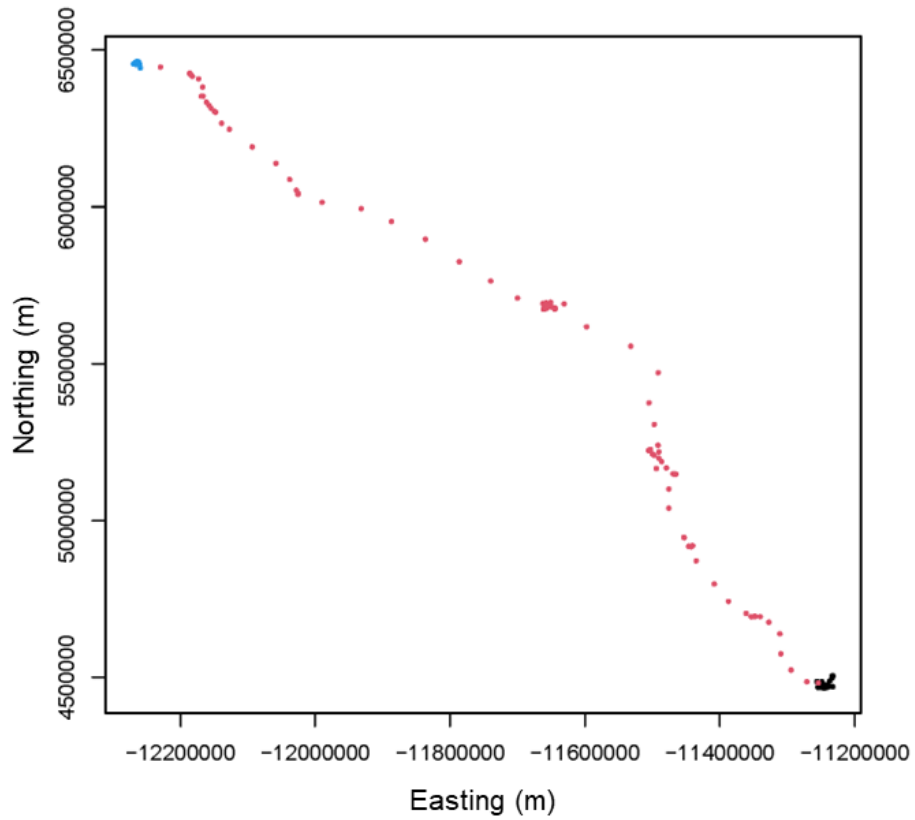
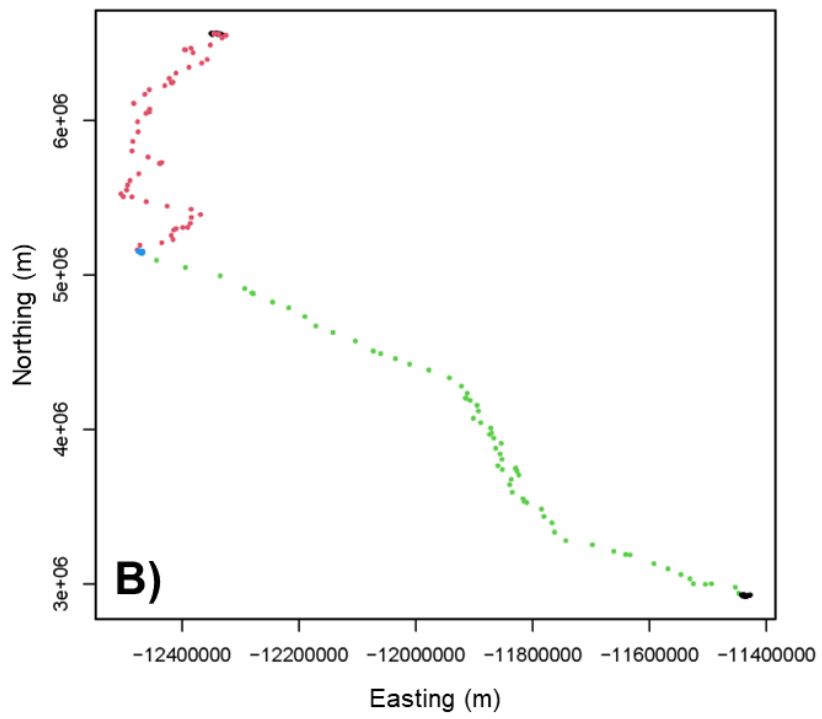
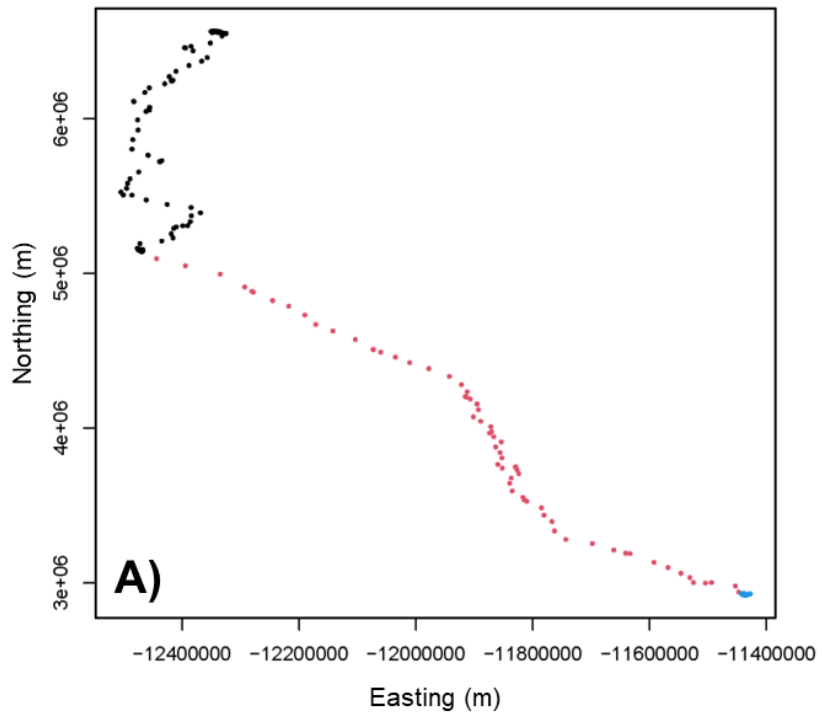


Figure 5.1: Movement path of a ferruginous hawk (hawk ID 192a; spring 2014) performing a spring migration from its wintering grounds in the southern United States to its breeding territory in southeastern Alberta, Canada. Black dots represent the wintering grounds, blue dots represent the breeding grounds, and red dots represent the migratory period as fit by our model.



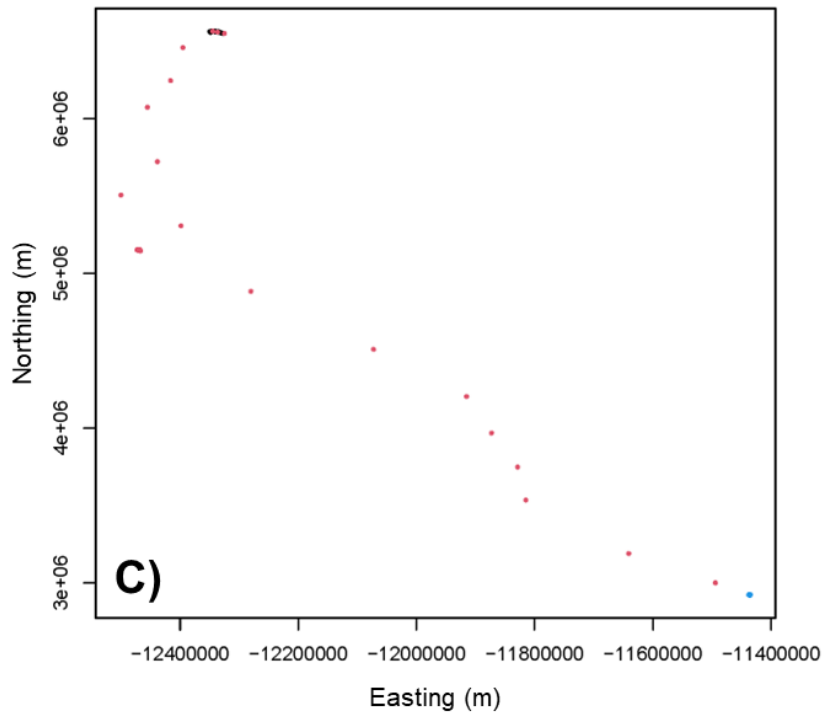
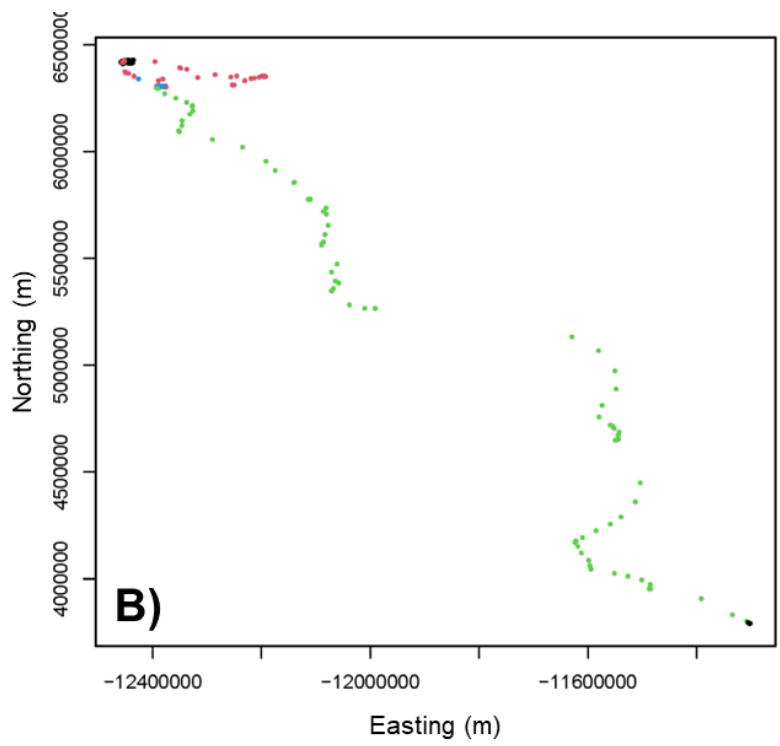
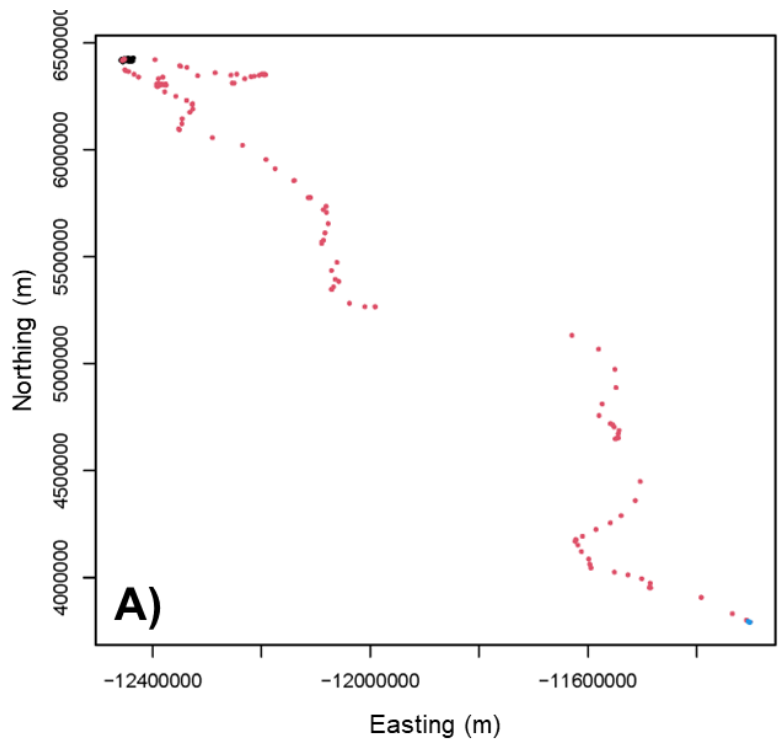


Figure 5.2: Movement path of a ferruginous hawk (hawk ID 196a; fall 2013) performing a fall migration from its breeding territory in Alberta, Canada, to its wintering grounds in the United States, including a stopover. Panel A) represents the model fit from the $k = 1$ model to the 1-hour fix rate data. Here, black dots represent the breeding grounds, blue dots represent what the model identifies as the wintering grounds, and red dots represent the migratory period. Panel B) represents the model fit from the $k = 2$ model to the 1-hour fix rate data. Here, black dots represent the breeding and wintering grounds, blue dots represent the stopover site, and red and green dots represent the first and second migrations, respectively. Panel C) represents the model fit from the $k = 1$ model to the 24-hour fix rate data. Each point is coloured similarly to in Panel A).



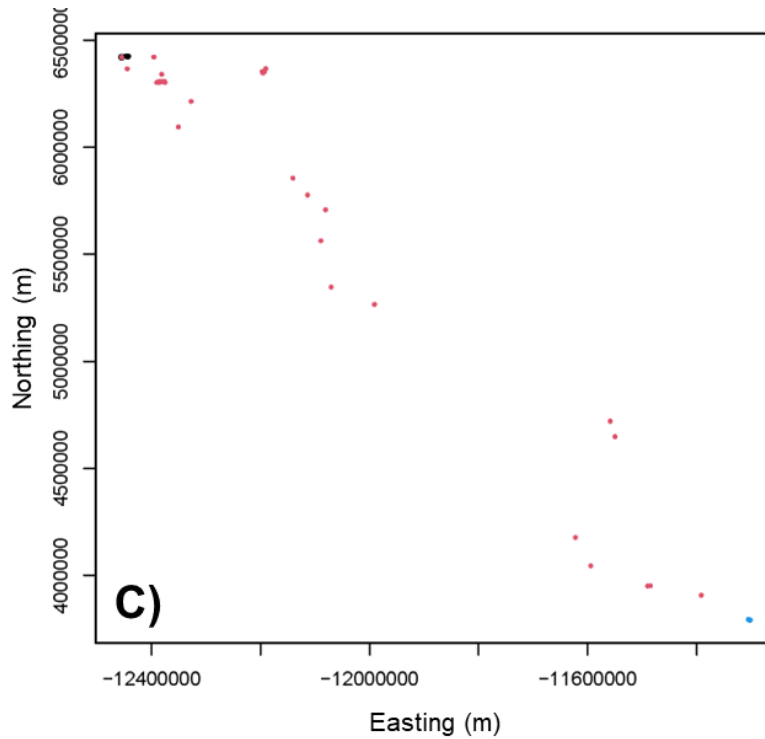


Figure 5.3: Movement path of a ferruginous hawk (hawk ID 191a; fall 2016) performing a fall migration from its breeding territory in Alberta, Canada, to its wintering grounds in the southern United States, including a pre-migratory movement. Canada. Panel A) represents the model fit from the $c = 1$ model to the 1-hour fix rate data. Here, black dots represent the breeding grounds, blue dots represent what the model identifies as the wintering grounds, and red dots represent the migratory period. Panel B) represents the model fit from the $c = 2$ model to the 1-hour fix rate data. Here, black dots represent the breeding and wintering grounds, blue dots represent the period between pre-migration and migration, and red and green dots represent what the model identifies as the first and second migrations, respectively. Panel C) represents the model fit from the $c = 1$ model to the 24-hour fix rate data. Each point is coloured similarly to in Panel A).

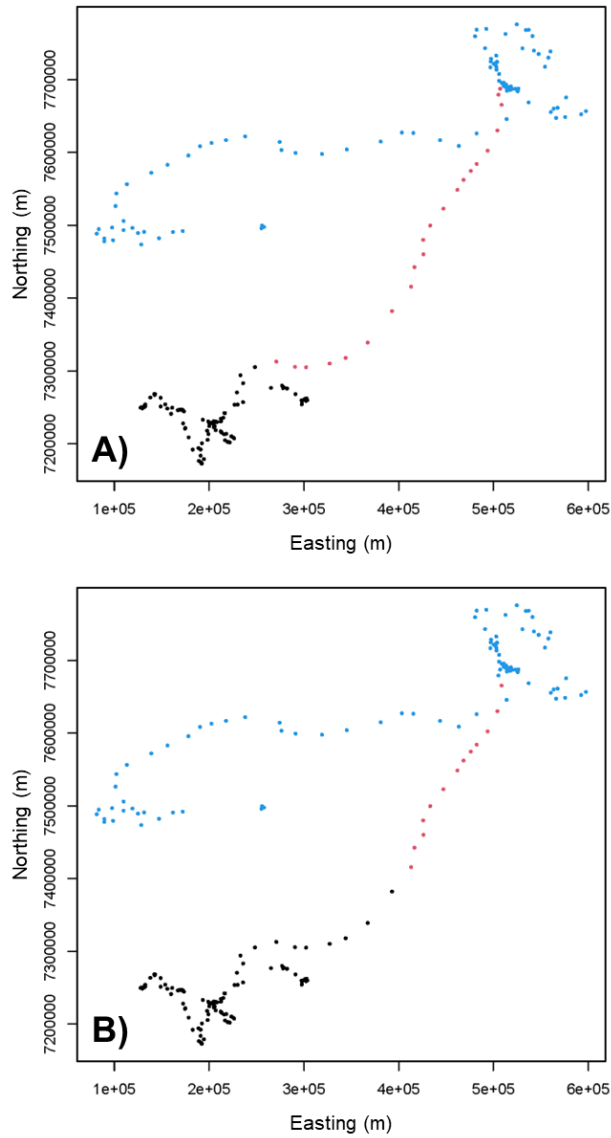
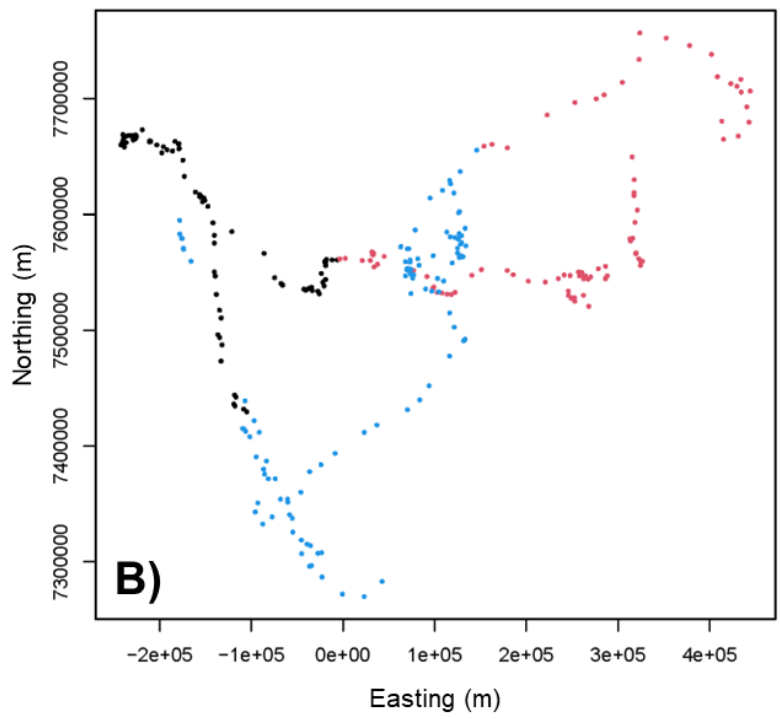
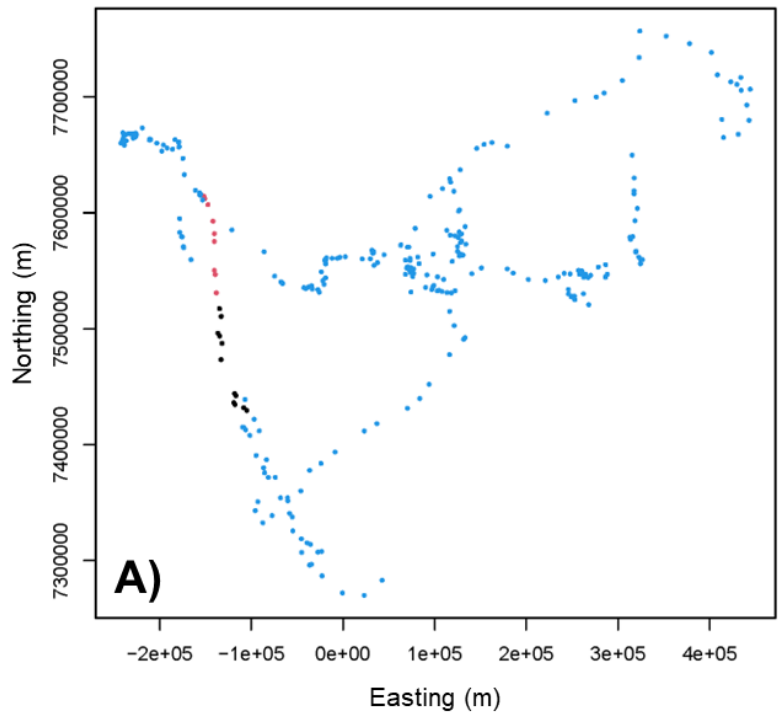


Figure 5.4: Movement path for a female caribou (caribou ID BL0560413; year 2016) in the Qamanirjuaq herd in Canada. Here, panel A) illustrates the migration timing estimates from our model, and panel B) illustrates the migration timing based on the NSD method developed by Bunnefeld et al. (2011). In both panels, black dots represent the wintering grounds, red dots represent migratory movement, and blue dots represent post-migratory movement. The calving grounds can be visually identified as a tightly packed clump of points just east of the end of migration.



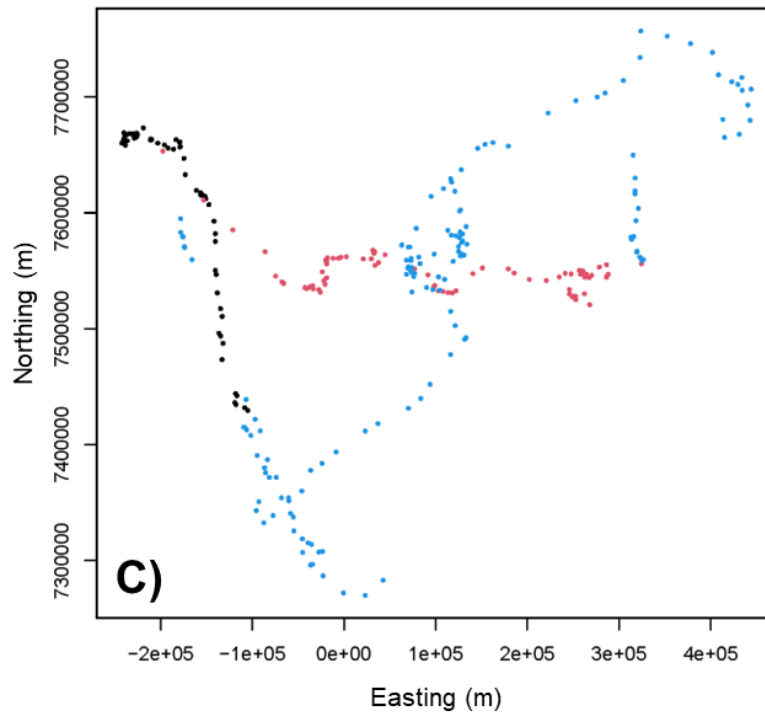


Figure 5.5: Movement path for a female caribou (caribou ID QM0830508; year 2011) in the Qamanirjuaq herd in Canada. In all three panels, black dots represent the wintering grounds, red dots represent migratory movement, and blue dots represent post-migratory movement. The calving grounds can be visually identified as a tightly packed clump of points just east of the end of migration. Here, panel A) illustrates the migration timing estimates from our model without *a priori* knowledge of calving phenology, and panel B) illustrates the migration timing based on the NSD method developed by Bunnefeld et al. (2011). Panel C) displays the fit from our model after using the technique developed by DeMars et al. (2013) to estimate t_2 , the onset of calving and end of spring migration.

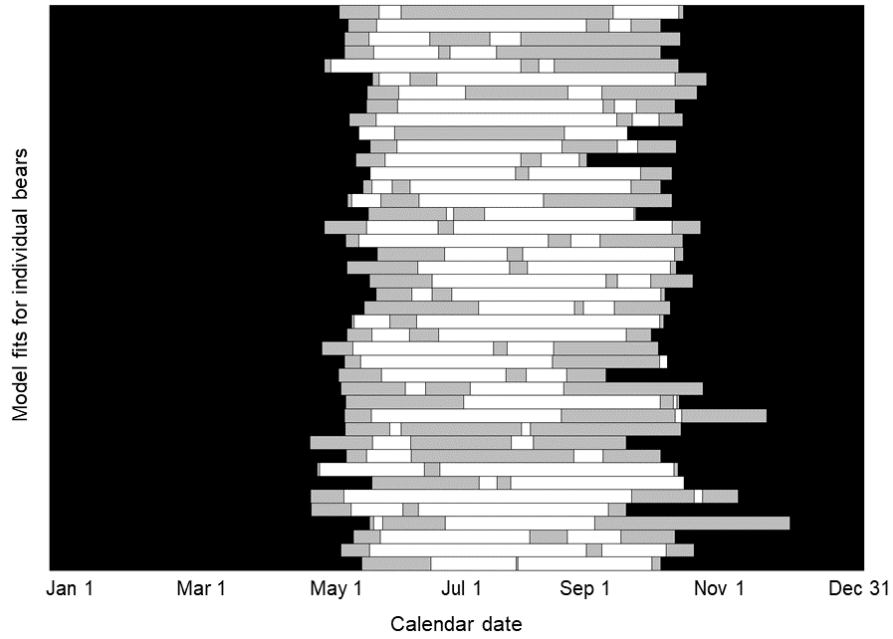


Figure 5.6: Distribution of theoretical Mackenzie Delta brown bear migratory patterns for 30 individuals (46 bear-years). Portions of the graph shaded in black represent the denning period each year, gray-shaded portions represent non-migratory portions (either before, between, or after both the migrations), and white portions represent theoretical migrations identified by the $c = 2$ migration model.

6 General conclusion

6.1 Statistical models as a window into animal cognition

Identifying exactly why animals make the decisions they do is extremely difficult. We cannot directly perceive these cognitive processes but we can develop statistical models that elucidate this behaviour. This realization has inspired exciting and innovative modelling work which has improved our knowledge of animal foraging and memory (van Moorter et al., 2009; Fagan et al., 2013; Pritchard et al., 2016; Lewis et al., 2021). Chapters 2, 3, 4, and 5 contribute to this wealth of literature and advance the budding field of memory-informed movement ecology. We developed a statistical model that can characterize spatiotemporal memory in moving animals, specifically by identifying how long they wait before returning to previously visited patches. The model builds on existing work, expanding on the "time since last visit" concept (Schlägel and Lewis, 2014; Schlägel et al., 2017) to account for animals that return to these patches after a specific time lag (Janmaat et al., 2013; Edwards and Derocher, 2015). In Chapter 3 we documented seasonal revisitation patterns in brown bears and, using the model described in Chapter 2, identified spatiotemporal memory as a driver of these movements. The model developed in Chapter 5 takes a statistical approach to identify behavioural shifts in migratory animals. The model estimates when animals start and stop migrating while also describing how movement patterns change during migration. Mechanistic links between memory and movement have been explored using a variety of simulation-based approaches that generate realistic, memory-informed foraging movements (Augar et al., 2013; Riotte-Lambert et al., 2015; Bracis and Mueller, 2017; Aarts et al., 2021). We built on the principles of these simulated foragers in Chapter 4, using repeated simulations as a model for learning in animals. Our model

connects spatial memory and learning which recent work has suggested are intertwined (Jesmer et al., 2018; Lewis et al., 2021). Taken together, the original work presented here has produced important conclusions about optimal foraging and animal cognition while also providing diverse opportunities for future research.

A key component of the work discussed here involves the implementation of temporal dynamics into spatial memory for movement models. These dynamics come about as a result of many different mechanisms, from depletion-recovery dynamics (González-Gómez et al., 2011) to prey vigilance (Schlägel et al., 2017) to seasonally available resources (Janmaat et al., 2013; Lafontaine et al., 2017), all of which can be handled by the model described in Chapter 2. Chapter 5 focuses on identifying the temporal extent of migration, using movement data to estimate the temporal extent of this behaviour. Both of these models required optimizing a likelihood function that contained some sort of temporal parameter (in Chapter 2, μ and σ ; in Chapter 5, t_1 and t_2). In both these cases, optimizing the likelihood function was made difficult by the temporal parameters, which produced many local optima. These numerical problems need to be addressed for ecologists to further explore models with temporal parameters, as they have many uses in ecology, and we handled these issues in both chapters to efficiently obtain accurate maximum likelihood estimates for both models.

We developed and applied many numerical tools to draw valuable inference from animal movement data in Chapters 2-5. The R Template Model Builder (TMB; Kristensen et al., 2016) package sped up the optimization of the models from Chapters 2 and 5. TMB uses automatic differentiation to accurately and quickly obtain maximum likelihood estimates for complex statistical models, and the work discussed here would not have been possible without it. Numerical and computational advancements like these may not seem immediately applicable

for advancing movement ecology as a field, but they are vital. Chapter 4 centres around a well-known numerical technique (Bayesian MCMC sampling) in an entirely new context: simulating how animals learn. For this to be possible, we ran MCMC using an objective function that simulated an animal path, producing a metric of foraging success as its output. This framework is applicable across disciplines, from simple laboratory tasks to complex cognitive problems encountered by wild animals. The numerical innovations produced by the work described here will allow movement ecologists to continue exploring how animals perceive, memorize, and learn about their environments.

6.2 Spatiotemporal predictability and memory

The way animals use memory is theorized to depend heavily on the variability of their environment (McNamara and Houston, 1987; Fagan et al., 2013). In homogeneous environments, there are not many unique cues to remember, and in extremely heterogeneous environments, these cues are far too abundant and complex (Boyer and Walsh, 2010; Wauters et al., 2010). On a temporal scale, not only does heterogeneity of the landscape contribute to animal movement patterns, but so does predictability. Memory-informed movement has been theorized to be more useful under temporally predictable resources (Mueller et al., 2011), and when these resources are distributed heterogeneously in space, migratory patterns are expected to arise (Mueller and Fagan, 2008; Berbert and Fagan, 2012). The spatial complexity and heterogeneity of an animal's environment should also affect its perceptual range (Olden et al., 2004). Taken together, Chapters 3 and 5 suggest that migration is not the only behaviour that can arise from these environmental conditions. Brown bears in the Mackenzie Delta region forage for a wide variety of temporally predictable resources that are distributed heterogeneously on the landscape. They use time-dependent

spatial memory to navigate to these resources when they become nutritionally valuable. These seasonal movements did not align with traditional definitions of migration (Dingle and Drake, 2007), however, as no consistent migratory signal was identified for these bears in Chapter 5. These results represent an important and unique application of this theory to wild animals.

Chapter 4 expands on these results by mechanistically incorporating learning and behavioural plasticity into simulated animal movements. These behaviours require long-term tracking data for individual animals, which are infrequently available, but mechanistic simulation modelling is an alternative for identifying the value of behavioural plasticity for animals in uncertain environments. Simulated foragers were more efficient when equipped with long-term memory in temporally predictable environments, aligning with existing theory. Our individual-based model for simulated foragers was heavily informed by the model developed by Avgar et al. (2013), with a key difference being the implementation of long-distance, directed navigations to previously visited patches. In environments with spatially "clumped" resources, simulated foraging paths with many long-distance navigations were inefficient because too much time was spent travelling, but short-distance navigations allowed the simulated foragers to efficiently exploit multiple resource patches. The framework displayed in Chapter 4 can be used to further explore theory about spatiotemporal heterogeneity, predictability, and memory in animals with many different foraging strategies.

In reality, it is likely that different food resources exhibit different temporal patterns of availability, suggesting that foraging animals may revisit these resources at different timings. Territorial animals that live in seasonal environments encounter this variability in at least two distinct stages: the seasonal availability of food brought about by the region's climate, and the depletion-

recovery dynamics of food the individual eats within its territory (Davies and Houston, 1981; Berger-Tal and Bar-David, 2015). The model from Chapter 2 does not explicitly account for this although it may be possible to extend it in a way that allows for multiple time lags of revisitation.

6.3 Management applications

Understanding the value that familiarity and memory provides for wild animals informs the success of translocation and reintroduction protocols. Animals are translocated for many reasons; some of these protocols facilitate population growth while others mitigate human-wildlife conflict (Barton et al., 2015). Translocated animals are unique case studies for cognitive ecologists because the animal must learn the spatiotemporal configuration of its new environment with little prior information (Jesmer et al., 2018; Falcón-Cortés et al., 2021; Cumming et al., 2022). Animals with advanced cognitive and navigation capacities, including brown bears, are susceptible to returning to their original home range, rendering the translocation a failure (Kemink and Kesler, 2013; Milligan et al., 2018; Lorand et al., 2022). We can use the model from Chapter 2 to identify animal species that frequently navigate to previously visited locations, and as a result may not be worth translocating. Adapting the model from Chapter 4 to a simulated translocation could more explicitly forecast these processes. The success of translocation and reintroduction protocols, which can be expensive and difficult, depends on how well ecologists understand the cognitive drivers of animal movement.

Understanding where animals go is crucial for appropriately designing protected areas, which preserve landscape connectivity and gene flow (Geldmann et al., 2013; Maxwell et al., 2020). Defining the spatial extent of protected areas must be done properly to fulfill the implied management goals, and simulation-

based models have been used to compare the predicted outcome of different designs (Malishev and Kramer-Schadt, 2021; Chetcuti et al., 2022; D’Elia et al., 2022). Chapter 4 suggests that the spatial distribution of resources has direct implications on animal fitness. The learning-based simulation algorithm could be applied to animals in proposed protected area designs. For migratory species, certain spatial areas are more valuable for conservation than others. Specifically, stopover sites have been identified as candidates for protected areas due to the energetic importance they provide for migratory animals (Bonter et al., 2009; Linscott and Senner, 2021). The model described in Chapter 5 can be used to identify stopover sites, among other steps of a migratory animal’s life cycle. Accurately partitioning an animal’s movement path into behaviourally meaningful segments allows ecologists to prioritize high-quality habitat for protection.

6.4 The future of movement ecology

The model developed in Chapter 2 can be applied to many ecological systems, connecting theory on memory-informed movement with tracking data. For example, the model could be applied to a population of home range-bound animals living in less predictable ecosystems. Polar bears (*Ursus maritimus*), for example, are a close relative of brown bears but spend most of their time on sea ice, a dynamic and unpredictable environment (Auger-Méthé et al., 2016b; Lunn et al., 2016). Polar bears display site fidelity to on-land locations (Cherry et al., 2013; McCall et al., 2016) and exploring how often they return to previously visited areas of the sea ice could contribute to theory about memory and spatiotemporal predictability. Taken together, analyses of independent populations can be synthesized into conclusions about how memory is used to achieve different ecological goals. We can also expand on these models by linking them with mechanistic approaches that predict animal space-use. Incorporating mechanis-

tic models allows us to handle complex feedbacks between animals and their environments (Potts and Börger, 2022). We can also use mechanistic models to verify the accuracy of statistical models (Potts et al., 2022). Augmenting the model described in Chapter 2 to account for external variables that covary with an animal’s movement, such as resources that deplete and recover, has potential for powerful inference on animal cognition and movement.

The model described in Chapter 5 allows ecologists to estimate the temporal phenology of animal migration with minimal data. Ecologists often use seasonal boundaries to delineate periods in which an animal’s movement behaviour may change, but these seasons are not always defined precisely, typically by months (Allegue et al., 2022; Vales et al., 2022). Notably, Chapter 3 tested a similar approach that defined resources based on their seasonal availability, which was outperformed by the memory-only model for brown bears. We suggest that meaningful changes in habitat selection or other behaviours can be elucidated using the model described in Chapter 5, particularly for migratory animals. For data-rich systems this model could also be used to compare migration phenology across years for individual animals, or link migration timing to external and internal covariates. The model is very simple and as a result, it is easy to tweak what metrics are incorporated and how they are modelled statistically to better encompass how certain animals migrate. Chapters 2 and 5 can even be coupled to characterize changes in animal cognition throughout the migratory cycle.

Chapter 4 presents a novel framework that explains how animals make decisions by incorporating the outcome of previous decisions. The model builds on statistical decision theory and while we applied it to foraging, Bayesian MCMC can simulate learning in many other ecological situations, as long as the value of a task can be quantified using some objective function. The application of approximate Bayesian computation to other problems in ecology (Beaumont,

2010) suggests that our model could be "fit" to data. This approach may be most effective in laboratory studies where these decisions are under the control and surveillance of scientists, but using this approach we could potentially estimate parameters like k from animal tracking data.

Technological advances in animal tracking and remote sensing have driven methodological and scientific advances in movement ecology for decades (Kays et al., 2015), and it is likely that this trend will continue. A likely consequence of these developments will be high-resolution movement data that much more accurately approximates an animal's continuous-time path. While the data used to characterize movement may change, there is no reason to suggest that this correlates in any way to the timescale at which animals make decisions. Movement ecologists will need to develop models (either in a discrete-time or continuous-time framework) that can infer how animals perceive complex spatial environments and remember this information, even when the input data are highly autocorrelated.

We still have much to learn about how animals perceive and remember their environments. Nathan et al. (2008) divided the movement process into four components in their seminal movement ecology paper, two of which being the animal's external (environmental) and internal (cognitive) states. The former has received great attention in literature through resource selection analysis and other related methods, but as technology broadens the capability with which ecologists can analyze animal movement, characterizing the latter has become popular. Linking spatiotemporal memory with animal movement is one of the key challenges facing the next generation of movement ecologists, carrying value for theoreticians and conservationists alike. These extremely complex processes are difficult to quantify in wild animals but the diversity of approaches described in Chapters 2-5 have advanced our progress towards this goal. As the world

around us changes rapidly and predictably, understanding how animals move will be as important as ever, and the future of this question lies in learning, cognition, and memory.

References

- Aarts, G., Mul, E., Fieberg, J., Brasseur, S., van Gils, J. A., Matthiopoulos, J., and Riotte-Lambert, L. (2021). Individual-level memory is sufficient to create spatial segregation among neighboring colonies of central place foragers. *The American Naturalist*, 198(2):E37–E52.
- Abrahms, B., Hazen, E. L., Aikens, E. O., Savoca, M. S., Goldbogen, J. A., Bograd, S. J., Jacox, M. G., Irvine, L. M., Palacios, D. M., and Mate, B. R. (2019). Memory and resource tracking drive blue whale migrations. *Proceedings of the National Academy of Sciences*, 116(12):5582–5587.
- Abril-Colón, I., Alonso, J. C., Palacín, C., Álvarez Martínez, J. M., and Uceró, A. (2022). Short-distance nocturnal migration in an island endemic bustard. *Ibis*, n/a(n/a).
- Aiken, S., Dallwitz, M., Consaul, L., McJannet, C., Boles, R., Argus, G., Gillett, J., Scott, P., Elven, R., LeBlanc, M., Gillespie, L., Brysting, A., Solstad, H., and Harris, J. (2007). *Flora of the Canadian Arctic Archipelago: Descriptions, Illustrations, Identification, and Information Retrieval*. NRC Research Press, National Research Council of Canada, Ottawa, Ontario.
- Albertsen, C. M., Whoriskey, K., Yurkowski, D., Nielsen, A., and Flemming, J. M. (2015). Fast fitting of non-Gaussian state-space models to animal movement data via Template Model Builder. *Ecology*, 96:2598–2604.
- Allegue, H., Guinet, C., Patrick, S. C., Hindell, M. A., McMahon, C. R., and Réale, D. (2022). Sex, body size, and boldness shape the seasonal foraging habitat selection in southern elephant seals. *Ecology and Evolution*, 12(1):e8457.
- Allen, T. A. and Fortin, N. J. (2013). The evolution of episodic memory. *Proceedings of the National Academy of Sciences*, 110(Supplement_2):10379–10386.
- Arthur, S. M., Manly, B. F. J., McDonald, L. L., and Garner, G. W. (1996). Assessing habitat selection when availability changes. *Ecology*, 77(1):215–227.
- Asensio, N., Brockelman, W. Y., Malaivijitnond, S., and Reichard, U. H. (2011). Gibbon travel paths are goal oriented. *Animal Cognition*, 14(3):395–405.
- Auger-Méthé, M., Albertsen, C. M., Jonsen, I. D., Derocher, A. E., Lidgard, D. C., Studholme, K. R., Bowen, W. D., Crossin, G. T., and Mills Flemming, J. (2017). Spatiotemporal modelling of marine movement data using Template Model Builder (TMB). *Marine Ecology Progress Series*, 565:237–249.
- Auger-Méthé, M., Derocher, A. E., DeMars, C. A., Plank, M. J., Codling, E. A., and Lewis, M. A. (2016a). Evaluating random search strategies in three mammals from distinct feeding guilds. *Journal of Animal Ecology*, 85(5):1411–1421.

- Auger-Méthé, M., Derocher, A. E., Plank, M. J., Codling, E. A., Lewis, M. A., and Börger, L. (2015). Differentiating the Lévy walk from a composite correlated random walk. *Methods in Ecology and Evolution*, 6(10):1179–1189.
- Auger-Méthé, M., Lewis, M. A., and Derocher, A. E. (2016b). Home ranges in moving habitats: polar bears and sea ice. *Ecography*, 39(1):26–35.
- Avgar, T., Baker, J. A., Brown, G. S., Hagens, J. S., Kittle, A. M., Mallon, E. E., McGreer, M. T., Mosser, A., Newmaster, S. G., Patterson, B. R., and et al. (2015). Space-use behaviour of woodland caribou based on a cognitive movement model. *Journal of Animal Ecology*, 84(4):1059–1070.
- Avgar, T., Deardon, R., and Fryxell, J. M. (2013). An empirically parameterized individual based model of animal movement, perception, and memory. *Ecological Modelling*, 251:158–172.
- Avgar, T., Potts, J. R., Lewis, M. A., and Boyce, M. S. (2016). Integrated step selection analysis: bridging the gap between resource selection and animal movement. *Methods in Ecology and Evolution*, 7(5):619–630.
- Barker, O. E. and Derocher, A. E. (2009). Brown bear (*Ursus arctos*) predation of broad whitefish (*Coregonus nasus*) in the Mackenzie Delta region, Northwest Territories. *Arctic*, 62(3):312–316.
- Barker, O. E. and Derocher, A. E. (2010). Habitat selection by arctic ground squirrels (*Spermophilus parryii*). *Journal of Mammalogy*, 91(5):1251–1260.
- Barker, O. E., Derocher, A. E., and Edwards, M. A. (2015). Use of arctic ground squirrels (*Urocitellus parryii*) by brown bears (*Ursus arctos*). *Polar Biology*, 38(3):369–379.
- Barraquand, F. and Benhamou, S. (2008). Animal movements in heterogeneous landscapes: Identifying profitable places and homogeneous movement bouts. *Ecology*, 89(12):3336–3348.
- Barton, P. S., Lentini, P. E., Alacs, E., Bau, S., Buckley, Y. M., Burns, E. L., Driscoll, D. A., Guja, L. K., Kujala, H., Lahoz-Monfort, J. J., Mortelliti, A., Nathan, R., Rowe, R., and Smith, A. L. (2015). Guidelines for using movement science to inform biodiversity policy. *Environmental Management*, 56(4):791–801.
- Bauder, J. M., Breininger, D. R., Bolt, M. R., Legare, M. L., Jenkins, C. L., Rothermel, B. B., and McGarigal, K. (2016). Seasonal variation in eastern indigo snake (*Drymarchon couperi*) movement patterns and space use in peninsular Florida at multiple temporal scales. *Herpetologica*, 72(3):214–226.
- Bauer, S. and Hoyer, B. J. (2014). Migratory animals couple biodiversity and ecosystem functioning worldwide. *Science*, 344(6179):1242552.

- Beaumont, M. A. (2010). Approximate Bayesian computation in evolution and ecology. *Annual Review of Ecology, Evolution, and Systematics*, 41:379–406.
- Bell, G. and Collins, S. (2008). Adaptation, extinction and global change. *Evolutionary Applications*, 1(1):3–16.
- Bennett, A. T. (1996). Do animals have cognitive maps? *Journal of Experimental Biology*, 199:219–224.
- Berbert, J. M. and Fagan, W. F. (2012). How the interplay between individual spatial memory and landscape persistence can generate population distribution patterns. *Ecological Complexity*, 12:1–12.
- Berger, J. O. (1985). *Statistical Decision Theory and Bayesian Analysis*. Springer Series in Statistics. Springer New York, New York, NY.
- Berger-Tal, O. and Avgar, T. (2012). The glass is half-full: Overestimating the quality of a novel environment is advantageous. *PLOS ONE*, 7(4):e34578.
- Berger-Tal, O. and Bar-David, S. (2015). Recursive movement patterns: review and synthesis across species. *Ecosphere*, 6(9):art149.
- Berger-Tal, O. and Saltz, D. (2014). Using the movement patterns of reintroduced animals to improve reintroduction success. *Current Zoology*, 60(4):515–526.
- Blackwell, P. G., Niu, M., Lambert, M. S., and LaPoint, S. D. (2016). Exact Bayesian inference for animal movement in continuous time. *Methods in Ecology and Evolution*, 7(2):184–195.
- Bohart, A. M., Lunn, N. J., Derocher, A. E., and McGeachy, D. (2021). Migration dynamics of polar bears (*ursus maritimus*) in western Hudson Bay. *Behavioral Ecology*, 32(3):440–451.
- Bonter, D. N., Gauthreaux Jr, S. A., and Donovan, T. M. (2009). Characteristics of important stopover locations for migrating birds: Remote sensing with radar in the Great Lakes Basin. *Conservation Biology*, 23(2):440–448.
- Borger, L., Dalziel, B. D., and Fryxell, J. M. (2008). Are there general mechanisms of animal home range behaviour? a review and prospects for future research. *Ecology Letters*, 11(6):637–50.
- Boyce, M. S. and McDonald, L. L. (1999). Relating populations to habitats using resource selection functions. *Trends in Ecology & Evolution*, 14(7):268–272.
- Boyer, D. and Walsh, P. D. (2010). Modelling the mobility of living organisms in heterogeneous landscapes: does memory improve foraging success? *Philosophical Transactions: Mathematical, Physical and Engineering Sciences*, 368(1933):5645–5659.

- Bracis, C., Gurarie, E., Rutter, J. D., and Goodwin, R. A. (2018). Remembering the good and the bad: memory-based mediation of the food–safety trade-off in dynamic landscapes. *Theoretical Ecology*, 11(3):305–319.
- Bracis, C. and Mueller, T. (2017). Memory, not just perception, plays an important role in terrestrial mammalian migration. *Proceedings of the Royal Society B: Biological Sciences*, 284(1855):20170449.
- Buck, C. L. and Barnes, B. M. (1999). Annual cycle of body composition and hibernation in free-living arctic ground squirrels. *Journal of Mammalogy*, 80(2):430–442.
- Bunnefeld, N., Börger, L., van Moorter, B., Rolandsen, C. M., Dettki, H., Solberg, E. J., and Ericsson, G. (2011). A model-driven approach to quantify migration patterns: individual, regional and yearly differences. *Journal of Animal Ecology*, 80(2):466–476.
- Burn, C. R. and Kokelj, S. V. (2009). The environment and permafrost of the Mackenzie Delta area. *Permafrost and Periglacial Processes*, 20(2):83–105.
- Burnham, K. P. and Anderson, D. R. (2004). Multimodel inference. *Sociological Methods & Research*, 33(2):261–304.
- Burt, H. (1940). Territorial behavior and populations of some small mammals in southern Michigan. *Miscellaneous Publications of the Museum of Zoology*, 45:70.
- Burt, W. H. (1943). Territoriality and home range concepts as applied to mammals. *Journal of Mammalogy*, 24(3):346–352.
- Byholm, P., Beal, M., Isaksson, N., Lötberg, U., and Åkesson, S. (2022). Paternal transmission of migration knowledge in a long-distance bird migrant. *Nature Communications*, 13(11):1566.
- Cagnacci, F., Focardi, S., Ghisla, A., van Moorter, B., Merrill, E. H., Gurarie, E., Heurich, M., Mysterud, A., Linnell, J., Panzacchi, M., May, R., Nygård, T., Rolandsen, C., and Hebblewhite, M. (2016). How many routes lead to migration? Comparison of methods to assess and characterize migratory movements. *Journal of Animal Ecology*, 85(1):54–68.
- Calenge, C. (2006). The package “adehabitat” for the R software: A tool for the analysis of space and habitat use by animals. *Ecological Modelling*, 197(3):516–519.
- Calsbeek, R. and Sinervo, B. (2002). An experimental test of the ideal despotic distribution. *Journal of Animal Ecology*, 71(3):513–523.
- Cantrell, R. S., Cosner, C., Deangelis, D. L., and Padron, V. (2007). The ideal free distribution as an evolutionarily stable strategy. *Journal of Biological Dynamics*, 1(3):249–271.

- Castellano, S., Cadeddu, G., and Cermelli, P. (2012). Computational mate choice: Theory and empirical evidence. *Behavioural Processes*, 90(2):261–277.
- Castro, L. and Wasserman, E. A. (2010). Animal learning. *WIREs Cognitive Science*, 1(1):89–98.
- Charnov, E. L. (1976). Optimal foraging, the marginal value theorem. *Theoretical Population Biology*, 9(2):129–136.
- Chen, W., Adamczewski, J. Z., White, L., Croft, B., Gunn, A., Football, A., Leblanc, S. G., Russell, D. E., and Tracz, B. (2018). Impacts of climate-driven habitat change on the peak calving date of the Bathurst caribou in Arctic Canada. *Polar Biology*, 41(5):953–967.
- Cherry, S. G., Derocher, A. E., Thiemann, G. W., and Lunn, N. J. (2013). Migration phenology and seasonal fidelity of an Arctic marine predator in relation to sea ice dynamics. *Journal of Animal Ecology*, 82(4):912–921.
- Chetcuti, J., Kunin, W. E., and Bullock, J. M. (2022). Species’ movement influence responses to habitat fragmentation. *Diversity and Distributions*, n/a(n/a).
- Chevin, L.-M., Lande, R., and Mace, G. M. (2010). Adaptation, plasticity, and extinction in a changing environment: Towards a predictive theory. *PLOS Biology*, 8(4):e1000357.
- Chib, S. and Greenberg, E. (1995). Understanding the Metropolis-Hastings algorithm. *The American Statistician*, 49(4):327–335.
- Christiansen, F., Esteban, N., Mortimer, J. A., Dujon, A. M., and Hays, G. C. (2016). Diel and seasonal patterns in activity and home range size of green turtles on their foraging grounds revealed by extended Fastloc-GPS tracking. *Marine Biology*, 164(1).
- Clapham, M., Nevin, O. T., Ramsey, A. D., and Rosell, F. (2012). A hypothetico-deductive approach to assessing the social function of chemical signalling in a non-territorial solitary carnivore. *PLoS One*, 7(4):e35404.
- Clayton, N. S. and Dickinson, A. (1998). Episodic-like memory during cache recovery by scrub jays. *Nature*, 395(6699):272–4.
- Codling, E. A., Plank, M. J., and Benhamou, S. (2008). Random walk models in biology. *J R Soc Interface*, 5(25):813–34.
- Collett, M., Chittka, L., and Collett, T. S. (2013). Spatial memory in insect navigation. *Current Biology*, 23(17):R789–R800.
- Courville, A. C., Daw, N. D., and Touretzky, D. S. (2006). Bayesian theories of conditioning in a changing world. *Trends in Cognitive Sciences*, 10(7):294–300.

- Cowles, M. K. and Carlin, B. P. (1996). Markov chain Monte Carlo convergence diagnostics: A comparative review. *Journal of the American Statistical Association*, 91(434):883–904.
- Crystal, J. D. (2018). Animal models of episodic memory. *Comparative Cognition & Behavior Reviews*, 13:105–122.
- Cumming, G. S., Henry, D. A. W., and Reynolds, C. (2022). Translocation experiment gives new insights into the navigation capacity of an African duck. *Diversity and Distributions*, n/a(n/a).
- Dahle, B. and Swenson, J. E. (2003). Home ranges in adult Scandinavian brown bears *Ursus arctos*: effect of population density, mass, sex, reproductive status and habitat type. *Journal of Zoology*, 260:329–355.
- Dall, S., Giraldeau, L., Olsson, O., Mcnamara, J., and Stephens, D. (2005). Information and its use by animals in evolutionary ecology. *Trends in Ecology & Evolution*, 20(4):187–193.
- Dalziel, B. D., Morales, J. M., and Fryxell, J. M. (2008). Fitting probability distributions to animal movement trajectories: using artificial neural networks to link distance, resources, and memory. *Am Nat*, 172(2):248–58.
- Darwin, C. R. (1839). *Journal of Researches into the Geology and Natural History of the Various Countries Visited by HMS Beagle*. Harper & Brothers, New York, USA, 1 edition.
- Davidson, S. C., Bohrer, G., Gurarie, E., LaPoint, S., Mahoney, P. J., Boelman, N. T., Eitel, J. U. H., Prugh, L. R., Vierling, L. A., Jennewein, J., Grier, E., Couriot, O., Kelly, A. P., Meddens, A. J. H., Oliver, R. Y., Kays, R., Wikelski, M., Aarvak, T., Ackerman, J. T., Alves, J. A., Bayne, E., Bedrosian, B., Belant, J. L., Berdahl, A. M., Berlin, A. M., Berteaux, D., Bêty, J., Boiko, D., Booms, T. L., Borg, B. L., Boutin, S., Boyd, W. S., Brides, K., Brown, S., Bulyuk, V. N., Burnham, K. K., Cabot, D., Casazza, M., Christie, K., Craig, E. H., Davis, S. E., Davison, T., Demma, D., DeSorbo, C. R., Dixon, A., Domenech, R., Eichhorn, G., Elliott, K., Evenson, J. R., Exo, K.-M., Ferguson, S. H., Fiedler, W., Fisk, A., Fort, J., Franke, A., Fuller, M. R., Garthe, S., Gauthier, G., Gilchrist, G., Glazov, P., Gray, C. E., Grémillet, D., Griffin, L., Hallworth, M. T., Harrison, A.-L., Hennin, H. L., Hipfner, J. M., Hodson, J., Johnson, J. A., Joly, K., Jones, K., Katzner, T. E., Kidd, J. W., Knight, E. C., Kochert, M. N., Kölzsch, A., Kruckenberg, H., Lagassé, B. J., Lai, S., Lamarre, J.-F., Lanctot, R. B., Larter, N. C., Latham, A. D. M., Latty, C. J., Lawler, J. P., Léandri-Breton, D.-J., Lee, H., Lewis, S. B., Love, O. P., Madsen, J., Maftei, M., Mallory, M. L., Mangipane, B., Markovets, M. Y., Marra, P. P., McGuire, R., McIntyre, C. L., McKinnon, E. A., Miller, T. A., Moonen, S., Mu, T., Müskens, G. J. D. M., Ng, J., Nicholson, K. L., Øien, I. J., Overton, C., Owen, P. A., Patterson, A., Petersen, A., Pokrovsky, I., Powell, L. L., Prieto, R., Quillfeldt, P., Rausch, J., Russell, K.,

- Saalfeld, S. T., Schekkerman, H., Schmutz, J. A., Schwemmer, P., Seip, D. R., Shreading, A., Silva, M. A., Smith, B. W., Smith, F., Smith, J. P., Snell, K. R. S., Sokolov, A., Sokolov, V., Solovyeva, D. V., Sorum, M. S., Tertitski, G., Therrien, J. F., Thorup, K., Tibbitts, T. L., Tulp, I., Uher-Koch, B. D., van Bemmelen, R. S. A., Van Wilgenburg, S., Von Duyke, A. L., Watson, J. L., Watts, B. D., Williams, J. A., Wilson, M. T., Wright, J. R., Yates, M. A., Yurkowski, D. J., Żydelis, R., and Hebblewhite, M. (2020). Ecological insights from three decades of animal movement tracking across a changing Arctic. *Science*, 370(6517):712–715.
- Davies, N. and Houston, A. (1981). Owners and satellites: The economics of territory defence in the pied wagtail, *Motacilla alba*. *Journal of Animal Ecology*, 50(1):157–180.
- Dayan, P. and Daw, N. D. (2008). Decision theory, reinforcement learning, and the brain. *Cognitive, Affective, & Behavioral Neuroscience*, 8(4):429–453.
- de Waal, F. B. M. (1991). Complementary methods and convergent evidence in the study of primate social cognition. *Behaviour*, 118(3–4):297–320.
- DeAngelis, D. L. and Diaz, S. G. (2019). Decision-making in agent-based modeling: A current review and future prospectus. *Frontiers in Ecology and Evolution*, 6:237.
- DeMars, C. A., Auger-Méthé, M., Schlägel, U. E., and Boutin, S. (2013). Inferring parturition and neonate survival from movement patterns of female ungulates: a case study using woodland caribou. *Ecology and Evolution*, 3(12):4149–4160.
- Dennis, B. and Taper, M. L. (1994). Density dependence in time series observations of natural populations: Estimation and testing. *Ecological Monographs*, 64(2):205–224.
- DeWitt, T. J., Sih, A., and Wilson, D. S. (1998). Costs and limits of phenotypic plasticity. *Trends in Ecology & Evolution*, 13(2):77–81.
- Dingle, H. and Drake, V. A. (2007). What is migration? *BioScience*, 57(2):113–121.
- Donaldson-Matasci, M. C., Lachmann, . M., and Bergstrom, C. T. (2008). Phenotypic diversity as an adaptation to environmental uncertainty. *Evolutionary Ecology Research*, 10(4):493–515.
- Duchesne, T., Fortin, D., and Rivest, L. P. (2015). Equivalence between step selection functions and biased correlated random walks for statistical inference on animal movement. *PLoS One*, 10(4):e0122947.
- Ducks Unlimited (2002). Lower Mackenzie River Delta, Northwest Territories Earth Cover Classification User’s Guide. Technical report, Ducks Unlimited Inc., Rancho Cordova, USA.

- Dunn, R. E., Wanless, S., Daunt, F., Harris, M. P., and Green, J. A. (2020). A year in the life of a North Atlantic seabird: behavioural and energetic adjustments during the annual cycle. *Scientific Reports*, 10(11):5993.
- D’Elia, J., Schumaker, N. H., Marcot, B. G., Miewald, T., Watkins, S., and Yanahan, A. D. (2022). Condors in space: an individual-based population model for California condor reintroduction planning. *Landscape Ecology*.
- Eacott, M. J. and Easton, A. (2010). Episodic memory in animals: Remembering which occasion. *Neuropsychologia*, 48(8):2273–2280.
- Edelhoff, H., Signer, J., and Balkenhol, N. (2016). Path segmentation for beginners: an overview of current methods for detecting changes in animal movement patterns. *Movement Ecology*, 4(1):21.
- Edenius, L. (1997). Field test of a GPS location system for moose *alces alces* under Scandinavian boreal conditions. *Wildlife Biology*, 3(1):39–43.
- Edwards, M., Derocher, A. E., Hobson, K., Branigan, M., and Nagy, J. (2011). Fast carnivores and slow herbivores: differential foraging strategies among grizzly bears in the Canadian Arctic. *Oecologia*, 165:877–889.
- Edwards, M. A. and Derocher, A. E. (2015). Mating-related behaviour of grizzly bears inhabiting marginal habitat at the periphery of their North American range. *Behavioural Processes*, 111:75–83.
- Edwards, M. A., Derocher, A. E., and Nagy, J. A. (2013). Home range size variation in female arctic grizzly bears relative to reproductive status and resource availability. *PLoS One*, 8(7):e68130.
- Edwards, M. A., Nagy, J. A., and Derocher, A. E. (2009). Low site fidelity and home range drift in a wide-ranging, large Arctic omnivore. *Animal Behaviour*, 77(1):23–28.
- Egevang, C., Stenhouse, I. J., Phillips, R. A., Petersen, A., Fox, J. W., and Silk, J. R. D. (2010). Tracking of Arctic terns *sterna paradisaea* reveals longest animal migration. *Proceedings of the National Academy of Sciences*, 107(5):2078–2081.
- Ellison, A. M. (2004). Bayesian inference in ecology. *Ecology Letters*, 7(6):509–520.
- Evans, S. R. and Bearhop, S. (2022). Variation in movement strategies: Capital versus income migration. *Journal of Animal Ecology*, n/a(n/a).
- Fagan, W. F., Gurarie, E., Bewick, S., Howard, A., Cantrell, R. S., and Cosner, C. (2017). Perceptual ranges, information gathering, and foraging success in dynamic landscapes. *The American Naturalist*, 189(5):474–489.

- Fagan, W. F., Lewis, M. A., Auger-Méthé, M., Avgar, T., Benhamou, S., Breed, G., LaDage, L., Schlägel, U. E., Tang, W.-w., Papastamatiou, Y. P., Forester, J., and Mueller, T. (2013). Spatial memory and animal movement. *Ecology Letters*, 16(10):1316–1329.
- Fagan, W. F., Saborio, C., Hoffman, T. D., Gurarie, E., Cantrell, R. S., and Cosner, C. (2022). What’s in a resource gradient? Comparing alternative cues for foraging in dynamic environments via movement, perception, and memory. *Theoretical Ecology*.
- Falcón-Cortés, A., Boyer, D., Merrill, E., Frair, J. L., and Morales, J. M. (2021). Hierarchical, memory-based movement models for translocated elk (*cervus canadensis*). *Frontiers in Ecology and Evolution*, 9:497.
- Farnsworth, K. D. and Beecham, J. A. (1999). How do grazers achieve their distribution? A continuum of models from random diffusion to the ideal free distribution using biased random walks. *The American Naturalist*, 153(5):509–526.
- Fauchald, P. and Tveraa, T. (2003). Using first-passage time in the analysis of area-restricted search and habitat selection. *Ecology*, 84(2):282–288.
- Ferguson, S. H. and McLoughlin, P. D. (2000). Effect of energy availability, seasonality, and geographic range on brown bear life history. *Ecography*, 23(2):193–200.
- Festa-Bianchet, M., Ray, J., Boutin, S., Côté, S., and Gunn, A. (2011). Conservation of caribou (*rangifer tarandus*) in Canada: an uncertain future. *Canadian Journal of Zoology*, 89(5):419–434.
- Fischer, S. M. and Lewis, M. A. (2021). A robust and efficient algorithm to find profile likelihood confidence intervals. *Statistics and Computing*, 31(4):38.
- Fleck, E. S. and Gunn, A. (1982). Characteristics of three barren-ground caribou calving grounds in the Northwest Territories. Technical Report 7, Northwest Territories Wildlife Service.
- Fleming, C. H. and Calabrese, J. M. (2017). A new kernel density estimator for accurate home-range and species-range area estimation. *Methods in Ecology and Evolution*, 8(5):571–579.
- Fletcher, R. J., Maxwell, C. W., Andrews, J. E., and Helmeý-Hartman, W. L. (2013). Signal detection theory clarifies the concept of perceptual range and its relevance to landscape connectivity. *Landscape Ecology*, 28(1):57–67.
- Forester, J. D., Im, H. K., and Rathouz, P. J. (2009). Accounting for animal movement in estimation of resource selection functions: sampling and data analysis. *Ecology*, 90(12):3554–3565.

- Fortin, D., Beyer, H. L., Boyce, M. S., Smith, D. W., Duchesne, T., and Mao, J. S. (2005). Wolves influence elk movements: Behavior shapes a trophic cascade in Yellowstone National Park. *Ecology*, 86(5):1320–1330.
- Franklin, K. A., Nicoll, M. A. C., Butler, S. J., Norris, K., Ratcliffe, N., Nakagawa, S., and Gill, J. A. (2022). Individual repeatability of avian migration phenology: A systematic review and meta-analysis. *Journal of Animal Ecology*, n/a(n/a).
- Fraser, K. C., Davies, K. T. A., Davy, C. M., Ford, A. T., Flockhart, D. T. T., and Martins, E. G. (2018). Tracking the conservation promise of movement ecology. *Frontiers in Ecology and Evolution*, 6.
- Fretwell, S. D. and Lucas, H. L. (1969). On territorial behavior and other factors influencing habitat distribution in birds. *Acta Biotheoretica*, 19(1):16–36.
- Fryxell, J. M. and Holt, R. D. (2013). Environmental change and the evolution of migration. *Ecology*, 94(6):1274–1279.
- Fullman, T. J., Person, B. T., Prichard, A. K., and Parrett, L. S. (2021). Variation in winter site fidelity within and among individuals influences movement behavior in a partially migratory ungulate. *PLOS ONE*, 16(9):e0258128.
- Gaillard, J. M., Hebblewhite, M., Loison, A., Fuller, M., Powell, R., Basille, M., and Van Moorter, B. (2010). Habitat-performance relationships: finding the right metric at a given spatial scale. *Philos Trans R Soc Lond B Biol Sci*, 365(1550):2255–65.
- Gaillard, J.-M. and Yoccoz, N. G. (2003). Temporal variation in survival of mammals: A case of environmental canalization? *Ecology*, 84(12):3294–3306.
- Gau, R. J., Case, R. L., Fenner, D., and McLoughlin, P. D. (2002). Feeding patterns of barren-ground grizzly bears in the central Canadian Arctic. *Arctic*, 55(4):339–344.
- Gehr, B., Bonnot, N. C., Heurich, M., Cagnacci, F., Ciuti, S., Hewison, A. J. M., Gaillard, J.-M., Ranc, N., Premier, J., Vogt, K., Hofer, E., Ryser, A., Vimercati, E., and Keller, L. (2020). Stay home, stay safe—site familiarity reduces predation risk in a large herbivore in two contrasting study sites. *Journal of Animal Ecology*, 89(6):1329–1339.
- Geldmann, J., Barnes, M., Coad, L., Craigie, I. D., Hockings, M., and Burgess, N. D. (2013). Effectiveness of terrestrial protected areas in reducing habitat loss and population declines. *Biological Conservation*, 161:230–238.
- Gende, S. M. and Quinn, T. P. (2004). The relative importance of prey density and social dominance in determining energy intake by bears feeding on Pacific salmon. *Canadian Journal of Zoology*, 82(1):75–85.

- Gerber, B. D., Hooten, M. B., Peck, C. P., Rice, M. B., Gammonley, J. H., Apa, A. D., Davis, A. J., and Lemaître, J. (2019). Extreme site fidelity as an optimal strategy in an unpredictable and homogeneous environment. *Functional Ecology*, 33(9):1695–1707.
- Gibbs, J. P. and Breisch, A. R. (2001). Climate warming and calling phenology of frogs near Ithaca, New York, 1900-1999. *Conservation Biology*, 15(4):1175–1178.
- Gibson, G. and Wagner, G. (2000). Canalization in evolutionary genetics: a stabilizing theory? *BioEssays*, 22(4):372–380.
- González-Gómez, P. L., Bozinovic, F., and Vásquez, R. A. (2011). Elements of episodic-like memory in free-living hummingbirds, energetic consequences. *Animal Behaviour*, 81(6):1257–1262.
- Graham, R. T., Witt, M. J., Castellanos, D. W., Remolina, F., Maxwell, S., Godley, B. J., and Hawkes, L. A. (2012). Satellite tracking of manta rays highlights challenges to their conservation. *PLoS One*, 7(5):e36834.
- Green, M., Alerstam, T., Clausen, P., Drent, R., and Ebbinge, B. S. (2002). Dark-bellied brent geese *branta bernicla bernicla*, as recorded by satellite telemetry, do not minimize flight distance during spring migration. *Ibis*, 144(1):106–121.
- Green, R. F. (1980). Bayesian birds: A simple example of Oaten’s stochastic model of optimal foraging. *Theoretical Population Biology*, 18(2):244–256.
- Green, R. F. (2006). A simpler, more general method of finding the optimal foraging strategy for Bayesian birds. *Oikos*, 112(2):274–284.
- Griffiths, T. L., Kemp, C., and Tenenbaum, J. B. (2001). *Bayesian Models of Cognition*, page 59–100. Cambridge University Press, 1 edition.
- Grimm, V., Berger, U., Bastiansen, F., Eliassen, S., Ginot, V., Giske, J., Goss-Custard, J., Grand, T., Heinz, S. K., Huse, G., and et al. (2006). A standard protocol for describing individual-based and agent-based models. *Ecological Modelling*, 198(1):115–126.
- Gunn, A. and Miller, F. L. (1986). Traditional behaviour and fidelity to caribou calving grounds by barren-ground caribou. *Rangifer*, page 151–158.
- Gunn, A., Poole, K. G., and Nishi, J. S. (2012). A conceptual model for migratory tundra caribou to explain and predict why shifts in spatial fidelity of breeding cows to their calving grounds are infrequent. *Rangifer*, page 259–267.
- Gurarie, E., Andrews, R. D., and Laidre, K. L. (2009). A novel method for identifying behavioural changes in animal movement data. *Ecology Letters*, 12(5):395–408.

- Haché, S., Villard, M.-A., and Bayne, E. M. (2013). Experimental evidence for an ideal free distribution in a breeding population of a territorial songbird. *Ecology*, 94(4):861–869.
- Haest, B., Hüppop, O., and Bairlein, F. (2018). The influence of weather on avian spring migration phenology: What, where and when? *Global Change Biology*, 24(12):5769–5788.
- Halloran, D. W. and Pearson, A. M. (1972). Blood chemistry of the brown bear (*ursus arctos*) from southwestern Yukon Territory, Canada. *Canadian Journal of Zoology*, 50(6):827–833.
- Hanski, I., Erälahti, C., Kankare, M., Ovaskainen, O., and Sirén, H. (2004). Variation in migration propensity among individuals maintained by landscape structure. *Ecology Letters*, 7(10):958–966.
- Hardesty-Moore, M., Deinet, S., Freeman, R., Titcomb, G. C., Dillon, E. M., Stears, K., Klope, M., Bui, A., Orr, D., Young, H. S., Miller-ter Kuile, A., Hughey, L. F., and McCauley, D. J. (2018). Migration in the Anthropocene: how collective navigation, environmental system and taxonomy shape the vulnerability of migratory species. *Philosophical Transactions of the Royal Society B: Biological Sciences*, 373(1746):20170017.
- Harel, R. and Nathan, R. (2018). The characteristic time-scale of perceived information for decision-making: Departure from thermal columns in soaring birds. *Functional Ecology*, 32(8):2065–2072.
- Harris, J. A. and Bouton, M. E. (2020). Pavlovian conditioning under partial reinforcement: The effects of nonreinforced trials versus cumulative conditioned stimulus duration. *Journal of Experimental Psychology: Animal Learning and Cognition*, 46(3):256–272.
- Harris, S. M., Descamps, S., Sneddon, L. U., Bertrand, P., Chastel, O., and Patrick, S. C. (2020). Personality predicts foraging site fidelity and trip repeatability in a marine predator. *Journal of Animal Ecology*, 89(1):68–79.
- Hastings, W. K. (1970). Monte Carlo sampling methods using Markov chains and their applications. *Biometrika*, 57(1):97–109.
- Hays, G. C., Bailey, H., Bograd, S. J., Bowen, W. D., Campagna, C., Carmichael, R. H., Casale, P., Chiaradia, A., Costa, D. P., Cuevas, E., Nico de Bruyn, P. J., Dias, M. P., Duarte, C. M., Dunn, D. C., Dutton, P. H., Esteban, N., Friedlaender, A., Goetz, K. T., Godley, B. J., Halpin, P. N., Hamann, M., Hammerschlag, N., Harcourt, R., Harrison, A.-L., Hazen, E. L., Heupel, M. R., Hoyt, E., Humphries, N. E., Kot, C. Y., Lea, J. S. E., Marsh, H., Maxwell, S. M., McMahan, C. R., Notarbartolo di Sciarra, G., Palacios, D. M., Phillips, R. A., Righton, D., Schofield, G., Seminoff, J. A., Simpfendorfer, C. A., Sims, D. W., Takahashi, A., Tetley, M. J., Thums, M.,

- Trathan, P. N., Villegas-Amtmann, S., Wells, R. S., Whiting, S. D., Wildermann, N. E., and Sequeira, A. M. M. (2019). Translating marine animal tracking data into conservation policy and management. *Trends in Ecology & Evolution*, 34(5):459–473.
- Hebblewhite, M. and Merrill, E. H. (2011). Demographic balancing of migrant and resident elk in a partially migratory population through forage–predation tradeoffs. *Oikos*, 120(12):1860–1870.
- Herbig, J. L. and Szedlmayer, S. T. (2016). Movement patterns of gray triggerfish, *Balistes capricus*, around artificial reefs in the northern Gulf of Mexico. *Fisheries Management and Ecology*, 23(5):418–427.
- Hertel, A. G., Leclerc, M., Warren, D., Pelletier, F., Zedrosser, A., and Mueller, T. (2019). Don’t poke the bear: using tracking data to quantify behavioural syndromes in elusive wildlife. *Animal Behaviour*, 147:91–104.
- Holland, A. E., Byrne, M. E., Bryan, A. L., DeVault, T. L., Rhodes, O. E., and Beasley, J. C. (2017). Fine-scale assessment of home ranges and activity patterns for resident black vultures (*Coragyps atratus*) and turkey vultures (*Cathartes aura*). *PLoS One*, 12(7):e0179819.
- Hussey, N. E., Kessel, S. T., Aarestrup, K., Cooke, S. J., Cowley, P. D., Fisk, A. T., Harcourt, R. G., Holland, K. N., Iverson, S. J., Kocik, J. F., Mills Fleming, J. E., and Whoriskey, F. G. (2015). Aquatic animal telemetry: A panoramic window into the underwater world. *Science*, 348(6240):1255642.
- Jacobs, L. F. and Menzel, R. (2014). Navigation outside of the box: what the lab can learn from the field and what the field can learn from the lab. *Movement Ecology*, 2(1):3.
- Janmaat, K. R., Boesch, C., Byrne, R., Chapman, C. A., Gone Bi, Z. B., Head, J. S., Robbins, M. M., Wrangham, R. W., and Polansky, L. (2016). Spatio-temporal complexity of chimpanzee food: How cognitive adaptations can counteract the ephemeral nature of ripe fruit. *American Journal of Primatology*, 78(6):626–45.
- Janmaat, K. R. L., Ban, S. D., and Boesch, C. (2013). Chimpanzees use long-term spatial memory to monitor large fruit trees and remember feeding experiences across seasons. *Animal Behaviour*, 86(6):1183–1205.
- Jerde, C. L. and Visscher, D. R. (2005). GPS measurement error influences on movement model parameterization. *Ecological Applications*, 15(3):806–810.
- Jesmer, B. R., Merkle, J. A., Goheen, J. R., Aikens, E. O., Beck, J. L., Courtemanch, A. B., Hurley, M. A., McWhirter, D. E., Miyasaki, H. M., Monteith, K. L., and Kauffman, M. J. (2018). Is ungulate migration culturally transmitted? evidence of social learning from translocated animals. *Science*, 361(6406):1023–1025.

Jetz, W., Tertitski, G., Kays, R., Mueller, U., Wikelski, M., Åkesson, S., Anisimov, Y., Antonov, A., Arnold, W., Bairlein, F., Baltà, O., Baum, D., Beck, M., Belonovich, O., Belyaev, M., Berger, M., Berthold, P., Bittner, S., Blake, S., Block, B., Bloche, D., Boehning-Gaese, K., Bohrer, G., Bojarinova, J., Bommas, G., Bourski, O., Bragin, A., Bragin, A., Bristol, R., Brlík, V., Buljuk, V., Cagnacci, F., Carlson, B., Chapple, T. K., Chefira, K. F., Cheng, Y., Chernetsov, N., Cierlik, G., Christiansen, S. S., Clarabuch, O., Cochran, W., Cornelius, J. M., Couzin, I., Crofoot, M. C., Cruz, S., Davydov, A., Davidson, S., Dech, S., Dechmann, D., Demidova, E., Dettmann, J., Dittmar, S., Dorofeev, D., Drenckhahn, D., Dubyanskiy, V., Egorov, N., Ehnbohm, S., Ellis-Soto, D., Ewald, R., Feare, C., Fefelov, I., Fehérvári, P., Fiedler, W., Flack, A., Froböse, M., Fufachev, I., Futoran, P., Gabyshev, V., Gagliardo, A., Garthe, S., Gashkov, S., Gibson, L., Goymann, W., Gruppe, G., Guglielmo, C., Hartl, P., Hedenström, A., Hegemann, A., Heine, G., Ruiz, M. H., Hofer, H., Huber, F., Iannarilli, F., Illa, M., Isaev, A., Jakobsen, B., Jenni, L., Jenni-Eiermann, S., Jesmer, B., Jiguet, F., Karimova, T., Kasdin, N. J., Kazansky, F., Kirillin, R., Klinner, T., Knopp, A., Kölzsch, A., Kondratyev, A., Krondorf, M., Ktitorov, P., Kulikova, O., Kumar, R. S., Künzer, C., Larionov, A., Larose, C., Liechti, F., Linek, N., Lohr, A., Lushchekina, A., Mansfield, K., Matantseva, M., Markovets, M., Marra, P., Masello, J. F., Melzheimer, J., Menz, M. H. M., Menzie, S., Meshcheryagina, S., Miquelle, D., Morozov, V., Mukhin, A., Müller, I., Mueller, T., Navedo, J. G., Nathan, R., Nelson, L., Németh, Z., Newman, S., Norris, R., Okhlopkov, I., Oleś, W., Oliver, R., O'Mara, T., Palatitz, P., Partecke, J., Pavlick, R., Pedenko, A., Pham, J., Piechowski, D., Pierce, A., Piersma, T., Pitz, W., Plettmeier, D., Pokrovskaya, I., Pokrovskaya, L., Pokrovsky, I., Pot, M., Procházka, P., Quillfeldt, P., Rakhimberdiev, E., Ramenofsky, M., Ranipeta, A., Rapczyński, J., Remisiewicz, M., Rozhnov, V., Rienks, F., Rozhnov, V., Rutz, C., Sakhvon, V., Sapir, N., Safi, K., Schäubelhut, F., Schimel, D., Schmidt, A., Shamoun-Baranes, J., Sharikov, A., Shearer, L., Shemyakin, E., Sherub, S., Shipley, R., Sica, Y., Smith, T. B., Simonov, S., Snell, K., Sokolov, A., Sokolov, V., Solomina, O., Soloviev, M., Spina, F., Spoelstra, K., Storhas, M., Sviridova, T., Swenson, G., Taylor, P., Thorup, K., Tsvey, A., Tucker, M., Turner, W., van der Jeugd, H., van Schalkwyk, L., van Toor, M., Viljoen, P., Visser, M. E., Volkmmer, T., Volkov, A., Volkov, S., Volkov, O., von Rönne, J. A. C., Vorneweg, B., Wachter, B., Waldenström, J., Wegmann, M., Wehr, A., Weinzierl, R., Weppler, J., Wilcove, D., Wild, T., Williams, H. J., Wilshire, J., Wingfield, J., Wunder, M., Yachmennikova, A., Yanco, S., Yohannes, E., Zeller, A., Ziegler, C., Zięcik, A., and Zook, C. (2022). Biological Earth observation with animal sensors. *Trends in Ecology & Evolution*, 37(4):293–298.

Johnson, A. R., Wiens, J. A., Milne, B. T., and Crist, T. O. (1992). Animal movements and population dynamics in heterogeneous landscapes. *Landscape Ecology*, 7(1):63–75.

Johnson, D. H. (1980). The comparison of usage and availability measurements for evaluating resource preference. *Ecology*, 61(1):65–71.

- Jonsen, I. D., Basson, M., Bestley, S., Bravington, M. V., Patterson, T. A., Pedersen, M. W., Thomson, R., Thygesen, U. H., and Wotherspoon, S. J. (2013). State-space models for bio-loggers: A methodological road map. *Deep Sea Research Part II: Topical Studies in Oceanography*, 88-89:34–46.
- Joo, R., Boone, M. E., Clay, T. A., Patrick, S. C., Clusella-Trullas, S., and Basille, M. (2020). Navigating through the R packages for movement. *Journal of Animal Ecology*, 89(1):248–267.
- Joo, R., Picardi, S., Boone, M. E., Clay, T. A., Patrick, S. C., Romero-Romero, V. S., and Basille, M. (2022). Recent trends in movement ecology of animals and human mobility. *Movement Ecology*, 10(1):26.
- Kartzinel, T. R. and Pringle, R. M. (2020). Multiple dimensions of dietary diversity in large mammalian herbivores. *Journal of Animal Ecology*, 89(6):1482–1496.
- Katz, J. S. and Wright, A. A. (2006). Same/different abstract-concept learning by pigeons. *Journal of Experimental Psychology: Animal Behavior Processes*, 32(1):80–86.
- Kauffman, M. J., Cagnacci, F., Chamaillé-Jammes, S., Hebblewhite, M., Hopcraft, J. G. C., Merkle, J. A., Mueller, T., Mysterud, A., Peters, W., Roettger, C., Steingisser, A., Meacham, J. E., Abera, K., Adamczewski, J., Aikens, E. O., Bartlam-Brooks, H., Bennitt, E., Berger, J., Boyd, C., Côté, S. D., Debeffe, L., Dekrout, A. S., Dejid, N., Donadio, E., Dziba, L., Fagan, W. F., Fischer, C., Focardi, S., Fryxell, J. M., Fynn, R. W. S., Geremia, C., González, B. A., Gunn, A., Gurarie, E., Heurich, M., Hilty, J., Hurley, M., Johnson, A., Joly, K., Kaczensky, P., Kendall, C. J., Kochkarev, P., Kolpaschikov, L., Kowalczyk, R., van Langevelde, F., Li, B. V., Lobora, A. L., Loison, A., Madiri, T. H., Mallon, D., Marchand, P., Medellin, R. A., Meisingset, E., Merrill, E., Middleton, A. D., Monteith, K. L., Morjan, M., Morrison, T. A., Mumme, S., Naidoo, R., Novaro, A., Ogutu, J. O., Olson, K. A., Oteng-Yeboah, A., Ovejero, R. J. A., Owen-Smith, N., Paasivaara, A., Packer, C., Panchenko, D., Pedrotti, L., Plumptre, A. J., Rolandsen, C. M., Said, S., Salemgareyev, A., Savchenko, A., Savchenko, P., Sawyer, H., Selebatso, M., Skroch, M., Solberg, E., Stabach, J. A., Strand, O., Sutor, M. J., Tachiki, Y., Trainor, A., Tshipa, A., Virani, M. Z., Vynne, C., Ward, S., Wittemyer, G., Xu, W., and Zuther, S. (2021). Mapping out a future for ungulate migrations. *Science*, 372(6542):566–569.
- Kavčič, I., Adamič, M., Kaczensky, P., Krofel, M., Kobal, M., and Jerina, K. (2015). Fast food bears: brown bear diet in a human-dominated landscape with intensive supplemental feeding. *Wildlife Biology*, 21(1):1–8.
- Kays, R., Crofoot, M. C., Jetz, W., and Wikelski, M. (2015). Terrestrial animal tracking as an eye on life and planet. *Science*, 348(6240):aaa2478.

- Kellert, S. R., Black, M., Rush, C. R., and Bath, A. J. (1996). Human culture and large carnivore conservation in North America. *Conservation Biology*, 10(4):977–990.
- Kemink, K. M. and Kesler, D. C. (2013). Using movement ecology to inform translocation efforts: a case study with an endangered lekking bird species. *Animal Conservation*, 16(4):449–457.
- Killick, R. and Eckley, I. (2014). changepoint: an r package for changepoint analysis. *Journal of Statistical Software*, 58(33):1–19.
- Killick, R., Fearnhead, P., and Eckley, I. A. (2012). Optimal detection of change-points with a linear computational cost. *Journal of the American Statistical Association*, 107(500):1590–1598.
- Kiltie, R. A. (2000). Scaling of visual acuity with body size in mammals and birds. *Functional Ecology*, 14(2):226–234.
- Krebs, J. R., Kacelnik, A., and Taylor, P. (1978). Test of optimal sampling by foraging great tits. *Nature*, 275(5675):27–31.
- Kriska, G., Horváth, G., and Andrikovics, S. (1998). Why do mayflies lay their eggs en masse on dry asphalt roads? Water-imitating polarized light reflected from asphalt attracts Ephemeroptera. *Journal of Experimental Biology*, 201(15):2273–2286.
- Kristensen, K., Nielsen, A., Berg, C. W., Skaug, H., and Bell, B. M. (2016). TMB: Automatic differentiation and Laplace approximation. *Journal of Statistical Software*, 70:1–21.
- Kunst, R. M. (2008). Cross validation of prediction models for seasonal time series by parametric bootstrapping. *Austrian Journal of Statistics*, 37(3):271–284.
- Kürten, N., Schmaljohann, H., Bichet, C., Haest, B., Vedder, O., González-Solís, J., and Bouwhuis, S. (2022). High individual repeatability of the migratory behaviour of a long-distance migratory seabird. *Movement Ecology*, 10(11):1–16.
- Lafontaine, A., Drapeau, P., Fortin, D., and St-Laurent, M.-H. (2017). Many places called home: the adaptive value of seasonal adjustments in range fidelity. *Journal of Animal Ecology*, 86(3):624–633.
- Lamb, C. T., Mowat, G., McLellan, B. N., Nielsen, S. E., and Boutin, S. (2017). Forbidden fruit: human settlement and abundant fruit create an ecological trap for an apex omnivore. *Journal of Animal Ecology*, 86(1):55–65.
- Lavielle, M. (2005). Using penalized contrasts for the change-point problem. *Signal Processing*, 85(8):1501–1510.

- Le Corre, M., Dussault, C., and Côté, S. D. (2014). Detecting changes in the annual movements of terrestrial migratory species: using the first-passage time to document the spring migration of caribou. *Movement Ecology*, 2(1):19.
- Le Corre, M., Dussault, C., and Côté, S. D. (2017). Weather conditions and variation in timing of spring and fall migrations of migratory caribou. *Journal of Mammalogy*, 98(1):260–271.
- Lea, S. E., McLaren, I. P., Dow, S. M., and Graft, D. A. (2012). The cognitive mechanisms of optimal sampling. *Behavioural Processes*, 89(2):77–85.
- Lele, S. R., Dennis, B., and Lutscher, F. (2007). Data cloning: easy maximum likelihood estimation for complex ecological models using Bayesian Markov chain Monte Carlo methods. *Ecology Letters*, 10(7):551–563.
- Lent, P. C. (1966). Calving and related social behavior in the barren-ground caribou. *Zeitschrift für Tierpsychologie*, 23(6):701–756.
- Lewis, M. A., Fagan, W. F., Auger-Méthé, M., Frair, J., Fryxell, J. M., Gros, C., Gurarie, E., Healy, S. D., and Merkle, J. A. (2021). Learning and animal movement. *Frontiers in Ecology and Evolution*, 9.
- Liefting, M., Hoffmann, A. A., and Ellers, J. (2009). Plasticity versus environmental canalization: Population differences in thermal responses along a latitudinal gradient in *drosophila serrata*. *Evolution*, 63(8):1954–1963.
- Limiñana, R., Soutullo, A., and Urios, V. (2007). Autumn migration of Montagu’s harriers *circus pygargus* tracked by satellite telemetry. *Journal of Ornithology*, 148(4):517–523.
- Linscott, J. A. and Senner, N. R. (2021). Beyond refueling: Investigating the diversity of functions of migratory stopover events. *Ornithological Applications*, 123(1):duaa074.
- Lorand, C., Robert, A., Gastineau, A., Mihoub, J.-B., and Bessa-Gomes, C. (2022). Effectiveness of interventions for managing human-large carnivore conflicts worldwide: Scare them off, don’t remove them. *Science of The Total Environment*, 838:156195.
- Lunn, N. J., Servanty, S., Regehr, E. V., Converse, S. J., Richardson, E., and Stirling, I. (2016). Demography of an apex predator at the edge of its range: impacts of changing sea ice on polar bears in Hudson Bay. *Ecological Applications*, 26(5):1302–1320.
- Luttbeg, B. (1996). A comparative Bayes tactic for mate assessment and choice. *Behavioral Ecology*, 7(4):451–460.
- López-López, P., Limiñana, R., Mellone, U., and Urios, V. (2010). From the Mediterranean Sea to Madagascar: Are there ecological barriers for the long-distance migrant Eleonora’s falcon? *Landscape Ecology*, 25(5):803–813.

- Macdonald, D. W. (1983). The ecology of carnivore social behaviour. *Nature*, 301(58995899):379–384.
- Macdonald, D. W. and Johnson, D. D. P. (2015). Patchwork planet: the resource dispersion hypothesis, society, and the ecology of life. *Journal of Zoology*, 295(2):75–107.
- Macdonald, R. W., Paton, D. W., Carmack, E. C., and Omstedt, A. (1995). The freshwater budget and under-ice spreading of Mackenzie River water in the Canadian Beaufort Sea based on salinity and $^{18}\text{O}/^{16}\text{O}$ measurements in water and ice. *Journal of Geophysical Research*, 100(C1).
- Mace, R. D., Waller, J. S., Manley, T. L., Lyon, J., and Zuuring, H. (1996). Relationships among grizzly bears, roads and habitat in the Swan Mountains, Montana. *Journal of Applied Ecology*, 33(6):1395–1404.
- MacHutchon, A. G. and Wellwood, D. W. (2003). Grizzly bear food habits in the northern Yukon, Canada. *Ursus*, 14(2):225–235.
- Madon, B. and Hingrat, Y. (2014). Deciphering behavioral changes in animal movement with a ‘multiple change point algorithm- classification tree’ framework. *Frontiers in Ecology and Evolution*, 2.
- Malishev, M. and Kramer-Schadt, S. (2021). Movement, models, and metabolism: Individual-based energy budget models as next-generation extensions for predicting animal movement outcomes across scales. *Ecological Modelling*, 441:109413.
- Mallory, C. D., Williamson, S. N., Campbell, M. W., and Boyce, M. S. (2020). Response of barren-ground caribou to advancing spring phenology. *Oecologia*, 192(3):837–852.
- Manchi, S. and Swenson, J. E. (2005). Denning behaviour of Scandinavian brown bears *Ursus arctos*. *Wildlife Biology*, 11(2):123–132.
- Manly, B. F., McDonald, L. L., Thomas, D. L., McDonald, T. L., and Erickson, W. P. (1993). *Resource selection by animals*. Chapman & Hall.
- Manly, B. F. J. (1974). A model for certain types of selection experiments. *Biometrics*, 30(2):281–294.
- Marchand, P., Garel, M., Bourgoin, G., Duparc, A., Dubray, D., Maillard, D., and Loison, A. (2017). Combining familiarity and landscape features helps break down the barriers between movements and home ranges in a non-territorial large herbivore. *J Anim Ecol*, 86(2):371–383.
- Martin, H. W., Hebblewhite, M., and Merrill, E. H. (2022). Large herbivores in a partially migratory population search for the ideal free home. *Ecology*, n/a(n/a):e3652.

- Martin-Ordas, G., Haun, D., Colmenares, F., and Call, J. (2010). Keeping track of time: evidence for episodic-like memory in great apes. *Anim Cogn*, 13(2):331–40.
- Masson-Delmotte, V., Zhai, P., Pirani, A., L., C. S., Péan, C., Berger, S., Caud, N., Chen, Y., Goldfarb, L., Gomis, M. I., Huang, M., Leitzell, K., Lonnoy, E., Matthews, J. B. R., Maycock, T. K., Waterfield, T., Yelekçi, O., Yu, R., and Zhou, B. (2021). Climate change 2021: The physical science basis. Contribution of Working Group I to the Sixth Assessment Report of the Intergovernmental Panel on Climate Change. Technical report, Intergovernmental Panel on Climate Change.
- Maxwell, S. L., Cazalis, V., Dudley, N., Hoffmann, M., Rodrigues, A. S. L., Stolton, S., Visconti, P., Woodley, S., Kingston, N., Lewis, E., Maron, M., Strassburg, B. B. N., Wenger, A., Jonas, H. D., Venter, O., and Watson, J. E. M. (2020). Area-based conservation in the twenty-first century. *Nature*, 586(78287828):217–227.
- McCall, A. G., Pilfold, N. W., Derocher, A. E., and Lunn, N. J. (2016). Seasonal habitat selection by adult female polar bears in western Hudson Bay. *Population Ecology*, 58(3):407–419.
- McClintock, B. T., Johnson, D. S., Hooten, M. B., Hoef, J. M. V., and Morales, J. M. (2014). When to be discrete: the importance of time formulation in understanding animal movement. *Movement Ecology*, 2(21):14.
- McLoughlin, P. D., Case, R. L., Gau, R. J., Cluff, D. H., Mulders, R., and Messier, F. (2002). Hierarchical habitat selection by barren-ground grizzly bears in the central Canadian Arctic. *Oecologia*, 132(1):102–108.
- McNamara, J. and Houston, A. (1980). The application of statistical decision theory to animal behaviour. *Journal of Theoretical Biology*, 85(4):673–690.
- McNamara, J. M., Green, R. F., and Olsson, O. (2006). Bayes’ theorem and its applications in animal behaviour. *Oikos*, 112(2):243–251.
- McNamara, J. M. and Houston, A. I. (1987). Memory and the efficient use of information. *Journal of Theoretical Biology*, 125(4):385–395.
- Merilä, J. and Hendry, A. P. (2014). Climate change, adaptation, and phenotypic plasticity: the problem and the evidence. *Evolutionary Applications*, 7(1):1–14.
- Merkle, J. A., Fortin, D., and Morales, J. M. (2014). A memory-based foraging tactic reveals an adaptive mechanism for restricted space use. *Ecology Letters*, 17(8):924–931.
- Merkle, J. A., Sawyer, H., Monteith, K. L., Dwinell, S. P. H., Fralick, G. L., and Kauffman, M. J. (2019). Spatial memory shapes migration and its benefits: evidence from a large herbivore. *Ecology Letters*, 22(11):1797–1805.

- Mettke-Hofmann, C., Lorentzen, S., Schlicht, E., Schneider, J., and Werner, F. (2009). Spatial neophilia and spatial neophobia in resident and migratory warblers (*sylvia*). *Ethology*, 115(5):482–492.
- Middleton, A. D., Sawyer, H., Merkle, J. A., Kauffman, M. J., Cole, E. K., Dewey, S. R., Gude, J. A., Gustine, D. D., McWhirter, D. E., Proffitt, K. M., and White, P. (2020). Conserving transboundary wildlife migrations: recent insights from the Greater Yellowstone Ecosystem. *Frontiers in Ecology and the Environment*, 18(2):83–91.
- Mikle, N. L., Graves, T. A., and Olexa, E. M. (2019). To forage or flee: lessons from an elk migration near a protected area. *Ecosphere*, 10(4):e02693.
- Milligan, S., Brown, L., Hobson, D., Frame, P., and Stenhouse, G. (2018). Factors affecting the success of grizzly bear translocations. *The Journal of Wildlife Management*, 82(3):519–530.
- Moorcroft, P. R., Lewis, M. A., and Crabtree, R. L. (2006). Mechanistic home range models capture spatial patterns and dynamics of coyote territories in Yellowstone. *Proceedings of the Royal Society B: Biological Sciences*, 273(1594):1651–1659.
- Morales, J. M., Haydon, D. T., Frair, J., Holsinger, K. E., and Fryxell, J. M. (2004). Extracting more out of relocation data: Building movement models as mixtures of random walks. *Ecology*, 85(9):2436–2445.
- Mueller, T. and Fagan, W. F. (2008). Search and navigation in dynamic environments – from individual behaviors to population distributions. *Oikos*, 117(5):654–664.
- Mueller, T., Fagan, W. F., and Grimm, V. (2011). Integrating individual search and navigation behaviors in mechanistic movement models. *Theoretical Ecology*, 4(3):341–355.
- Muhly, T. B., Johnson, C. A., Hebblewhite, M., Neilson, E. W., Fortin, D., Fryxell, J. M., Latham, A. D. M., Latham, M. C., McLoughlin, P. D., Merrill, E., Paquet, P. C., Patterson, B. R., Schmiegelow, F., Scurrah, F., and Musiani, M. (2019). Functional response of wolves to human development across boreal North America. *Ecology and Evolution*, 9(18):10801–10815.
- Munoz-Lopez, M. and Morris, R. (2009). Episodic memory: Assessment in animals. *Encyclopedia of Neuroscience*, 3:1173–1182. journalAbbreviation: Encyclopedia of Neuroscience.
- Murphy, K. J., Ciuti, S., and Kane, A. (2020). An introduction to agent-based models as an accessible surrogate to field-based research and teaching. *Ecology and Evolution*, 10(22):12482–12498.

- Murray, G., Boxall, P., and Wein, R. (2005). Distribution, abundance, and utilization of wild berries by the Gwich'in people in the Mackenzie River Delta region. *Economic Botany*, 59(2):174–184.
- Møller, A. P. (2009). Successful city dwellers: a comparative study of the ecological characteristics of urban birds in the western Palearctic. *Oecologia*, 159(4):849–858.
- Møller, A. P. and Erritzøe, J. (2010). Flight distance and eye size in birds. *Ethology*, 116(5):458–465.
- Nagy, J. and Haroldson, M. (1990). Comparisons of some home range and population parameters among four grizzly bear populations in Canada. *Bears: Their Biology and Management*, 8:227–235.
- Nagy, J. A., Johnson, D. L., Larter, N. C., Campbell, M. W., Derocher, A. E., Kelly, A., Dumond, M., Allaire, D., and Croft, B. (2011). Subpopulation structure of caribou (*rangifer tarandus* L.) in arctic and subarctic Canada. *Ecological Applications*, 21(6):2334–2348.
- Nagy, J. A., Russell, R. H., Pearson, A. M., Kingsley, M. C. S., and Larsen, C. B. (1983). A study of grizzly bears on the barren grounds of Tuktoyaktuk Peninsula and Richards Island, Northwest Territories, 1974 to 1978. Technical report, Canadian Wildlife Service, Edmonton, AB, Canada.
- Nathan, R., Getz, W. M., Revilla, E., Holyoak, M., Kadmon, R., Saltz, D., and Smouse, P. E. (2008). A movement ecology paradigm for unifying organismal movement research. *Proceedings of the National Academy of Sciences*, 105(49):19052–19059.
- Nathan, R., Monk, C. T., Arlinghaus, R., Adam, T., Alós, J., Assaf, M., Baktoft, H., Beardsworth, C. E., Bertram, M. G., Bijleveld, A. I., Brodin, T., Brooks, J. L., Campos-Candela, A., Cooke, S. J., Gjelland, K. O., Gupte, P. R., Harel, R., Hellström, G., Jeltsch, F., Killen, S. S., Klefoth, T., Langrock, R., Lennox, R. J., Lourie, E., Madden, J. R., Orchan, Y., Pauwels, I. S., Ríha, M., Roeleke, M., Schlägel, U. E., Shohami, D., Signer, J., Toledo, S., Vilc, O., Westrelin, S., Whiteside, M. A., and Jarić, I. (2022). Big-data approaches lead to an increased understanding of the ecology of animal movement. *Science*, 375(6582):eabg1780.
- Netz, C., Ramesh, A., Gismann, J., Gupte, P. R., and Weissing, F. J. (2022). Details matter when modelling the effects of animal personality on the spatial distribution of foragers. *Proceedings of the Royal Society B: Biological Sciences*, 289(1970):20210903.
- Nevoux, M., Forcada, J., Barbraud, C., Croxall, J., and Weimerskirch, H. (2010). Bet-hedging response to environmental variability, an intraspecific comparison. *Ecology*, 91(8):2416–2427.

- Normand, E. and Boesch, C. (2009). Sophisticated Euclidean maps in forest chimpanzees. *Animal Behaviour*, 77(5):1195–1201.
- Norment, C. and Fuller, M. (1997). Breeding-season frugivory by Harris’ sparrows (*Zonotrichia querula*) and white-crowned sparrows (*Zonotrichia leucophrys*) in a low-arctic ecosystem. *Canadian Journal of Zoology*, 75(7):670–679.
- Olden, J. D., Schooley, R. L., Monroe, J. B., and Poff, N. L. (2004). Context-dependent perceptual ranges and their relevance to animal movements in landscapes. *Journal of Animal Ecology*, 73(6):1190–1194.
- Oliveira-Santos, L. G. R., Forester, J. D., Piovezan, U., Tomas, W. M., and Fernandez, F. A. S. (2016). Incorporating animal spatial memory in step selection functions. *Journal of Animal Ecology*, 85(2):516–524.
- O’Keefe, J. and Nadel, L. (1978). *The Hippocampus as a Cognitive Map*. Oxford University Press, Oxford, UK.
- Pan, L. and Wu, L. (1998). A hybrid global optimization method for inverse estimation of hydraulic parameters: Annealing-simplex method. *Water Resources Research*, 34(9):2261–2269.
- Panakhova, E., Buresova, O., and Bures, J. (1984). Persistence of spatial memory in the Morris water tank task. *International Journal of Psychophysiology*, 2(1):5–10.
- Parrish, J. D. (2000). Behavioral, energetic, and conservation implications of foraging plasticity during migration. *Studies in Avian Biology*, 20:18.
- Parzen, E. (1961). On estimation of a probability density function and mode. *The Annals of Mathematical Statistics*, 33:1065–1076.
- Pasitschniak-Arts, M. (1993). *Ursus arctos*. *Mammalian Species*, 439(1):1–10.
- Pavlov, I. (1927). *Conditioned reflexes*. Oxford University Press.
- Pearce, J. M. (1987). A model for stimulus generalization in Pavlovian conditioning. *Psychological Review*, 94(1):61–73.
- Pearce, J. M. (2008). *Animal Learning and Cognition: An Introduction*. Psychology Press, New York, NY, 3 edition.
- Polak, T. and Saltz, D. (2011). Reintroduction as an ecosystem restoration technique. *Conservation Biology*, 25(3):424–424.
- Porsild, A. and Cody, W. (1980). *Vascular plants of continental Northwest Territories, Canada*, volume 1. National Museum of Natural Sciences, National Museums of Canada, Ottawa, ON.

- Postlethwaite, C. M. and Dennis, T. E. (2013). Effects of temporal resolution on an inferential model of animal movement. *PLOS ONE*, 8(5):e57640.
- Potts, J. R., Auger-Méthé, M., Mokross, K., and Lewis, M. A. (2014). A generalized residual technique for analysing complex movement models using earth mover’s distance. *Methods in Ecology and Evolution*, 5(10):1012–1022.
- Potts, J. R. and Börger, L. (2022). How to scale up from animal movement decisions to spatio-temporal patterns: an approach via step selection. *bioRxiv*, page 2022.07.19.500568.
- Potts, J. R., Börger, L., Strickland, B. K., and Street, G. M. (2022). Assessing the predictive power of step selection functions: How social and environmental interactions affect animal space use. *Methods in Ecology and Evolution*, n/a(n/a).
- Potts, J. R. and Lewis, M. A. (2014). How do animal territories form and change? Lessons from 20 years of mechanistic modelling. *Proceedings of the Royal Society B: Biological Sciences*, 281(1784):20140231.
- Potts, J. R. and Lewis, M. A. (2016). How memory of direct animal interactions can lead to territorial pattern formation. *Journal of The Royal Society Interface*, 13(118):20160059.
- Pritchard, D. J., Hurly, T. A., Tello-Ramos, M. C., and Healy, S. D. (2016). Why study cognition in the wild (and how to test it)? *Journal of the Experimental Analysis of Behavior*, 105(1):41–55.
- Prokopenko, C. M., Boyce, M. S., Avgar, T., and Tulloch, A. (2017). Characterizing wildlife behavioural responses to roads using integrated step selection analysis. *Journal of Applied Ecology*, 54(2):470–479.
- Pulido, F. (2007). The genetics and evolution of avian migration. *BioScience*, 57(2):165–174.
- R Core Team (2021). *R: A Language and Environment for Statistical Computing*. R Foundation for Statistical Computing, Vienna, Austria.
- Raftery, A. E. and Lewis, S. (1992). *How Many Iterations in the Gibbs Sampler?*, page 763–773. Oxford University Press.
- Railsback, S. F. (2022). Suboptimal foraging theory: How inaccurate predictions and approximations can make better models of adaptive behavior. *Ecology*, n/a(n/a):e3721.
- Ranc, N., Cagnacci, F., and Moorcroft, P. R. (2022). Memory drives the formation of animal home ranges: Evidence from a reintroduction. *Ecology Letters*, n/a(n/a).

- Ranc, N., Moorcroft, P. R., Ossi, F., and Cagnacci, F. (2021). Experimental evidence of memory-based foraging decisions in a large wild mammal. *Proceedings of the National Academy of Sciences*, 118(15):e2014856118.
- Rappole, J. H. and Warner, D. W. (1976). Relationships between behavior, physiology and weather in avian transients at a migration stopover site. *Oecologia*, 26(3):193–212.
- Rescorla, R. A. and Wagner, A. R. (1972). A theory of Pavlovian conditioning: Variations in the effectiveness of reinforcement and nonreinforcement. In Black, A. H. and Prokasy, W. F., editors, *Classical conditioning II: Current research and theory*, pages 64–99. Appleton-Century-Crofts, New York, NY.
- Richter, L., Balkenhol, N., Raab, C., Reinecke, H., Meißner, M., Herzog, S., Isselstein, J., and Signer, J. (2020). So close and yet so different: the importance of considering temporal dynamics to understand habitat selection. *Basic and Applied Ecology*, 43:99–109.
- Riotte-Lambert, L., Benhamou, S., and Chamaillé-Jammes, S. (2017). From randomness to traplining: a framework for the study of routine movement behavior. *Behavioral Ecology*, 28(1):280–287.
- Riotte-Lambert, L., Benhamou, S., Chamaillé-Jammes, S., Adler, A. E. F. R., and Bronstein, E. J. L. (2015). How memory-based movement leads to non-territorial spatial segregation. *The American Naturalist*, 185(4):E103–E116.
- Robbins, C., Fortin, J., Rode, K. D., Farley, S. D., Shipley, L. A., and Felicetti, L. A. (2007). Optimizing protein intake as a foraging strategy to maximize mass gain in an omnivore. *Oikos*, 116(10):1675–1682.
- Robertson, B. A. and Chalfoun, A. D. (2016). Evolutionary traps as keys to understanding behavioral maladaptation. *Current Opinion in Behavioral Sciences*, 12:12–17.
- Robertson, B. A., Rehage, J. S., and Sih, A. (2013). Ecological novelty and the emergence of evolutionary traps. *Trends in Ecology & Evolution*, 28(9):552–560.
- Roff, D. A. and Fairbairn, D. J. (2007). The evolution and genetics of migration in insects. *BioScience*, 57(2):155–164.
- Rotics, S., Kaatz, M., Turjeman, S., Zurell, D., Wikelski, M., Sapir, N., Eggers, U., Fiedler, W., Jeltsch, F., and Nathan, R. (2018). Early arrival at breeding grounds: Causes, costs and a trade-off with overwintering latitude. *Journal of Animal Ecology*, 87(6):1627–1638.
- Rubner, Y., Tomasi, C., and Guibas, L. J. (2000). The earth mover’s distance as a metric for image retrieval. *International Journal of Computer Vision*, 40(2):99–121.

- Salewski, V., Thoma, M., and Schaub, M. (2007). Stopover of migrating birds: simultaneous analysis of different marking methods enhances the power of capture–recapture analyses. *Journal of Ornithology*, 148(1):29–37.
- Schick, R. S., Loarie, S. R., Colchero, F., Best, B. D., Boustany, A., Conde, D. A., Halpin, P. N., Joppa, L. N., McClellan, C. M., and Clark, J. S. (2008). Understanding movement data and movement processes: current and emerging directions. *Ecology Letters*, 11(12):1338–1350.
- Schlather, M. (2012). Construction of covariance functions and unconditional simulation of random fields. In Porcu, E., Montero, J., and Schlather, M., editors, *Advances and Challenges in Space-time Modelling of Natural Events*, Lecture Notes in Statistics, page 25–54. Springer.
- Schlägel, U. E. and Lewis, M. A. (2014). Detecting effects of spatial memory and dynamic information on animal movement decisions. *Methods in Ecology and Evolution*, 5(11):1236–1246.
- Schlägel, U. E., Merrill, E. H., and Lewis, M. A. (2017). Territory surveillance and prey management: Wolves keep track of space and time. *Ecology and Evolution*, 7(20):8388–8405.
- Schmaljohann, H., Eikenaar, C., and Sapir, N. (2022). Understanding the ecological and evolutionary function of stopover in migrating birds. *Biological Reviews*, 97(4):1231–1252.
- Schmidt, K. A., Dall, S. R. X., and Gils, J. A. V. (2010). The ecology of information: an overview on the ecological significance of making informed decisions. *Oikos*, 119(2):304–316.
- Schmutz, J. K., Flockhart, D. T. T., Houston, C. S., and McLoughlin, P. D. (2008). Demography of ferruginous hawks breeding in western Canada. *Journal of Wildlife Management*, 72(6):1352–1360.
- Schmutz, J. K. and Fyfe, R. W. (1987). Migration and mortality of Alberta ferruginous hawks. *The Condor*, 89(1):169–174.
- Sciaini, M., Fritsch, M., Scherer, C., Simpkins, C. E., and Golding, N. (2018). NLMR and landscapetools: An integrated environment for simulating and modifying neutral landscape models in R. *Methods in Ecology and Evolution*, 9(11):2240–2248.
- Scott, R. C. and Resetarits, W. J. (2022). Spatially explicit habitat selection: Testing contagion and the ideal free distribution with *culex* mosquitoes. *The American Naturalist*, page 000–000.
- Seddon, P. J., Armstrong, D. P., and Maloney, R. F. (2007). Developing the science of reintroduction biology. *Conservation Biology*, 21(2):303–312.

- Seip, D. R. (1992). Factors limiting woodland caribou populations and their interrelationships with wolves and moose in southeastern British Columbia. *Canadian Journal of Zoology*, 70(8):1494–1503.
- Self, S. G. and Liang, K.-Y. (1987). Asymptotic properties of maximum likelihood estimators and likelihood ratio tests under nonstandard conditions. *Journal of the American Statistical Association*, 82(398):605–610.
- Selva, N., Teitelbaum, C. S., Sergiel, A., Zwijacz-Kozica, T., Zięba, F., Bojarska, K., and Mueller, T. (2017). Supplementary ungulate feeding affects movement behavior of brown bears. *Basic and Applied Ecology*, 24:68–76.
- Shevtsova, A., Ojala, A., Neuvonen, S., Vieno, M., and Haukioja, E. (1995). Growth and reproduction of dwarf shrubs in a subarctic plant community: Annual variation and above-ground interactions with neighbours. *Journal of Ecology*, 83(2):263–275.
- Singh, N. J., Allen, A. M., and Ericsson, G. (2016). Quantifying migration behaviour using net squared displacement approach: Clarifications and caveats. *PLOS ONE*, 11(3):e0149594.
- Siniff, D. and Jessen, C. (1969). A simulation model of animal movement patterns. *Advances in Ecological Research*, 6:185–219.
- Skaug, H. J. and Fournier, D. A. (2006). Automatic approximation of the marginal likelihood in non-Gaussian hierarchical models. *Computational Statistics & Data Analysis*, 51(2):699–709.
- Snell-Rood, E. C. (2013). An overview of the evolutionary causes and consequences of behavioural plasticity. *Animal Behaviour*, 85(5):1004–1011.
- Soriano-Redondo, A., Acácio, M., Franco, A. M. A., Herlander Martins, B., Moreira, F., Rogerson, K., and Catry, I. (2020). Testing alternative methods for estimation of bird migration phenology from GPS tracking data. *Ibis*, 162(2):581–588.
- Sorum, M. S., Joly, K., Wells, A. G., Cameron, M. D., Hilderbrand, G. V., and Gustine, D. D. (2019). Den-site characteristics and selection by brown bears (*Ursus arctos*) in the central Brooks Range of Alaska. *Ecosphere*, 10(8):e02822.
- Spence, K. W. (1936). The nature of discrimination learning in animals. *Psychological Review*, 43(5):427–449.
- Steyaert, S. M., Leclerc, M., Pelletier, F., Kindberg, J., Brunberg, S., Swenson, J. E., and Zedrosser, A. (2016). Human shields mediate sexual conflict in a top predator. *Proceedings of the Royal Society B: Biological Sciences*, 283(1833).
- Sturz, B. R., Bodily, K. D., and Katz, J. S. (2006). Evidence against integration of spatial maps in humans. *Animal Cognition*, 9(3):207–17.

- Suraci, J. P., Frank, L. G., Oriol-Cotterill, A., Ekwanga, S., Williams, T. M., and Wilmers, C. C. (2019). Behavior-specific habitat selection by African lions may promote their persistence in a human-dominated landscape. *Ecology*, 100(4):e02644.
- Tang, W. and Bennett, D. A. (2010). Agent-based modeling of animal movement: A review. *Geography Compass*, 4(7):682–700.
- Thomas, D. A. and Riccio, D. C. (1979). Forgetting of a CS attribute in a conditioned suppression paradigm. *Animal Learning & Behavior*, 7(2):191–195.
- Thurfjell, H., Ciuti, S., and Boyce, M. S. (2014). Applications of step-selection functions in ecology and conservation. *Movement Ecology*, 2(4):1–12.
- Tolman, E. C. (1948). Cognitive maps in rats and men. *The Psychological Review*, 55(4):189–208.
- Torney, C. J., Lamont, M., Debell, L., Angohiatok, R. J., Leclerc, L.-M., and Berdahl, A. M. (2018). Inferring the rules of social interaction in migrating caribou. *Philosophical Transactions of the Royal Society B: Biological Sciences*, 373(1746):20170385.
- Tucker, M. A., Böhning-Gaese, K., Fagan, W. F., Fryxell, J. M., Van Moorter, B., Alberts, S. C., Ali, A. H., Allen, A. M., Attias, N., Avgar, T., Bartlam-Brooks, H., Bayarbaatar, B., Belant, J. L., Bertassoni, A., Beyer, D., Bidner, L., van Beest, F. M., Blake, S., Blaum, N., Bracis, C., Brown, D., de Bruyn, P. J. N., Cagnacci, F., Calabrese, J. M., Camilo-Alves, C., Chamailé-Jammes, S., Chiaradia, A., Davidson, S. C., Dennis, T., DeStefano, S., Diefenbach, D., Douglas-Hamilton, I., Fennessy, J., Fichtel, C., Fiedler, W., Fischer, C., Fischhoff, I., Fleming, C. H., Ford, A. T., Fritz, S. A., Gehr, B., Goheen, J. R., Gurarie, E., Hebblewhite, M., Heurich, M., Hewison, A. J. M., Hof, C., Hurme, E., Isbell, L. A., Janssen, R., Jeltsch, F., Kaczensky, P., Kane, A., Kappeler, P. M., Kauffman, M., Kays, R., Kimuyu, D., Koch, F., Kranstauber, B., LaPoint, S., Leimgruber, P., Linnell, J. D. C., López-López, P., Markham, A. C., Mattisson, J., Medici, E. P., Mellone, U., Merrill, E., de Miranda Mourão, G., Morato, R. G., Morellet, N., Morrison, T. A., Díaz-Muñoz, S. L., Mysterud, A., Nandintsetseg, D., Nathan, R., Niamir, A., Odden, J., O’Hara, R. B., Oliveira-Santos, L. G. R., Olson, K. A., Patterson, B. D., Cunha de Paula, R., Pedrotti, L., Reineking, B., Rimmler, M., Rogers, T. L., Rolandsen, C. M., Rosenberry, C. S., Rubenstein, D. I., Safi, K., Saïd, S., Sapir, N., Sawyer, H., Schmidt, N. M., Selva, N., Sergiel, A., Shiilegdamba, E., Silva, J. P., Singh, N., Solberg, E. J., Spiegel, O., Strand, O., Sundaresan, S., Ullmann, W., Voigt, U., Wall, J., Wattles, D., Wikelski, M., Wilmers, C. C., Wilson, J. W., Wittemyer, G., Zięba, F., Zwijacz-Kozica, T., and Mueller, T. (2018). Moving in the anthropocene: Global reductions in terrestrial mammalian movements. *Science*, 359(6374):466–469.

- Vales, D. J., Nielson, R. M., and Middleton, M. P. (2022). Black-tailed deer seasonal habitat selection: accounting for missing global positioning system fixes. *The Journal of Wildlife Management*, n/a(n/a):e22305.
- Valone, T. J. (2006). Are animals capable of Bayesian updating? an empirical review. *Oikos*, 112(2):252–259.
- van Baaren, J. and Candolin, U. (2018). Plasticity in a changing world: behavioural responses to human perturbations. *Current Opinion in Insect Science*, 27:21–25.
- van Moorter, B., Visscher, D., Benhamou, S., Börger, L., Boyce, M. S., and Gaillard, J.-M. (2009). Memory keeps you at home: a mechanistic model for home range emergence. *Oikos*, 118(5):641–652.
- van Moorter, B., Visscher, D. R., Jerde, C. L., Frair, J. L., and Merrill, E. H. (2010). Identifying movement states from location data using cluster analysis. *Journal of Wildlife Management*, 74(3):588–594.
- Vaserstein, L. N. (1969). Markov processes over denumerable products of spaces, describing large systems of automata. *Problemy Peredachi Informat-sii*, 5(3):64–72.
- Vergara, P. M., Soto, G. E., Moreira-Arce, D., Rodewald, A. D., Meneses, L. O., and Perez-Hernandez, C. G. (2016). Foraging behaviour in Magellanic woodpeckers is consistent with a multi-scale assessment of tree quality. *PLoS One*, 11(7):e0159096.
- Vors, L. S. and Boyce, M. S. (2009). Global declines of caribou and reindeer. *Global Change Biology*, 15(11):2626–2633.
- Vámos, T. I. F. and Shaw, R. C. (2022). How does selection shape spatial memory in the wild? *Current Opinion in Behavioral Sciences*, 45:101117.
- Wang, Y.-S., Blackwell, P. G., Merkle, J. A., and Potts, J. R. (2019). Continuous time resource selection analysis for moving animals. *Methods in Ecology and Evolution*, 10(10):1664–1678.
- Watson, J. L. (2020). *Ferruginous Hawk (Buteo regalis) Home Range and Resource Use on Northern Grasslands in Canada*. M.sc., University of Alberta, Edmonton, AB, Canada.
- Watson, J. W., Banasch, U., Byer, T., Svingen, D. N., McCready, R., Cruz, M. A., Hanni, D., Lafón, A., and Gerhardt, R. (2018). Migration patterns, timing, and seasonal destinations of adult ferruginous hawks (*buteo regalis*). *Journal of Raptor Research*, 52(3):267–281.
- Watson, J. W. and Keren, I. N. (2019). Repeatability in migration of ferruginous hawks (*buteo regalis*) and implications for nomadism. *The Wilson Journal of Ornithology*, 131(3):561–570.

- Wauters, L. A., Verbeylen, G., Preatoni, D., Martinoli, A., and Matthysen, E. (2010). Dispersal and habitat cuing of Eurasian red squirrels in fragmented habitats. *Population Ecology*, 52(4):527–536.
- Weng, K. C., Foley, D. G., Ganong, J. E., Perle, C., Shillinger, G. L., and Block, B. A. (2008). Migration of an upper trophic level predator, the salmon shark *lamna ditropis*, between distant ecoregions. *Marine Ecology Progress Series*, 372:253–264.
- Whoriskey, K., Auger-Methe, M., Albertsen, C. M., Whoriskey, F. G., Binder, T. R., Krueger, C. C., and Mills Flemming, J. (2017). A hidden Markov movement model for rapidly identifying behavioral states from animal tracks. *Ecol Evol*, 7(7):2112–2121.
- Wiktander, U., Olsson, O., and Nilsson, S. J. (2001). Seasonal variation in home-range size, and habitat area requirement of the lesser spotted woodpecker (*Dendrocopos minor*) in southern Sweden. *Biological Conservation*, 100:387–385.
- Wilcove, D. S. and Wikelski, M. (2008). Going, going, gone: Is animal migration disappearing? *PLOS Biology*, 6(7):e188.
- Wilmers, C. C., Nickel, B., Bryce, C. M., Smith, J. A., Wheat, R. E., and Yovovich, V. (2015). The golden age of bio-logging: how animal-borne sensors are advancing the frontiers of ecology. *Ecology*, 96(7):1741–1753.
- Wirsing, A. J., Quinn, T. P., Cunningham, C. J., Adams, J. R., Craig, A. D., and Waits, L. P. (2018). Alaskan brown bears (*Ursus arctos*) aggregate and display fidelity to foraging neighborhoods while preying on Pacific salmon along small streams. *Ecology and Evolution*, 8(17):9048–9061.
- Wolfson, D. W., Andersen, D. E., and Fieberg, J. R. (2022). Using piecewise regression to identify biological phenomena in biotelemetry datasets. *Journal of Animal Ecology*, 91(9):1755–1769.
- Wong, B. B. and Candolin, U. (2015). Behavioral responses to changing environments. *Behavioral Ecology*, 26(3):665–673.
- Worton, B. J. (1989). Kernel methods for estimating the utilization distribution in home-range studies. *Ecology*, 70(1):164–168.

Appendices

Appendix A: Supplementary Figures and Tables for Chapter 2

	Description
\mathbf{x}_t	The animal's location at time t
ϕ_t	The heading at which the animal arrives at \mathbf{x}_t at time t
Z_t	The animal's cognitive map at time t ; a spatially discrete function over a 2-D square grid
z_t	The grid cell within Z in which the animal is located at time t
\mathbf{A}	Markov chain matrix describing state-switching probabilities
f_s	Conditional likelihood function of the animal's spatial position given the animal is in the stationary movement state
g_s	Conditional likelihood function of the animal's headings given it is in the stationary movement state
ρ_s	Mean "step length" for animals when in the stationary state
f_{ns}	Conditional likelihood function of the animal's spatial position given the animal is in the non-stationary movement state
g_{ns}	Conditional likelihood function of the animal's headings given it is in the non-stationary movement state
k	Resource-independent movement kernel representing the probability of moving to any spatial location given the animal's current location; part of f_{ns} and remains constant in all four versions of the model
W	Environmental weighting function measuring the relative quality or attractiveness of any point in space to the animal; part of f_{ns} and varies in each version of the model (W_N, W_R, W_M , and W_{RM} for the null, resource-only, memory-only, and resource-memory models, respectively)
Θ_1	Parameter vector containing ρ_{ns} and κ , the two parameters incorporated in k ; remains constant in all four versions of the model
Θ_2	Parameter vector containing all parameters incorporated into W ; varies in each version of the model ($\Theta_{2,N}, \Theta_{2,R}, \Theta_{2,M}$, and $\Theta_{2,RM}$ for the null, resource-only, memory-only, and resource-memory models, respectively)
P	Number of resource covariates included in the resource-only and resource-memory models
φ	Gaussian distribution function
δ_s	Probability that the animal begins its movement path in the stationary movement state (in the model fitting process, estimated based on the data)
t^*	Number of time steps that are omitted from the movement track for model fitting, to allow the animal to "train" its memory
T	Number of time steps included in the model fitting (the total length of the animal's movement path is $t^* + T$ time indices)
K	Number of simulated "available points" per observed step used in model fitting

Table A.1: Description of all functions and quantities included in the model that were not fit as parameters. For parameters that were fit in the model, see Table 2.1.

		$K = 10$				$K = 50$			
		N	R	M	RM	N	R	M	RM
$T = 600$	N	20	7	2	21	27	4	3	16
	R	0	24	0	26	0	26	0	24
	M	3	0	24	23	0	0	25	25
	RM	0	2	5	43	0	0	2	48
$T = 1200$	N	28	1	1	20	29	2	1	18
	R	0	35	0	15	0	32	0	18
	M	0	0	15	35	0	0	20	30
	RM	0	0	1	49	0	0	0	50

Table A.2: Breakdown of model selection counts using AIC for different types of simulated tracks. The row represents the "true" model that the tracks were simulated from (N = null; R = resource-only; M = memory-only; RM = resource-memory), while the column represents the model that was identified as the most parsimonious explanation of the data using AIC. Treatment groups are identified by the outer left and upper portions of the table and are separated by shading.

		$K = 10$					$K = 50$				
		N-R	N-M	N-RM	R-RM	M-RM	N-R	N-M	N-RM	R-RM	M-RM
$T = 600$	N	5	2	26	25	9	3	3	17	18	27
	R	50	24	50	22	50	50	22	50	20	50
	M	4	45	46	45	22	3	48	50	50	23
	RM	50	47	50	47	45	50	49	50	50	48
$T = 1200$	N	0	0	21	24	27	1	1	19	19	24
	R	50	31	50	13	50	50	29	50	16	50
	M	2	48	50	50	33	0	50	50	50	28
	RM	50	50	50	50	49	50	49	50	50	50

Table A.3: Breakdown of likelihood ratio test results for different types of simulated tracks. The row represents the "true" model that the tracks were simulated from (N = null; R = resource-only; M = memory-only; RM = resource-memory), while the column represents the two models that were compared using a likelihood ratio test. Counts represent the number of simulated tracks (50 per cell) that registered a p-value below 0.05 for the indicated likelihood ratio test (for example, the "N-R" column indicates likelihood ratio tests determining whether the resource-only model is significantly more explanatory than the null model). Treatment groups are identified by the outer left and upper portions of the table and are separated by shading.

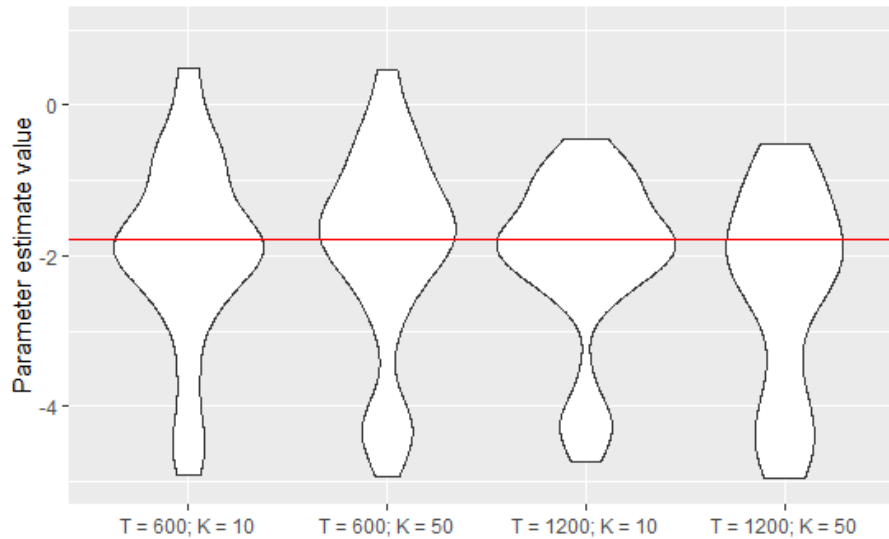


Figure A.1: Violin plot of parameter estimates for α parameter in the resource-memory model for our four treatment groups (detailed on the x-axis), with 50 simulations per treatment. The true value of $\log_{10} \frac{1}{60} \approx -1.78$ is denoted by a horizontal red line.

Appendix B: Supplementary Material for Chapter 3

Generating the berry density raster

We generated a vegetation class raster using the decision tree from Ducks Unlimited (2002) to classify each 30 x 30 m grid cell in the Mackenzie Delta region into one of 46 classes. Table B.1 describes each class as well as its value for the berry probability raster used in the model.

Description	Berry probability	Percent of landscape
Open needleleaf	0.5	0.397
Woodland needleleaf (other)	1	1.481
Woodland needleleaf (moss)	1	0.303
Woodland needleleaf (lichen)	1	0.524
Closed deciduous	0.5	0.082
Open deciduous	0.5	0.344
Closed tall shrub	0	1.476
Open tall shrub	0	0.007
Medium willow shrub	0	0.480
Medium-tall willow shrub	0	0.356
Medium-tall shrub (other)	0	0.027
Low shrub (other)	0	14.087
Low shrub (recently burned)	0	0.352
Low shrub (wet)	0	0.004
Low shrub (floodplain)	0	0.688
Low shrub (delta lowlands)	0	1.243
Low shrub - wet graminoid	0	0.012
Low shrub - tussock	0	1.135
Low shrub (upland)	0.5	0.368
Dwarf shrub (other)	1	9.097
Dwarf shrub (tussock)	0	5.331
Dwarf shrub (lichen)	1	2.239
Dwarf shrub (unknown - Kendall area)	0.5	0.046
Dwarf shrub (tussock/ <i>Dryas</i>)	0	0.072
Dwarf shrub (<i>Dryas</i> /heather)	0.5	0.796
Dwarf shrub (sloped hummocks)	0	0.035
Dwarf shrub (wet graminoid)	0.5	0.160
Tussock tundra	0.5	1.407
Lichen	0.5	0.243
Wet graminoid (wetland depressions or lake edges)	0	1.762
Wet graminoid (northern delta)	0	1.429
Wet graminoid (floodplain)	0	1.101
Wet graminoid (some shrubs)	0	0.111
Wet graminoid (unknown)	0	0.003
Dwarf shrub mosaic (wet)	0.5	0.355
Dwarf shrub mosaic (very wet)	0.5	0.761
Aquatic bed	0	0.014
Emergent vegetation	0	1.002
Emergent and other wet wetland areas	0	1.424
Clear water	0	20.108
Turbid water	0	25.385
Sparse vegetation	0	0.394
Sparse / non-vegetated (unsure)	0	0.030
Non-vegetated	0	0.670
Other	0	0.001
Unclassified	0	2.655

Table B.1: Classification method used to generate the berry density raster for the resource-only and resource-memory models. The name of each original vegetation class is shown along with the assigned probability, representing how correlated each habitat type is to the presence of berries, as well as the percentage of the landscape that is covered by each class.

Supplementary tables

Appendix C: Overview, Design Concepts, and Details (ODD) protocol for Chapter 4

Purpose

We developed a model heavily influenced by Avgar et al. (2013) to simulate the movement of spatially informed foragers. The model includes four parameters that, when combined, quantify an animal's foraging strategy. These parameters are intended to measure behaviourally plastic qualities of an animal as opposed to genetic or morphological traits. We assessed the adaptive value of different foraging strategies using a net energetic gain metric, which weighs the animal's resource intake against the energetic cost of movement. We do not specifically liken the model to any animal taxon, but we note that many common behavioural processes (e.g., migration and sociality) are not included in the model.

State variables and scales

The model consists of one individual (henceforth referred to as an "animal") that moves throughout a bounded spatial landscape. The animal performs discrete-time, continuous-space movements at constant temporal intervals of 1 arbitrary time unit (tu). The landscape is a 100 x 100 arbitrary length unit (lu) square in two-dimensional space. Each spatial point on the landscape \mathbf{x} and time index t has a resource quality $Q(\mathbf{x}, t) \in [0, 1]$ representing the energetic value of resources at that point. For mathematical convenience, we formulated $Q(\mathbf{x}, t)$ as a piecewise constant function; all \mathbf{x} in any 1x1 lu "grid cell" have the same value of $Q(\mathbf{x}, t)$ at any time t . To prevent animals from getting "trapped" in corners or boundaries of the landscape, we assume that landscapes have wrap-around

ID	Model	ρ_{ns}	κ	β_1	β_2	β_3	β_4	β_5	β_6	β_0	β_d	μ	σ	λ	γ	α
GF1004	RM	0.357	0.403	0.113	-0.031	0.707	-0.019	-0.055	-0.111	0.1068	~ 1	350.6	9.1	0.460	0.729	-0.046
GM1046	RM	0.399	0.414	0.381	-1.341	0.732	-0.029	-0.015	-0.074	0.2011	0.7800	354.2	8.1	0.332	0.741	-0.259
GF1008	R	0.414	0.422	0.098	-0.885	1.536	-0.044	-0.127	-0.157	N/A	0	N/A	N/A	0.464	0.825	N/A
GF1086	RM	0.205	0.131	0.281	-1.307	2.579	-0.198	-0.006	-0.307	~ 0	0.9792	0.8	3.0	0.346	0.739	-4.617
GF1016	M	0.279	0.110	0	0	0	0	0	0	0.7311	0.9354	1.4	3.0	0.549	0.722	0.072
GF1041	R	0.376	0.465	0.165	-1.450	2.497	-0.030	-0.275	-0.269	N/A	0	N/A	N/A	0.338	0.752	N/A
GF1107	R	0.236	0.141	0.222	-0.718	2.433	-0.020	-0.311	-0.241	N/A	0	N/A	N/A	0.387	0.712	N/A
GF1130	N	0.394	0.400	0	0	0	0	0	0	N/A	0	N/A	N/A	0.421	0.728	N/A
GF1005	R	0.597	0.202	0.158	-0.926	3.538	-0.060	-0.169	-0.153	N/A	0	N/A	N/A	0.404	0.716	N/A
GF1096	RM	0.366	0.273	0.207	-2.017	1.970	-0.040	-0.132	-0.188	0.9997	0.5002	337.0	16.4	0.330	0.755	-0.129
GF1167	M	0.420	0.427	0	0	0	0	0	0	0.7311	~ 1	361.1	3.8	0.310	0.716	-0.274
GF1079	RM	0.341	0.573	0.156	-2.434	2.829	-0.021	-0.071	-0.151	~ 0	0.5000	0.8	3.0	0.096	0.740	-6.436
GF1089	M	0.267	0.033	0	0	0	0	0	0	0.7311	0.9306	0.8	3.0	0.292	0.688	-0.064
GF1141	M	0.363	0.060	0	0	0	0	0	0	0.7311	0.9945	354.8	3.0	0.509	0.685	-0.344
GM1133	M	0.324	0.000	0	0	0	0	0	0	0.7311	~ 1	47.4	22.3	0.495	0.698	-0.306
GF1087	RM	0.344	0.078	0.677	-1.405	-13.080	-36.366	-0.755	0.359	0.5200	0.8604	351.9	5.0	0.280	0.668	-1.030
GF1108	N	0.326	0.003	0	0	0	0	0	0	N/A	0	N/A	N/A	0.115	0.822	N/A
GF1143	RM	0.331	0.477	-0.020	-1.243	3.271	-0.065	-0.126	-0.196	0.0007	0.5000	299.1	6.5	0.060	0.781	-1.076
GM1147	M	0.464	0.000	0	0	0	0	0	0	0.7311	~ 1	259.8	3.0	0.088	0.652	-0.512
GF1092	RM	0.241	0.000	0.189	-1.115	1.884	-0.096	-0.300	-0.250	0.0006	0.5005	334.6	30.8	0.314	0.602	-0.512
GF1146	M	0.319	0.159	0	0	0	0	0	0	0.7311	0.9885	346.8	3.0	0.097	0.701	-0.653

Table B.2a: 95% lower confidence bounds for the "best model" (as identified by BIC) for each bear, calculated using likelihood profiling. Bears are listed in ascending order by number of GPS fixes. Gray text in the table indicates a parameter value that was fixed and not estimated for that model, and gray "N/A" values indicate parameters that are not influential in the "best model" for that bear. Parameter estimates for β_0 and β_d that are very close to but not exactly 0 or 1 are indicated as such with a " \sim ". See Table 1 for descriptions of each parameter.

ID	Model	ρ_{ns}	κ	β_1	β_2	β_3	β_4	β_5	β_6	β_0	β_d	μ	σ	λ	γ	α
GF1004	RM	0.409	0.603	0.252	0.510	1.809	0.003	0.090	0.044	0.2813	~1	356.4	12.8	0.558	0.788	-0.015
GM1046	RM	0.458	0.619	0.574	-0.267	1.861	0.000	0.112	0.053	0.9122	~1	363.0	17.9	0.451	0.801	-0.100
GF1008	R	0.474	0.628	0.248	-0.005	2.536	-0.013	0.015	-0.008	N/A	0	N/A	N/A	0.590	0.877	N/A
GF1086	RM	0.235	0.328	0.527	-0.498	5.036	-0.030	0.196	-0.097	0.0111	~1	1.2	3.3	0.462	0.800	-1.496
GF1016	M	0.326	0.332	0	0	0	0	0	0	0.7311	0.9933	4.6	4.0	0.652	0.792	0.112
GF1041	R	0.436	0.687	0.307	-0.336	3.840	-0.005	0.058	0.067	N/A	0	N/A	N/A	0.462	0.815	N/A
GF1107	R	0.279	0.377	0.452	0.798	3.263	0.002	0.126	0.201	N/A	0	N/A	N/A	0.517	0.787	N/A
GF1130	N	0.468	0.658	0	0	0	0	0	0	N/A	0	N/A	N/A	0.552	0.803	N/A
GF1005	R	0.716	0.464	0.332	0.428	5.696	-0.008	0.002	0.021	N/A	0	N/A	N/A	0.541	0.796	N/A
GF1096	RM	0.436	0.531	0.404	-0.806	3.578	-0.001	0.052	0.005	~1	0.6815	363.2	40.4	0.485	0.830	-0.079
GF1167	M	0.512	0.725	0	0	0	0	0	0	0.7311	~1	368.6	12.5	0.467	0.802	-0.126
GF1079	RM	0.419	0.894	0.358	-1.088	4.354	0.014	0.135	0.051	~1	~1	1.3	3.4	0.264	0.827	-0.946
GF1089	M	0.331	0.340	0	0	0	0	0	0	0.7311	0.9990	5.4	13.1	0.466	0.786	0.068
GF1141	M	0.487	0.484	0	0	0	0	0	0	0.7311	~1	365.0	31.7	0.697	0.817	-0.023
GM1133	M	0.435	0.288	0	0	0	0	0	0	0.7311	~1	61.0	33.9	0.690	0.829	-0.111
GF1087	RM	0.466	0.518	1.769	0.273	6.502	-0.053	-0.182	1.132	~1	~1	359.5	12.0	0.513	0.808	-0.478
GF1108	N	0.437	0.421	0	0	0	0	0	0	N/A	0	N/A	N/A	0.463	0.927	N/A
GF1143	RM	0.457	0.977	0.312	-0.256	6.609	-0.006	0.508	0.802	~1	~1	366.0	182.5	0.353	0.903	-0.119
GM1147	M	0.674	0.381	0	0	0	0	0	0	0.7311	~1	261.8	3.2	0.359	0.820	-0.440
GF1092	RM	0.370	0.108	0.830	3.508	4.001	-0.020	0.544	0.564	~1	~1	368.0	55.3	0.614	0.801	0.106
GF1146	M	0.543	0.960	0	0	0	0	0	0	0.7311	~1	353.2	7.0	0.543	0.908	-0.114

Table B.2b: 95% upper confidence bounds for the "best model" (as identified by BIC) for each bear, calculated using likelihood profiling. Bears are listed in ascending order by number of GPS fixes. Gray text in the table indicates a parameter value that was fixed and not estimated for that model, and gray "N/A" values indicate parameters that are not influential in the "best model" for that bear. Parameter estimates for β_0 and β_d that are very close to but not exactly 0 or 1 are indicated as such with a "~". See Table 1 for descriptions of each parameter.

ID	Model	ρ_{ns}	κ	β_1	β_2	β_3	β_4	β_5	β_6	β_0	β_d	μ	σ	λ	γ	α
GF1004	RM	0.383	0.502	0.265	0.300	-0.265	-0.015	0.068	0.007	0.4360	~1	0.8	3.0	0.508	0.759	-1.611
GM1046	M	0.428	0.517	0	0	0	0	0	0	0.7311	~1	359.1	10.2	0.390	0.772	-0.126
GF1008	M	0.443	0.526	0	0	0	0	0	0	0.7311	~1	351.6	4.4	0.528	0.852	-0.133
GF1086	R	0.219	0.229	0.945	-0.792	3.529	-0.130	0.079	-0.120	N/A	0	N/A	N/A	0.403	0.770	N/A
GF1016	M	0.301	0.220	0	0	0	0	0	0	0.7311	0.9782	3.0	3.0	0.601	0.758	0.112
GF1041	N	0.405	0.578	0	0	0	0	0	0	N/A	0	N/A	N/A	0.399	0.785	N/A
GF1107	M	0.258	0.253	0	0	0	0	0	0	0.7311	~1	365.0	65.0	0.448	0.750	0.140
GF1130	RM	0.430	0.529	0.178	-0.110	-0.325	-0.051	0.002	-0.031	0.4415	~1	0.8	3.0	0.488	0.768	-1.762
GF1005	M	0.651	0.331	0	0	0	0	0	0	0.7311	0.9953	5.6	3.0	0.473	0.758	-0.256
GF1096	M	0.400	0.402	0	0	0	0	0	0	0.7311	~1	348.1	26.9	0.405	0.794	-0.079
GF1167	M	0.463	0.574	0	0	0	0	0	0	0.7311	~1	364.8	6.3	0.387	0.761	-0.126
GF1079	R	0.378	0.728	0.376	-2.161	2.508	0.012	-0.059	-0.141	N/A	0	N/A	N/A	0.171	0.786	N/A
GF1089	R	0.298	0.192	1.506	-0.783	1.243	-0.005	0.056	0.196	N/A	0	N/A	N/A	0.379	0.740	N/A
GF1141	M	0.419	0.529	0	0	0	0	0	0	0.7311	~1	365.0	11.9	0.606	0.754	-0.023
GM1133	M	0.374	0.080	0	0	0	0	0	0	0.7311	~1	54.5	26.7	0.595	0.768	-0.212
GF1087	M	0.400	0.295	0	0	0	0	0	0	0.7311	~1	357.9	9.2	0.396	0.744	-0.338
GF1108	N	0.376	0.211	0	0	0	0	0	0	N/A	0	N/A	N/A	0.273	0.880	N/A
GF1143	M	0.388	0.722	0	0	0	0	0	0	0.7311	~1	352.8	15.1	0.179	0.848	-0.119
GM1147	M	0.556	0.115	0	0	0	0	0	0	0.7311	~1	260.9	3.0	0.204	0.742	-0.477
GF1092	M	0.301	0.000	0	0	0	0	0	0	0.7311	~1	363.1	42.0	0.469	0.714	0.106
GF1146	M	0.412	0.549	0	0	0	0	0	0	0.7311	0.9998	350.0	3.0	0.286	0.819	-0.162

Table B.3: Parameter estimates for the "best model" (as identified by BIC) for each bear with explicit expression of resource seasonality. Bears are listed in ascending order by number of GPS fixes. Note that the second letter of the bear ID indicates the sex of the individual. Gray text in the table indicates a parameter value that was fixed and not estimated for that model, and gray "N/A" values indicate parameters that are not influential in the "best model" for that bear. Parameter estimates for β_0 and β_d that are very close to but not exactly 0 or 1 are indicated as such with a " \sim ".

boundaries (e.g., if the animal moves far enough to the left, it will eventually end up on the right side of the grid).

The landscape has two unique resources that are added together to produce the total resource quality $Q(\mathbf{x}, t)$ for each point and time. We define $Q_1(\mathbf{x}, t)$ and $Q_2(\mathbf{x}, t)$ to be the quality values for the first and second resources at point \mathbf{x} and time t , respectively. Both of these resource functions can take on values between 0 and 1, so to ensure that $Q(\mathbf{x}, t)$ is defined properly, we set $Q(\mathbf{x}, t) = (Q_1(\mathbf{x}, t) + Q_2(\mathbf{x}, t)) * 0.5$ for every point \mathbf{x} and time t .

We incorporated depletion-recovery dynamics to the landscape to ensure animals would be incentivized to move. When the animal visits any point in a grid cell, it consumes and depletes that cell's resources. Specifically, we decrement $Q_1(\mathbf{x}, t)$ and $Q_2(\mathbf{x}, t)$ by resource depletion parameter d_L for every point \mathbf{x} in the cell the animal visits at time t . If d_L is greater than the resource value at that time, the cell is depleted entirely and is assigned a resource value of 0. Each depleted resource recovers by r_L units each time step until reaches its original, pre-depletion value. We fixed d_L and r_L for all simulations (Table 4.1).

Process overview and scheduling

We tracked information storage in simulated animals using $C(\mathbf{x}, t)$, which represents the animal's estimation of resource quality for each point and time. As the animal perceives and remembers new information through movement, C is updated. The animal moves by choosing a "point of interest" to navigate to based on C . Points of interest may take more than 1 tu to reach, reflecting the numerous timescales at which animals make movement decisions (McClintock et al., 2014; Blackwell et al., 2016).

Design concepts

Fitness: Simulated animals perform the most basic version of "fitness-seeking" in that they search for points with a higher concentration of resources. Following Assumption A1, animals exhibit "habitat selection" for the different resources on the landscape. We introduce the parameter $h \in [0, 1]$ to quantify this relationship. When the animal visits a new location, it stores the value of that location as $\tilde{Q}(\mathbf{x}, t) = hQ_1(\mathbf{x}, t) + (1-h)Q_2(\mathbf{x}, t)$ rather than $Q(\mathbf{x}, t)$ (Figure 4.1). Per Assumption A4, animals will be more likely to navigate to nearby points, as this minimizes locomotive cost as well as the opportunity cost of navigating through potentially resource-poor habitat on the way to a faraway point of interest.

Sensing: Animals are not omniscient and must obtain information via perception. Typically, animals perceive nearby information more accurately (Avgar et al., 2015; Fagan et al., 2017). Mathematically, we formalize this using a perception function $p(\mathbf{x}, \mathbf{y})$. This function measures how accurately (ranging from 0 to 1) an animal located at \mathbf{x} perceives information about \mathbf{y} . We chose an exponential decay function (similar to Avgar et al., 2013) to represent this relationship:

$$p(\mathbf{x}, \mathbf{y}) = \exp\left(-\frac{d(\mathbf{x}, \mathbf{y})}{\rho}\right), \quad (\text{C.1})$$

where $d(\mathbf{x}, \mathbf{y})$ is the distance between \mathbf{x} and \mathbf{y} , accounting for wrap-around boundaries. We assume that the animal's perceptual ability increases with ρ , the parameter governing the animal's locomotive capability.

Memory: Assumption A2 states that the animal's reliance on memory decreases as the time since the formation of that memory increases. Mathematically, we

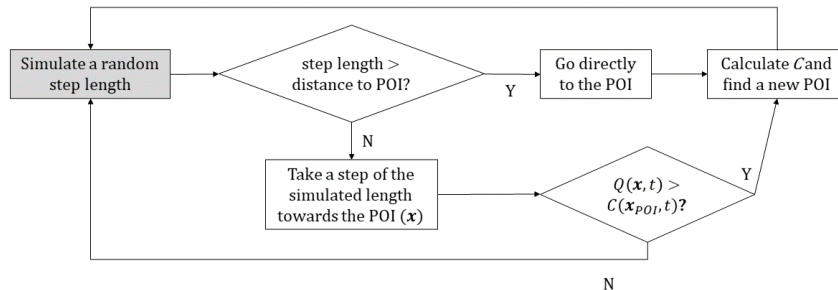


Figure C.1: Flowchart describing the individual-based simulation model for animal movement. At each time step, animals update their perception of the environment C , occasionally using it to choose a point of interest (POI) to navigate to. This navigation can take any number of time steps, as the animal does not typically stop navigating until it reaches the point.

used an exponential decay function to represent this (similarly to Avgar et al., 2013). The function $m(t)$ ranges between 0 and 1 and quantifies the animal's reliance on memory as a function of how long ago the memory was formed. Simply put, $m(t) = \exp(-\beta t)$. If $\beta = 0$, the animal effectively has an infinite memory, and as β becomes infinitely large, the animal begins to neglect its memory entirely.

Prediction: The animal estimates the resource quality at any point on the landscape using perception and memory, but if it has never visited a location on the grid, it must still make a naive "guess" about the resource quality there (Berger-Tal and Avgar, 2012; Avgar et al., 2013). Assumption A3 states that this guess is constant across space and time; in other words, the animal will treat all unvisited points equally throughout the simulation. We can represent this guess with $q \in [0, 1]$. Larger values of q will result in more exploratory movement as animals assign higher value to unvisited areas.

Stochasticity: Animal movement paths are stochastic, and as a result animals

will not always visit the patch that confers the highest expected benefit (i.e., the highest value of C). That being said, points with higher values of C are still more likely to be chosen as points of interest. When the animal is not currently en route to a point of interest, a new point of interest is picked using a Monte Carlo sampling technique. This involves simulating $N_r = 1000$ possible points of interest $\mathbf{x}_{t,1}, \mathbf{x}_{t,2}, \dots, \mathbf{x}_{t,N_r}$ and randomly picking one (denoted \mathbf{x}_t^P) based on the value of C . More specifically,

$$P(\mathbf{x}_{t,i} = \mathbf{x}_t^P) = \frac{C(\mathbf{x}_{t,i}, t)^\lambda}{\sum_{j=1}^{N_r} C(\mathbf{x}_{t,j}, t)^\lambda}, \quad (\text{C.2})$$

for any positive integer $i \leq N_r$. We include a fixed constant $\lambda \geq 0$ that controls the "determinism" of the animal's movements: as λ increases, it is more likely to choose the point with the highest value of C .

We simulate the $\mathbf{x}_{t,i}$ as end points of a movement "step" beginning at \mathbf{x}_{t-1} , where the lengths of each step follow an exponential distribution. The shape of this distribution results in smaller step lengths being more frequently sampled, following Assumption A4. We define $\gamma \geq 0$ as the "rate" parameter of the exponential distribution, quantifying the strength of the relationship between distance and point-of-interest selection. As γ approaches 0, every point on the grid has an equal chance of being selected (assuming equal values of C). If γ is large, all $\mathbf{x}_{t,i}$ will be close to the animal and it will not undertake long-distance navigations very often.

The animal navigates to points of interest by performing a biased random walk (Figure C.1). The lengths of each step along the navigation are simulated from a gamma distribution with mean and variance ρ . This distribution has an entirely positive support and is roughly bell-shaped for most values of ρ , including the value we used (Table 4.1). If simulated step lengths are longer than the distance to the point of interest (i.e., the animal would "overshoot" its

destination), the animal goes directly to the point of interest instead. Otherwise, it takes a step of the simulated length towards the point of interest. The heading of this step is simulated from a von Mises distribution where the mean heading is the heading required to reach the point of interest. The concentration parameter for this distribution, $\kappa \geq 0$, is a fixed quantity in this model (Table 4.1). It is recommended that large values of κ , which cause more directed movement to the point of interest, are used here. If one of the steps on the animal's navigation ends on a point that has better resources than the point of interest (i.e., $\tilde{Q}(\mathbf{x}_{t+1}, t+1) > C(\mathbf{x}_t^P, t+1)$), the animal "forgets" about the point of interest and prioritizes foraging at the newfound location. The algorithm restarts whenever the animal arrives at its point of interest.

Observation: We collected information about the animal's movement as well as its cumulative resource intake. We keep track of the animal's location \mathbf{x}_t , as well as the value of $Q(\mathbf{x}_t, t)$, for each time step t in the track. Note that while the animal exhibits relative preference for resources using \tilde{Q} , it still takes in equal amounts of both resources when it visits a patch.

Our model does not implement interaction or collectives since animals are solitary on the landscape. While we assume that animals can "adapt" to environmental conditions by modifying β, γ, q , and h between simulations, we do not allow for adaptation within a single simulation. We are not particularly focused on emergent properties such as home range formation.

Initialization

At the beginning of each simulation, we randomly generate a landscape and initialize the animal at a random point on that landscape. Initially, $C(\mathbf{x}, 0) = q$ for every point \mathbf{x} , as the animal has no prior experience on the grid.

Input

For each simulated animal movement path, we supplied two randomly generated landscapes (for Q_1 and Q_2 respectively) as inputs. We simulated our landscapes as Gaussian random fields, implying that each cell on the grid is a component of a multivariate Gaussian random variable (Schlather, 2012). In this case, the covariance between any two cells depends on the wrap-around distance between the two cells (closer cells have higher covariance). We then scaled the values such they all fell between 0 and 1.

To more accurately capture the patchiness of many real-world habitats, we defined a cut-off value \underline{Q} that could be used to make these landscapes more patchy. Under this rule, any grid cell with a value of Q below \underline{Q} would be set to 0. Increasing \underline{Q} decreases the overall resource quality of the landscape and is more likely to confine the animal to specific high-quality patches. Here, we used landscapes with $\underline{Q} = 0.6$ and $\underline{Q} = 0.9$ (Figure 4.2).

Submodels

Our main submodel is the calculation of C , the animal's spatial map of perceived resource quality. This calculation is composed of three mechanisms: perception ($p(\mathbf{x}, \mathbf{y})$), memory ($m(t)$), and default expectation (q). Figure 4.1 displays how these quantities are combined and weighted to produce C . This is mathematically formalized below:

$$C(\mathbf{x}, t) = \underbrace{p(\mathbf{x}, \mathbf{x}_t)\tilde{Q}(\mathbf{x}, t)}_{\text{perception}} + (1 - p(\mathbf{x}, \mathbf{x}_t)) \left(\underbrace{m(1)C(\mathbf{x}, t-1)}_{\text{memory}} + \underbrace{(1 - m(1))q}_{\text{expectation}} \right). \quad (\text{C.3})$$

Note that $m(1) = \exp(-\beta)$, which resembles the model from Avgar et al. (2013).

Appendix D: Determining the appropriate number of MCMC iterations

We determined an optimal number of iterations per MCMC chain by identifying when additional iterations did not substantially affect the posterior distribution of the four behavioural parameters. If some value N were to be sufficient as the number of iterations per chain, we would expect that a chain simulated for N iterations would produce similar posteriors when we added additional iterations to the chain. If simulating more iterations produced negligibly different posteriors, it is not computationally worthwhile to perform those iterations. To that end, we ran a chain of the MCMC sampling algorithm for our foraging task with 5000 iterations (what we deemed to be the largest computationally reasonable value). We then took the first N iterations of that chain and compared the posterior distribution from that subset with a slightly larger subset, the first $N + 500$ iterations. We used a static MCMC sampler in our analysis so the individual iterations were independent of each other, rendering this process similar to comparing two separate chains.

We compared posterior distributions using the earth mover’s distance, also known as the Wasserstein distance, a common tool for comparing multivariate distributions across many fields (Vaserstein, 1969; Rubner et al., 2000; Potts et al., 2014). The earth mover’s distance approximates the energy required to spatially transform one probability distribution such that it resembles another. As a result, lower values of this metric suggest higher distributional similarity, and an earth mover’s distance of 0 is only achieved between two perfectly identical probability distributions. Plotting the earth mover’s distance against N , the proposed number of iterations, for many different values of N (ranging from

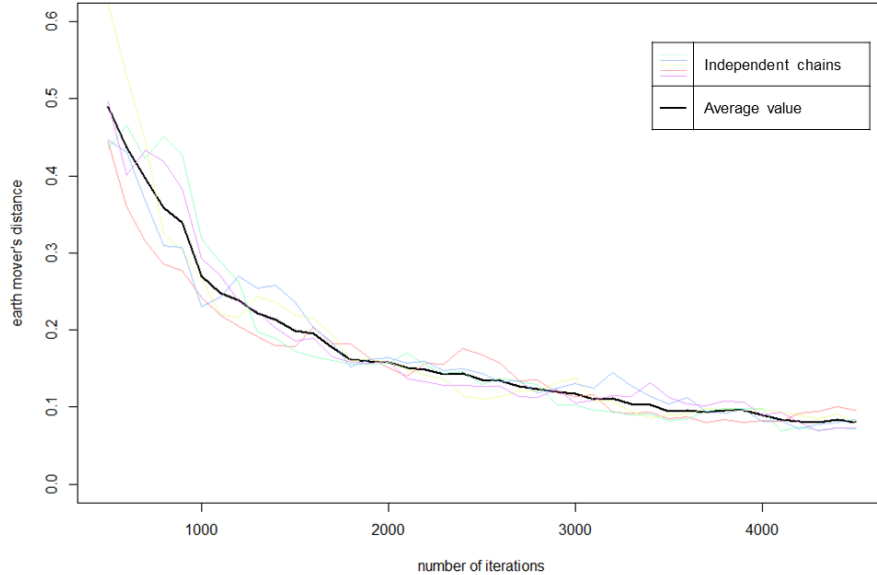


Figure D.1: Relationship between the number of iterations in a MCMC chain used to simulate the foraging task and distributional similarity, measured using the earth mover’s distance. We calculated the earth mover’s distance between the first N iterations of the chain and the first $N + 500$ iterations to evaluate the difference that adding 500 iterations would make to the posterior distribution of animal behaviour. The coloured lines represent five individual runs of the process, and the thicker black line represents the mean earth mover’s distance across these runs.

500 to 4500 by 100) led us to identify $N_{iter} = 2000$ as the appropriate number of iterations (Figure D.1). We ran the process described above five independent times to ensure that this relationship was similar with different random runs of the algorithm.

Appendix E: Simulation study for Chapter 5

We simulated movement paths intended to resemble ferruginous hawk migrations with and without stopovers. We then fit the $k = 1$ (one-migration) and $k = 2$ (two-migration) versions of the model to all these simulated paths and

compared the parsimony of each model type using Akaike Information Criterion (AIC) and Bayesian Information Criterion (BIC). We parameterized the model such that it resembled a typical fall hawk migration (where stopovers are more frequent). We simulated our paths as a series of 1-hour movements over a 200-day period, in line with the 1-hour fix rate data for fall migrant hawks. In both stopover and non-stopover cases the simulated birds departed from their breeding grounds after 119 days and arrived on their wintering grounds after 190 days (in line with examples from our results). We simulated 25 paths without any stopover behaviour and 25 paths with a 30-day stopover starting at day 130. To simulate our paths, we generated step lengths and turning angles independently using the probability distribution functions described in Equation 5.5. We simulated step lengths from an exponential distribution and turning angles from a von Mises distribution, where the parameters for these distributions varied depending on the time associated with each data point. In our simulation, we set $\rho_0 = 0.6$ km/hr, $\rho_1 = 7$ km/hr, $\kappa_0 = 0$, and $\kappa_1 = 0.5$. This gave us 4800 step lengths and turning angles from which we iteratively constructed a movement path. The real-life hawk data had many missing steps so we randomly removed $0.5(1 - \frac{2000}{4800}) = 29.1\bar{6}$ percent of the generated locations. Our simulated paths contained approximately 2000 pairs of consecutive data points (steps), resembling the real-life data. We fit the $k = 1$ and $k = 2$ models to these simulated paths using the same algorithm as the real data, obtaining parameter estimates and calculating AIC and BIC. These results are included in Supplementary File 1.